POLYVALENT SURFACE MODIFICATION OF HYDROCARBON POLYMERS VIA COVALENT LAYER-BY-LAYER SELF-ASSEMBLY

A Dissertation

by

KANG-SHYANG LIAO

Submitted to the Office of Graduate Studies of
Texas A&M University
in partial fulfillment of the requirements for the degree of

DOCTOR OF PHILOSOPHY

December 2008

Major Subject: Chemistry

POLYVALENT SURFACE MODIFICATION OF HYDROCARBON POLYMERS VIA COVALENT LAYER-BY-LAYER SELF-ASSEMBLY

A Dissertation

by

KANG-SHYANG LIAO

Submitted to the Office of Graduate Studies of
Texas A&M University
in partial fulfillment of the requirements for the degree of

DOCTOR OF PHILOSOPHY

Approved by:

Chair of Committee,	David E. Bergbreiter
Committee Members,	James D. Batteas
	Eric E. Simanek
	Jaime C. Grunlan
Head of Department,	David H. Russell

December 2008

Major Subject: Chemistry

ABSTRACT

Polyvalent Surface Modification of Hydrocarbon Polymers

via Covalent Layer-by-Layer Self-Assembly. (December 2008)

Kang-Shyang Liao, B.S., National Taiwan University

Chair of Advisory Committee: Dr. David E. Bergbreiter

Layer-by-layer (LbL) assembly based on ionic interactions has proven to be a versatile route for surface modification and construction of ultrathin nanocomposites. Covalent LbL assembly based on facile 'click' covalent bond formation is an effective alternative, especially for the applications where a more robust ultrathin films or nanocomposites is desired. The subject of this dissertation focuses on the design of three different covalent LbL assemblies and their applications on conductive thin films, superhydrophobic surfaces, and solute responsive surfaces, respectively.

Surface modification of PE substrates using covalent LbL assembly with PEI and Gantrez is a successful route to prepare a surface graft. The procedure is relative easy, fast and reproducible. Grafting multiple layers of PEI/Gantrez to the PE powder surface provided excellent coverage and promoted stable LbL film growth and excellent adhesion. This carbon black (CB) coated powder was compression molded into films, and their conductivity was measured, which revealed a percolation threshold below 0.01 wt % CB for the PEI-grafted system. Electrical conductivity of 0.2 S/cm was achieved with only 6 wt % CB, which is exceptional for a CB-filled PE film.

Direct amination of MWNTs with PEI is a convenient and simple method leading to highly functionalized product that contains 6-8 % by weight PEI. Superhydrophobic PE films can be formed either from ionic LbL self-assembly of MWNT-NH-PEIs and poly(acrylic acid) or from covalent LbL self-assembly of MWNT-NH-PEIs and Gantrez when the final graft is acrylated with octadecanoic acid. While the ionically assembled nanocomposite graft is labile under acid, the covalently assembled graft is more chemically robust.

Responsive surfaces with significant, reversible, reproducible wettability changes can be prepared by covalent LbL grafting using PNIPAM-*c*-PNASI and aminated silica nanoparticles. A 65º $\Delta\Theta$ value was observed with water vs. 1.4 M Na_2SO_4. The prepared film shows a high surface roughness of ~300 nm, which contributes to the large solute responsive $\Delta\Theta$ values. The surfaces are reconfigurable in different solute conditions and that the changes in water contact angle are likely due to combination of change in surface roughness along with swell and intercalation of the solute ions into the PNIPAM surface.

DEDICATION

To my parents, my brother, and Aide.

ACKNOWLEDGMENTS

First, I would like to sincerely thank Professor David Bergbreiter for his guidance throughout my graduate school career. Under his tutelage and guidance, I became a professional scientist and writer. I would also like to thank Professor Jaime Grunlan for our collaborations in the conductive thin films project and Professor James Batteas for the superhydrophobic and solute-responsive surfaces. Professor Grunlan and Professor Batteas opened up my vision to the field of material science and the amazing would of nanotechnology.

I would also like to acknowledge my undergraduate advisors, Professor Yuen-Ming Tsai and Professor Sheng-Hsien Chiu, for their guidance during my undergraduate years at National Taiwan University. They were not only my mentors, but also friends, who helped guide me through the world of chemistry and led me to the right direction earlier in my career as a chemist.

I would like to extend my thanks to Dr. Yeon-Seok Kim for his help on the project of conductive thin film and Albert Wan for his help on the superhydrophobic and solute-responsive surfaces project. I would also like to thank Hui Fu for taking over my solute-responsive project where I left off. It has been a wonderful experience working with all of you.

Finally, I would like to thank all of my friends and colleagues: Chi-Lin Tsai, Dr. Izabela Owsik, Dr. Jianhua Tian, Chayanant (Film) Hongfa, Christopher Hobbs, Haw-Lih Su, Yun-Chin (Jeff) Yang, and all other friends, with whom I have shared these wonderful five years with at Texas A&M University.

TABLE OF CONTENTS

CHAPTER Page

CHAPTER Page

CHAPTER Page

LIST OF SCHEMES

SCHEME Page

LIST OF FIGURES

FIGURE Page

FIGURE Page

FIGURE Page

FIGURE Page

LIST OF TABLES

TABLE Page

CHAPTER I

INTRODUCTION

Surface Modification Using Layer-by-Layer Self-Assembly

Modern approaches to layer-by-layer (LbL) assembly most often use ionic processes as first reported almost twenty years ago by Decher.[1] These LbL processes have become widely used methods for surface modification. In such processes[2-4], thin film surface grafts are assembled by alternate deposition of mutually attractive molecules or particles. Most commonly these species are positively and negatively charged polymers. This self-assembly approach to a multilayer graft requires formation of a charged surface as a first step. If an anionic surface is present, the first deposition step involves entropically favored assembly of a cationic polymer onto this anionic surface. This process is entropically favored because the polyvalent attachment of a single cationic polymer releases many cations and anions to solution. The product of this ionic assembly process is a surface with an excess of the polycation. Subsequent alternating depositions of more anionic and then cationic polymers produce additional "bilayers". This process can be automated and can be continued until the graft reaches the desired thickness or the surface has the desired properties. By varying experimental conditions, graft thicknesses can be reproducibly controlled. This LbL approach is simple and works on substrates of any shape. Recent reviews discuss this chemistry.[5-7]

While LbL assembly most often uses polyelectrolytes for graft construction, others

---

This dissertation follows the style of the *Journal of the American Chemical Society.*

have shown that other driving forces work too. For example, self-assembly of polymers that are hydrogen bond donors and acceptors is a non-ionic way to affect multilayer assembly.[8] In this scheme, an uncharged hydrogen bond acceptor polymer like poly(ethylene oxide) or poly(*N*-isopropylacrylamide) and a hydrogen bond donating polymer like poly(acrylic acid) are alternately deposited one on the other to form a multilayer graft.

Though ionic or hydrogen bond self-assembly processes are experimentally simple and broadly useful, they have some drawbacks. Specifically, ionic or hydrogen bonded LbL assemblies can dissemble under conditions where the ionic or hydrogen bonds are unstable.[8] For example, strongly acidic, strongly basic, or high salt solutions can affect these grafts' stability. Most often, this is not a problem. In other cases, facile disassembly of a multilayer grafts even provides advantages (e.g. in drug release applications).[7] Nonetheless, some applications are better served by more chemically robust multilayer grafts that withstand harsh conditions.

Covalent assembly is a third way to assembly multilayers grafts on diverse surfaces that provides this extra stability and is the subject of this review. This relatively 'new' way to make grafts is an approach to surface modification with ancient roots. Oriental lacquerware fabrication dates back to 4000 BC in China and Japan and has similarities to covalent multilayer assembly processes.[9,10] The sap used for the lacquerware coatings is an aqueous emulsion of phenolic lipids-polysaccharide-glycoprotein complexes derived from lacquer trees. The process that generates the product high gloss, durable coating is a layer-by-layer process involving as many as 40 repeated coating-drying-polishing-

rubbing-drying cycles. Enzymatic radical dimerization or polymerization of phenolics leads to covalent bonds during the drying cycle of what actually is an LbL process. The numerous perfectly preserved examples of lacquerware from the Qin dynasty (around 200 BC) of China afford an artistic and pleasing record that substantiates the notion that covalent multilayer grafts can be durable and useful.

Requirements and General Features for Covalent LbL Assembly

Covalent LbL assembly differs from ionic LbL assembly in a number of respects. First, while ionic LbL assembly only requires two mutually attractive polyelectrolytes, the polymers to be used as building blocks in covalent assembly have to possess complementary functional groups that can form stable covalent bonds *in-situ*. Second, these reactions preferably should be reactions that can be carried out under mild conditions. Ideally, these reactions would occur under ambient atmosphere so as to minimize the need for special environments for the assembly process. Third, if the reactions generate side products, the side products should be easily separated from the film so that contamination of the penultimate LbL assembly by impurities is avoided. In general, reactions that Sharpless has described as 'click' chemistry are ideal.[11] These general features of the covalent LbL assembly process and the materials that can be used are summarized graphically in Scheme 1.

For applications that require functional robust thin films or nanocomposites, covalent LbL assembly has potential advantages over traditional non-covalent LbL assembly methods. First, covalent bonding affords high stability to the product thin film

assembly allowing it to withstand harsh conditions such as extreme pH or extreme ionic strength.

Scheme 1. General features of the covalent LbL assembly process and the materials that can be used: (a) small molecules and a polymer; (b) polymers or copolymers; (c) a polymer and a nanoparticle; or (d) nanoparticles.

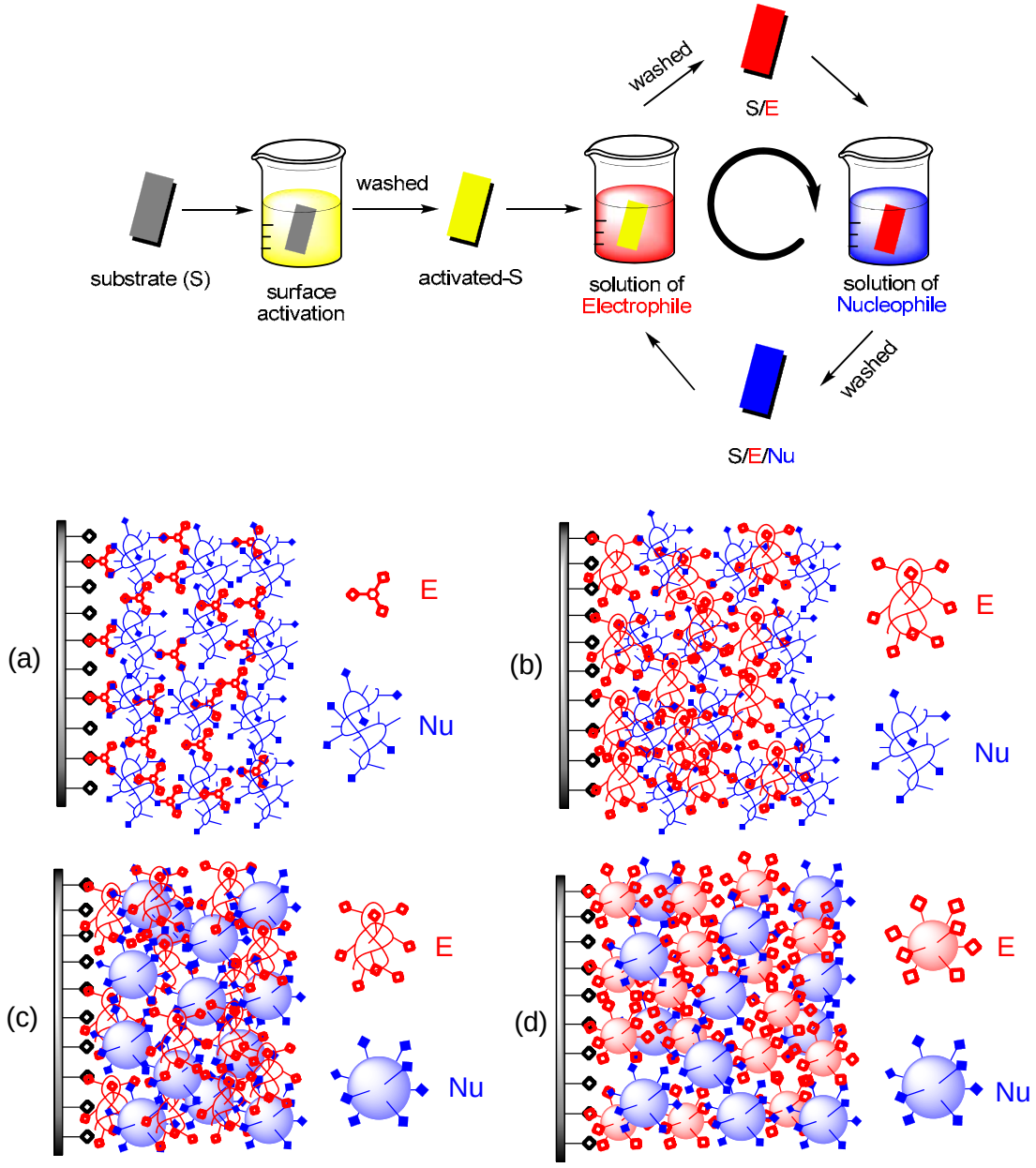

Second, *in-situ* covalent bond formation avoids post-assembly cross-linking which may change the properties of a multilayer grafts. Third, given the wide variety of functional polymers, many different sorts of reactions can be used to form a multilayer graft. Fourth, the chemistry can be carried out in either aqueous or organic solutions depending on the type of reactions that are used to couple the bilayers to one another. This can be advantageous if it is desirable to incorporate materials which do not dissolve or which cannot be used in the aqueous solutions normally used in ionic or hydrogen bond based LbL assembly procedures. Fifth, covalent bond formation is usually a spontaneous energetically favorable process so a newly deposited layer cannot readily disassemble from the previous layer. This makes it possible to incorporate small bifunctional molecules during the LbL process. Ionic or hydrogen bonding LbL assembly typically requires multiple interactions between polymers or nanoparticles disfavoring incorporation of a monofunctional anion or cation. This feature of covalent assembly also makes it possible to incorporate copolymers with a higher percentage of other functionality into the multilayer grafts. Finally, a covalent LbL assembly process leaves behind excess reactive groups inside the multilayer matrix that can further react with other molecules to tailor the product functional interfaces for other functions. In this highlight, we will describe the ideas involved in covalent LbL assembly. We will discuss the sorts of chemistry used in the covalent self-assembly processes and briefly note the applications of some of the functional thin films or nanocomposites made by these covalent LbL assembly methods.

Covalent LbL Assembly Based on Carbonyl Chemistry

The earliest example of chemistry used for covalent LbL assembly via stable covalent bond was chemistry that involved condensation reactions of nucleophiles and carbonyl derivatives. Such nucleophilic additions to carbonyl groups include reactions like amide, ester, urea, urethane, oxime, and imine bond formation using electrophilic polyfunctional or polymeric carbonyl derivatives like those shown below. Of these reactions, amide bond formation between an amine and an activated carboxylic acid is the most commonly used process for covalent self-assembly. This partly reflects the desirable stability of amide bonds but also reflects the ready availability of the reagents.

Bergbreiter and Crooks' groups described early examples of covalent LbL assembly using the commercially available poly(maleic anhydride)-*c*-poly(methylvinyl ether) copolymer (Gantrez, **1** (R = -CH_3)) as an electrophile in reaction of nucleophilic amine- or hydroxyl-terminated generation five (G5) poly(amidoamine) (**2** or **3)** or G5 poly(iminopropane-1,3-diyl) dendrimers.[12-14] LbL covalent assembly of these polyvalent anhydride polymers and polyvalent nucleophilic dendrimers on Au, Al, Si, or polymer substrates formed grafts like those in Scheme 1c that were 15-nm thick per bilayer.

Such LbL covalent assemblies impart new chemistry to their substrates. For example, these ultrathin multilayers on Au had pH-switchable permselectivity. Cyclic voltammetry studies showed that at pH 11, the graft's net negative charge due to CO_2Na groups excluded electroactive $Fe(CN)_6^{3-}$ anions but $Ru(NH_3)_6^{3+}$ cations had normal redox chemistry. At pH 4, the residual amine groups in the graft were positively charged and only the electroactive anions underwent redox chemistry.

Other work showed that the amic acid groups formed during the covalent reaction of amines and anhydrides in this covalent self-assembly could be imidized with mild heating to form impermeable monolithic films. When these imidized nanocomposites were formed on Al and a hydrophobic octadecyl layer was attached as a final step, the underlying Al was passivated against corrosion in $NaOH_{aq}$ or from pitting in neutral $NaCl_{aq}$ by these ultrathin covalently assembled coatings. Similar passivation of Al was also seen in work by Bruening's group when they formed films using Gantrez (**1**) and poly(allylamine) (**4**).[15] This work showed that the impedances of Al electrodes coated with a 27-nm, 3-bilayer Gantrez/poly(allylamine) film increased 10-fold after imidization of the intermediate covalent assembly at 150 ºC.

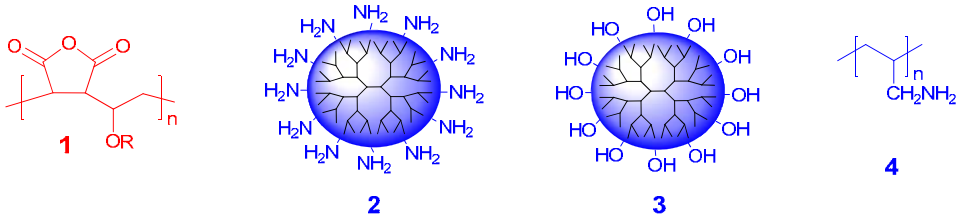

Blanchard and coworkers examined a variety of strategies for covalent multilayer growth including amide, ester, ether, urea, and urethane chemistry. They first demonstrated a polymer multilayer assembly by ester bond formation can act as an efficient sorbent for selected metal ions.[16] By alternative deposition of a 4-hydroxyphenyl-maleimide-vinyl ether (MVE) copolymer **5** and adipoyl chloride (**6**), an ester bond was formed between the hydroxyl group of copolymer **5** and the acid chloride. The growth of the multilayer assembly proceeded in a linear fashion as shown in Scheme 1a with growth proceeding at a rate of 1.6-nm/bilayer. Once the assembly was complete, the isopropylphosphonates were deprotected using bromotrimethylsilane. The

uptake of Zr^{4+} by the phosphonate groups inside the multilayers so formed was shown to be very fast (~20 sec) in a 5 mM of ethanolic $ZrOCl_2$ solution. The PO_3^{2-}/Zr^{4+} complexation inside the multilayers was predominantly 1:1, based on the 1:1 P/Zr ratio seen in an XPS analysis of the product. In their later work,[17,18] they synthesized a variety of MVE copolymers with different reactive side chains including amine (**7**), acid chloride (**8**) and hydroxyl groups (**9**). By coupling with a variety of bifunctional molecules including diacid chloride **6**, diepoxide **10**, diisocyanates **11**, diol **12** and diamine **13** in a LbL fashion, a combination of covalent LbL assembly with amide (**6**+**7**, **7**+**8**, **8**+**13**), ester (**6**+**9**, **8**+**9**, **8**+**12**), ether (**9**+**10**), urea (**7**+**11**) and urethane (**9**+**11**) interlayer bondings can be realized. The growth of the multilayer assembly of all cases proceeded in a linear fashion as shown in Scheme 1a. They further found that the addition of concentrated acid during polymer layer deposition for amide, ester, urea and urethane formation resulted in a 2- to 4-fold increase of the polymer loading density.[19] These findings suggested the mechanism is acid catalysis (HCl) and/or dehydration (H_2SO_4).

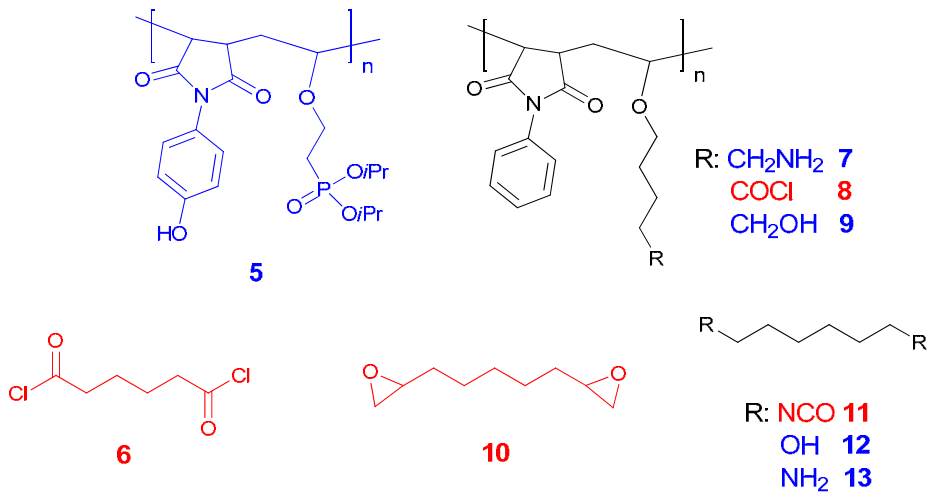

Akashi and coworkers also used covalent LbL assembly to prepare thermoresponsive ultrathin hydrogels. Systematic studies are carried out to discover the optimum ratio between thermoresponsive and reactive segments for multilayer growth. In their early work,[20] they used poly(vinylamine)-*c*-poly(*N*-vinylisobutyramide) (PVAm-*c*-PNVIBA, **14**) and poly(acrylic acid) (PAA) to assemble ultrathin hydrogels on a gold surface. The carboxylic acid group of PAA was activated by 1-ethyl-3-(3-(dimethylamino)propyl)-carbodiimide hydrochloride (EDC). The activated ester reacted with the amine group of PVAm-*c*-PNVIBA to form the amide bond. The growth of the multilayer assembly reached the maximum with 39 mol % of vinylamine units. The surface of the ultrathin hydrogels so formed became more hydrophobic above 30-40 ^{o}C, based on contact angle measurements. This phenomenon suggested that the phase transition was derived from the PNVIBA unit. In later work,[21] ultrathin hydrogels were fabricated using covalent LbL assembly using EDC activated PAA and poly(vinylamine)-*c*-poly(*N*-vinylformamide) (**15**) with at least 28 mol % of vinylamine units. Further work[22] also showed that the same chemistry could be used to fabricate thermoresponsive ultrathin hydrogels using poly(vinylamine hydrochloride) and poly(acrylic acid)-*c*-poly(*N*-isopropyl-acrylamide) (PAA-*c*-PNIPAM, **16**) with as low as 5 mol % of acrylic acid units. Permeabilities of ions through the hydrogel could be switched on/off by changing the temperature below or above the lower critical solution temperature (LCST) of PNIPAM.

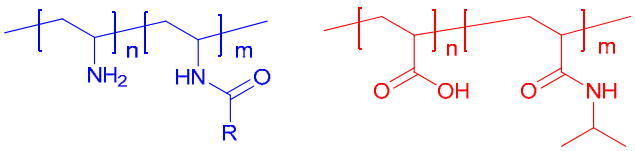

R: $CH(CH_3)_2$ **14**
H **15**

16

Srinivasan and coworkers studied the step-by-step covalent assembly of pyromellitic dianhydride (PMDA) and diaminodiphenyl ether on aminated silicon and quartz in supercritical carbon dioxide ($scCO_2$) and in dimethyl acetamide (DMAc), followed by thermal or chemical imidation.[23] The study showed that $scCO_2$, an environmentally friendly solvent, could be used to form mechanically robust and thermally stable ultrathin films. In their later work, they fabricated ultrathin polyimide films using covalent LbL assembly using hydroxyl polyimide (HPI, **17**) and terephthaloyl chloride (**18**) to form ester bonds between HPI layers.[24] The growth of the multilayer assembly proceeded in a linear fashion. Polymer substrates formed grafts like those in Scheme 1a that were 3-nm thick per bilayer. The resulting film showed good thermal stability at 300 ^{o}C under nitrogen for 1 h. UV-vis absorption spectrum taken after the thermal treatment was virtually indistinguishable from that before thermal treatment. The resulting LbL film also showed more mechanical resistant against indentation than the spin-coated HPI film of similar thickness due to the covalent nature of imide and ester bonds. Similar chemistry using HPI (**17**) and poly(thiophene-3-acetyl chloride) (**19**) to fabricate ultrathin composite films was also carried out.[25] The resulting films showed good thermal stability and moderate conductivity. In later work, the step-by-step growth of bifunctional reagents was extended to develop a covalent LbL

assembly process that coupled PMDA and a polyvalent G2 poly(amidoamine) dendrimer (**2**) on amine- and anhydride-derivatized silicon surfaces in $scCO_2$.[26] Copper acetylacetonate was then introduced into the amine groups inside the dendrimer matrix by metal chelation. Cu nanoparticles were formed after the copper salt was reduced by decomposing the acetylacetonate complex at 250 °C for 2 h in the presence of H_2 and N_2. Cu nanoparticle with an average diameter of 7- nm could be embedded inside the matrix of dendrimers.[27] A denser dispersion of nanoparticle was observed if the multilayers were assembled in $scCO_2$ rather than in THF. The assembled film in $scCO_2$ also showed greater stability toward polar solvent.

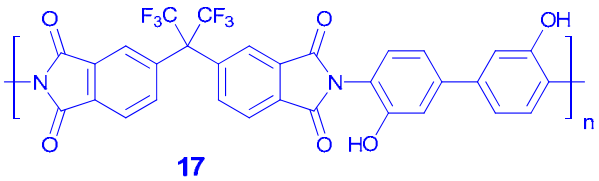

17

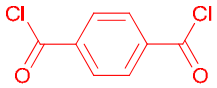

18

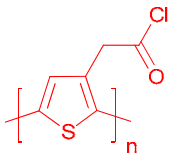

19

Covalent LbL assembly like ionic LbL assembly processes works with objects of varying shape. Li's work leading to fluorescent nanotubes of PEI (**20**) and 3,4,9,10-perylenetetracarboxylic dianhydride (**21**) prepared by covalent LbL assembly of this polyvalent nucleophilic polymer and dianhydride inside the pores of alumina membranes illustrates this.[28] After 10 covalent bilayers, the aluminum membrane was dissolved to liberate the 350-nm diameter nanotube products. Thinner 50-nm nanotubes were formed after three bilayer depositions. The flexible covalently assembled nanotubes so formed retain their fluorescent properties for up to 10 months.

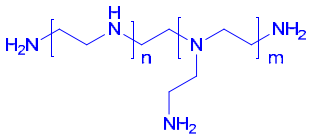

20

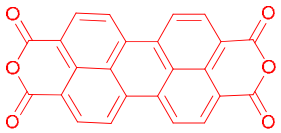

21

Wang and coworkers studied the covalent LbL assembly using amine and pentafluorophenyl ester functionalized poly(p-phenylenevinylene) (PPV) (**22** and **23**). This covalent LbL method was further applied to generate conjugated polymer micropatterns onto microstamped self-assembled monolayer.[29] The growth of the multilayer assembly proceeded in a complex behavior, which suggested a complicate adsorption-desorption mechanism. This phenomenon suggested that the formation of the multilayers was not solely governed by covalent bonds between amines and active esters, but hydrogen bond interactions between amines and carbonyl groups were also involved. Desorption of hydrogen-bonded parts took place to some extent with subsequent layer deposition. No significant changes were observed in both film thickness and UV/vis spectra after sonication of the assembled films in THF for several hours. On the contrary, the hydrogen-bonding-based PPV multilayer films were found to dissociate quickly under the same conditions in their parallel experiments.[30] The same chemistry could be applied to fabricate multilayer thin films using polymer **22** and pentafluorophenyl ester functionalized CdSe nanoparticle **24**.[31] The growth of the multilayer assembly proceeded in a linear fashion as shown in Scheme 1c with growth proceeding at a rate of 5.24-nm/bilayer. Preliminary work in which a 10-bilayer hybrid film containing CdSe nanoparticles was illuminated by white light suggested possible applications of this sort of covalent LbL assembly as an organic photovoltaic device. This early example of a

potential application of these covalent LbL nanocomposites had an optical-to-electrical power conversion efficiency of 0.71 % when illuminated by white light having an intensity of 10 mW/ cm^2.

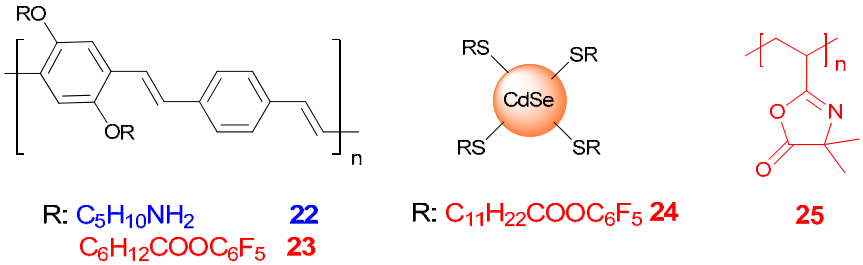

R: $C_5H_{10}NH_2$ **22**
$C_6H_{12}COOC_6F_5$ **23**

R: $C_{11}H_{22}COOC_6F_5$ **24**

25

Lynn and coworkers showed that nucleophilic addition of the amines of PEI (**20**) to the carbonyl group of poly(2-vinyl-4,4-dimethylazlactone) (**25**) provided a stepwise LbL "click" route to covalent multilayer assemblies coupled to each other via a diamide of 2,2-dimethylglycine.[32] These grafts thickness increased linearly with the number of bilayers at the rate of 6 nm per bilayer. The products retain unreactive azlactone groups and were quantitatively and rapidly consumed throughout the bulk of the thin film after the grafting process was complete by treatment with propylamine. Such chemistry suggests that these azlactone-containing LbL grafts will be amenable to post-fabrication to other blocking, patterning, or passivation for chemistry. An example of such post-fabrication chemistry was shown in a fluorescence patterning experiment that used a hydrazide-functionalized coumarin or a tetramethylrhodamine cadavarine dye on a PDMS stamp to create <100 μm fluorescent grid.

Condensation of an aldehyde-containing polymer (**26** and **28**) with an alkoxyamine-containing polymer (**27** and **29**) to form oximes has been used by Yu's group in covalent LbL assembly of conjugated polymers onto glass and gold substrates.[33] This work

showed that the functional group in the electrophilic polymer had to be an aldehyde – polymers with less reactive ketone groups are not reactive enough to 'click' to successfully form covalent LbL assemblies.[34] Later work by this group showed that this covalent assembly process produced multilayer films on gold substrates that were highly insulating and defect free with finely tunable capacitance based on the number of deposition layers.[35] Similar covalent LbL chemistry using imines was also described by Gao's group. In this case, the assembly process used glutaraldehyde and poly(allylamine hydrochloride) (PAH) and was carried out on $MnCO_3$ particle templates.[36] In this example, the template core was dissolved to yield chemically stable microcapsules – a result that suggested cross-linking of the imine-containing multilayer had occurred.

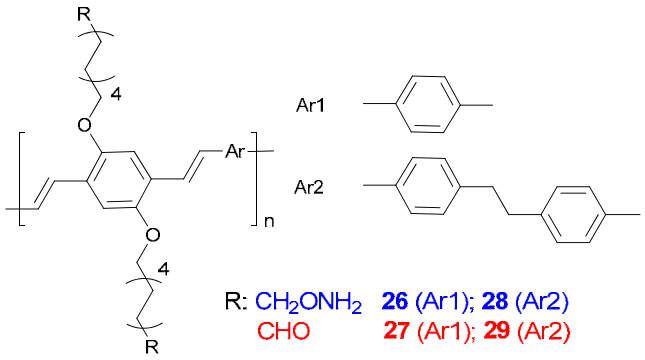

Finally, ester formation involving an inorganic acid (boronic acid) and poly(vinyl alcohol) (PVA) has been used in covalent LbL assembly multilayer films by the Yang's group.[37] In this case, a thiol containing a boronic acid group was assembled on gold nanoparticles (**30**). The pendant boronic acids rapidly formed cyclic boronate esters with PVA in an LbL process to form multilayer grafts containing Au nanoparticles. A linear increase of the absorbance from the surface plasmon band of gold nanoparticle

with the number of bilayers indicates a stepwise and uniform assembly. Unreacted boronic acid groups in the product grafted film in this case served as a handle to immobilize a glycosylated-protein - horseradish peroxidase - and this enzyme was subsequently shown to have been immobilized with good retention of its catalytic activity.

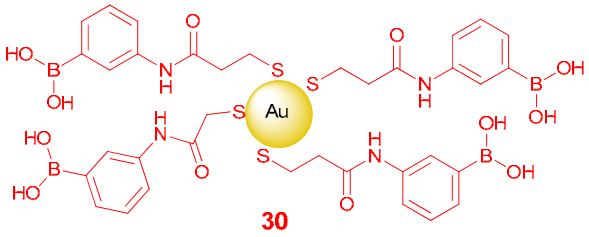

30

Covalent LbL Assembly Based on Aromatic Substitution Chemistry

Other covalent bond forming reactions are also suitable for covalent LbL assembly. For example, electrophilic aromatic substitution by a polymeric aryl diazonium salt (**31**) on an electron-rich polymer formed from formaldehyde and *m*-cresol (**32**) has been shown by several groups to be suitable as a way to assemble way to assemble grafts on substrates like quartz or sulfonated polystyrene latex.[38,39] This chemistry not only served as a way to covalently self assemble a multilayer graft that was stable to solvents like THF and DMF, it simultaneously introduced azo dye groups at each coupling event. That enabled Cao's group to follow the linear growth of the assembly process by UV-visible spectroscopy.

The Bergbreiter and Simanek groups reported using nucleophilic aromatic substitution of PEI (**20**) and cyanuric chloride (**33**) as a route to LbL covalent grafts on silica.[40] Water, instead of organic solvents, can be used as a solvent for the PEI grafting

in this case. The step-by-step process shows a trend of linear growth based on acid-base titration of the free amine groups of PEI-grafts and a 6-bilayer graft had a capacity of 1 mequiv of base/g.

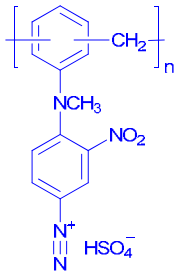

31

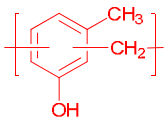

32

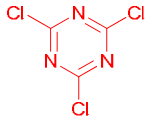

33

Covalent LbL Assembly Based on Cu-Catalyzed Azide-Alkyne [3+2] Cycloadditions

The recent development of Cu(I) catalyzed azide-alkyne [3+2] cycloadditions to form 1,2,3-triazoles have attracted interest in many areas of chemistry including this area of covalent self assembly. Caruso's group was the first to use such Cu-catalyzed [3+2] cycloadditions in covalent LbL assembly on quartz, silicon, or gold by alternately dipping the substrates into solutions of PAA copolymerized with either azide (**34**) or alkyne (**35**) functionality in the presence of Cu(I) and sodium ascorbate.[41] A subsequent study used this same chemistry was used to fabricate responsive polymer capsules whose size was pH dependent.[42] In that example, the multilayers were readily functionalized through a post-assembly reaction with a "clickable" rhodamine dye, showing again how covalently assembled LbL grafts can serve as a versatile platform for further functionalization.

Hawker also used this [3+2] cycloaddition chemistry for the covalent LbL assembly of dendritic thin films on silicon wafers.[43] Azide and alkyne-terminated dendrimers (**36** and **37**) derived from hydroxyl terminated 2,2-bis(methylol)propionic acid dendrimers from the 2nd to the 5th generation were used for the construction of the thin films. Film thickness growth was linear but depended on the dendrimer size, varying from 0.46 to 1.22 nm/triazole layer with 2nd to 5th generation dendrimers. Linear polymer analogs gave layers that were four times thicker/layer but rougher.

Bergbreiter also used azide-alkyne [3+2] cycloadditions to fabricate PNIPAM grafts on PE substrates.[44] Water-soluble PNIPAM copolymers containing pendant azide or alkyne groups (**38** and **39**) that can be thermally separated from aqueous solutions were used to alternately to assemble a multilayer graft. As was true in Caruso's work, free azide groups inside the grafts can be readily labeled with alkyne-terminated fluorescent reagent.

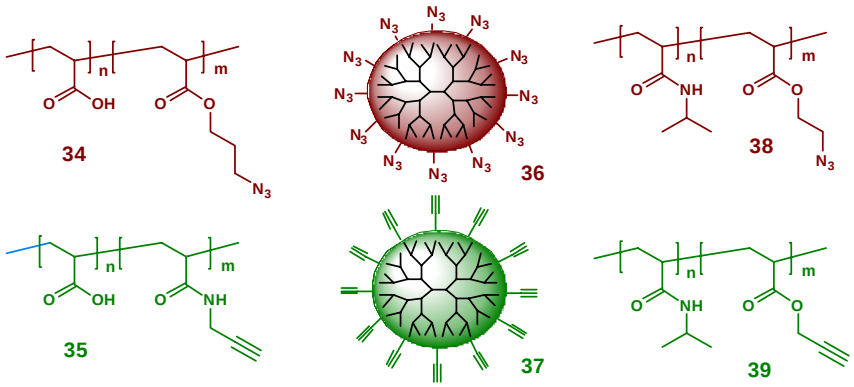

Conclusions

LbL assembly based on ionic interactions has proven to be a versatile route for surface modification and construction of ultrathin nanocomposites for the last two decades. Covalent LbL assembly based on facile ‘click’ covalent bond formation is an effective alternative, especially for the applications where a more robust ultrathin films or nanocomposites is desired. The scope of the chemistry that can be used and the potential for tailoring the product multilayer grafts after grafting is complete makes covalent LbL assembly even more attractive for applications in emerging areas such as nanotechnology and biomedicine.

CHAPTER II

SURFACE MODIFICATION OF POLYETHYLENE USING COVALENT LAYER-BY-LAYER SELF-ASSEMBLY WITH POLYETHYLENIMINE AND GANTREZ*

Introduction

Polymer surfaces are the phase boundaries between the bulk polymer and the environment. While the surface of a polymer usually is only a minor portion of the material, the performance of polymeric materials relies largely upon the properties of the surfaces in many applications. Most polymeric materials, especially hydrocarbon polymers, have a hydrophobic, chemically inert surface. Such untreated non-polar polymer surfaces often have problems in adhesion, coating, painting, etc. when they are exposed to a second more polar material. To solve these problems, a lot of research has been devoted to the surface modifications of such hydrophobic polymeric materials.[45]

Plasma treatment is one of the techniques used extensively to modify polymer surfaces. Plasma modification of polymer surfaces can be rapid and clean. However, only a few types of functional groups can be generated, the surface concentrations are relatively low, and such surfaces easily reconstruct. To achieve useful properties, other more long-lasting modifications are usually needed.[46-49]

Graft polymerization initiated on surfaces is a second approach to functionalize polymer surfaces. By generating initiators on surfaces, monomers in solution or vapor

*Reproduced in part with permission from Kim, Y.-S.; Liao, K.-S.; Jan, C. J.; Bergbreiter, D. E.; Grunlan, J. C. *Chem. Mater.* **2006**, *18*, 2997-3004.

phase can bind to the surface and in turn polymerize from the surfaces to form grafts. Almost any kind of graft can be attached to a surface so long as the corresponding monomer is suitable for that specific polymerization (radical, anionic, cationic, ATRP, etc.) However, the success of polymerization highly depends on the experimental conditions, which need careful control.[50,51]

A fourth more recent procedure for surface modification is layer-by-layer (LbL) self-assembly, or electrostatic (ionic) self-assembly.[2-4] This technique is based on alternating physisorption of oppositely charged polyelectrolytes. Such chemistry is a simple alternative to the grafting chemistry described above. LbL self-assembly features monomolecular layer deposition for each polyelectrolyte, precise control over the thickness, and can form defined three-dimensional structures. However, the substrates have to be polyelectrolytes. Second, the physisorption does not involve covalent bonding, and desorption of the oppositely charged layers in electrostatic self-assembly can occur if another strong electrolyte is present. Third, further modification of the surfaces is problematic.

Covalent LbL self-assembly, however, can be an alternative route to modify a surface in a stepwise covalent manner. In this chemistry, neutral or charged materials can be used in a variety of solvents. What is required is that a nucleophilic polymer reacts with an electrophilic polymer to form a covalent bond. While the size of a polymeric reagent may mean that only a small number of possible covalent bonds could form, this is not a problem. Indeed, such incomplete reactions leave excess functional

groups that can be used as nucleophiles or electrophiles in later assembly stages or in other subsequent chemistry.

In previous studies by our group,[12-14] reactions of the commercially available poly(methyl vinyl ether-*alt*-maleic anhydride) (Gantrez) with either an amine- or hydroxyl-terminated G5 poly(amidoamine) dendrimer, or a G5 poly(iminopropane-1,3-diyl) dendrimer were carried out. The ultrathin multilayers that formed had pH-switchable permselectivity toward electroactive anionic $Fe(CN)_6^{3-}$ and cationic $Ru(NH_3)_6^{3+}$ metal complexes as was shown in cyclic voltammetric studies. At high pH, films with these sorts of covalent LbL grafts have net negative charges that exclude anions but allow electroactive cations like $Ru(NH_3)_6^{3+}$ to diffuse to the electrode; at low pH, these covalent LbL grafts are positively charged and cations are excluded from the underlying electrode but electroactive anion like $Fe(CN)_6^{3-}$ can diffuse to the electrode.

When amine-terminated dendrimers were used in assembly of these covalent grafts, the amic acid groups formed during the bilayer assembly could be further imidized in subsequent thermal processing to form highly impermeable monolithic films on Au, Al or Si substrates. When a hydrophobic octadecyl layer was attached as a final step on these composites on Al, Al was passivated against corrosion in alkaline solution or from pitting in neutral chloride-containing solution by ultrathin covalent LbL grafts. Although these studies were promising, the potential of using this chemistry in real applications is problematic because the reagents are expensive, the reaction times are long and the procedure is significantly more difficult that ionic LbL assembly.

In my work, I explored the use of commercially available polyethylenimine (PEI), a simple analog of amine-terminated poly(amidoamine) dendrimer, and Gantrez to assemble covalent LbL grafts on oxidized PE substrates. Characterizations of the resulting substrates were carried out using ATR-IR spectrometry, titrimetric analyses, fluorescent analyses of assembled films with dansyl label, and thermogravimetric analyses (TGA) of assemblies with entrapped carbon black particles. The surface element composition of the product films was also analyzed by X-ray photoelectron spectroscopy (XPS).

In subsequent studies, polyethylenimine (PEI) was also grafted to the surface of irregularly shaped polyethylene (PE) particles. This work was carried out in an effort to facilitate formation of carbon black (CB) nanocomposite thin films. The details of this work will be presented in Chapter III.

Results and Discussion

Preparation of PEI/Gantrez Grafts on Oxidized PE Surfaces Using Covalent LbL Self-Assembly. To create a surface amenable to LbL assembly, PE substrates were modified according to the procedures shown in Scheme 2. First, PE was oxidized by chromic acid. The carboxylic acid groups formed in that oxidation process were then activated by ethyl chloroformate to form electrophilic mixed anhydride groups. A nucleophilic polymer, PEI, was then allowed to react with the anhydrides to form amide bonds. In the resulting surface, some amine groups of the PEI formed covalent amide bonds and some amine groups of the PEI formed ammonium carboxylates. To increase the nucleophilicity of this initial product, the surface was treated with an excess of triethylamine (Et_3N) in MeOH. This produced an amine-rich surface that was in turn allowed to react with an electrophilic polymer, poly(methyl vinyl ether-*alt*-maleic anhydride) (Gantrez). This step formed a new graft layer covalently by formation of amic acid bonds from the anhydride groups in Gantrez. As discussed above, this step produced an anhydride-rich surface because most of the excess anhydride groups did not react. These steps were repeated several times to yield a hyperbranched hydrophilic surface covered by a network of the PEI and Gantrez polymers with a high loading of amine, amic acid, and carboxylic acid functional groups. Repetition of these electrophilic and nucleophilic steps using 6 PEI treatments and 5 Gantrez treatments produced a grafted product described below as PEI-6/Gantrez-5. While this process has multiple steps, it is experimentally a rather simple process that is much like ionic LbL

deposition (Scheme 2). For example, the entire surface modification procedure required to prepare a PE/PEI-6/Gantrez-5 graft took approximately 12 h.

Scheme 2. The experimental procedure for covalent LbL assembly of PEI/Gantrez on oxidized PE powders.

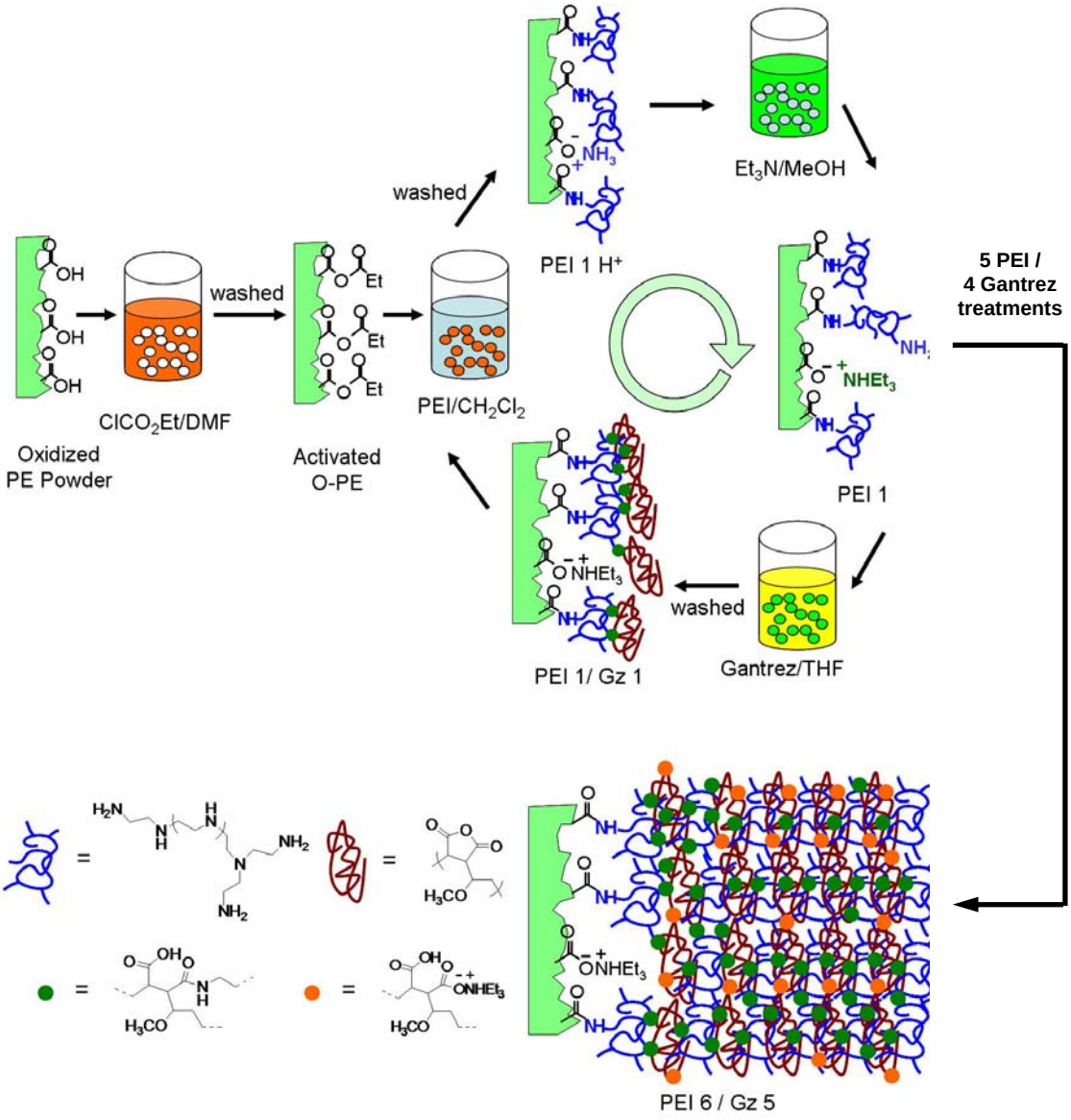

The Et_3N treatment between PEI and Gantrez stage was shown to be crucial for successful assembly of these covalent LbL grafts. This is because amine salts are formed when the PEI reacts with the Gantrez on the surface. Such protonation limits the ability of the PEI graft to react with the Gantrez in next stage. With triethylamine treatment, these salts are neutralized and the PEI is more reactive to Gantrez molecules in the next stage. As a result, the growth of each polymer layer increases prominently.

This covalent step-by-step assembly process is schematically shown in Scheme 2. This scheme is not necessarily fully correct and oversimplifies this LbL process. We suspect that, for example, amine groups from the PEI-1 stage can and do react with Gantrez polymer introduced when forming the PEI-3/Gantrez-3 stage. The surface grafts are more like homogeneous composite rather than the distinct layers of PEI/Gantrez shown in the scheme. Similar considerations also apply to ionic LbL chemistry.[2]

Characterization of PEI/Gantrez Grafts on Oxidized PE Substrates. Analysis of the progress of a synthetic process on a surface is particular challenging. The amounts of surface graft, even of a high density surface graft, correspond to trace contamination in an ordinary setting. For example, a 50-nm graft of poly(acrylic acid) (PAA) on a 1 cm^2 PE film incorporates 4 μg of PAA, an amount of material that can be difficult to analyze. To address the analytical challenges associated with the syntheses above, a multipronged approach using multiple physical and spectroscopic analyses of the same surface was used to verify the progress and nature of the grafting.

ATR-IR of PEI/Gantrez - PE Films. ATR-IR spectroscopy was a primary spectroscopic tool used to follow the progress of the grafting chemistry as shown in

Figure 1. The oxidized PE had a relatively small peak due to carboxylic acid carbonyl groups at 1710 cm^{-1}. After activation and PEI treatment, this acid carbonyl peak disappeared and an amide peak (1650 cm^{-1}) appeared. The Gantrez stages showed anhydride peaks at 1790 and 1730 cm^{-1}. A C-O peak ascribed to the methoxyl group around 1100 cm^{-1} was also present. The reaction of PEI and Gantrez to form a mixture of amic acids and ammonium carboxylate groups was confirmed by the disappearance of anhydride peaks and the appearance of amide and carboxylate peaks. Qualitatively, the growth of the grafting layers could be estimated by comparing the integral of the amide and carboxylate region (1650 and 1560 cm^{-1}) with that of the C-H region from PE itself (2910 and 2850 cm^{-1}). The final PEI-6 had a ratio of about 0.7, whereas the ratio was less than 0.05 with PEI-1.

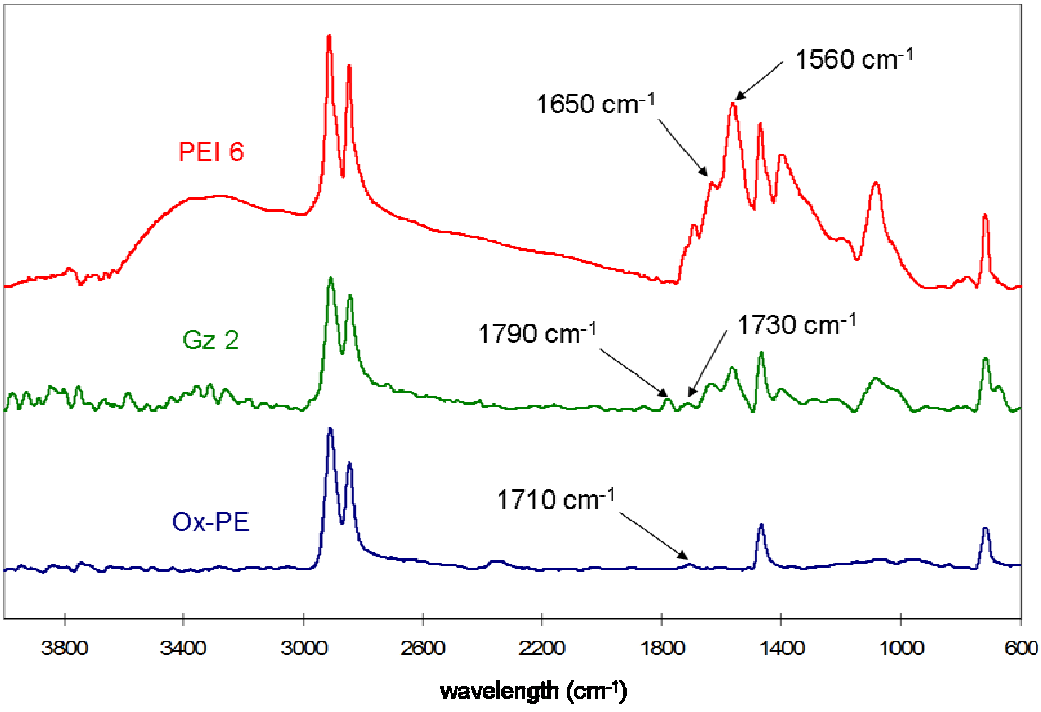

Figure 1. ATR-IR spectra of oxidized PE and PEI/Gantrez PE derivatives.

Titrimetric Analyses of PEI/Gantrez - PE Powders. The PEI/Gantrez covalent assembly process was also monitored by acid-base titration. The results, shown in Figure 2, revealed a linear growth of titratable groups. This chemistry included an extra step to get a high loading of amines in the product graft. Specifically, we found that using ethylenediamine as a crosslinker in a Gantrez pretreatment step increases the grafting of the anhydride-containing Gantrez. Presumably, this pretreatment process works by increasing the molecular weight of Gantrez molecules and agglomerating the Gantrez polymer into a more globular shape. My studies showed that the surface loading of each bilayer increased proportionally to the ethylenediamine added to the Gantrez solution. After six covalent stages of grafting using a PEI solution and an Gantrez solution prepared by mixing Gantrez with 0, 0.4, and 1.6 wt % ethylenediamine, the surface loading of the last PEI-6 stage reached 0.11, 0.27, and 0.89 mmol of basic groups per gram of PE particle, respectively.

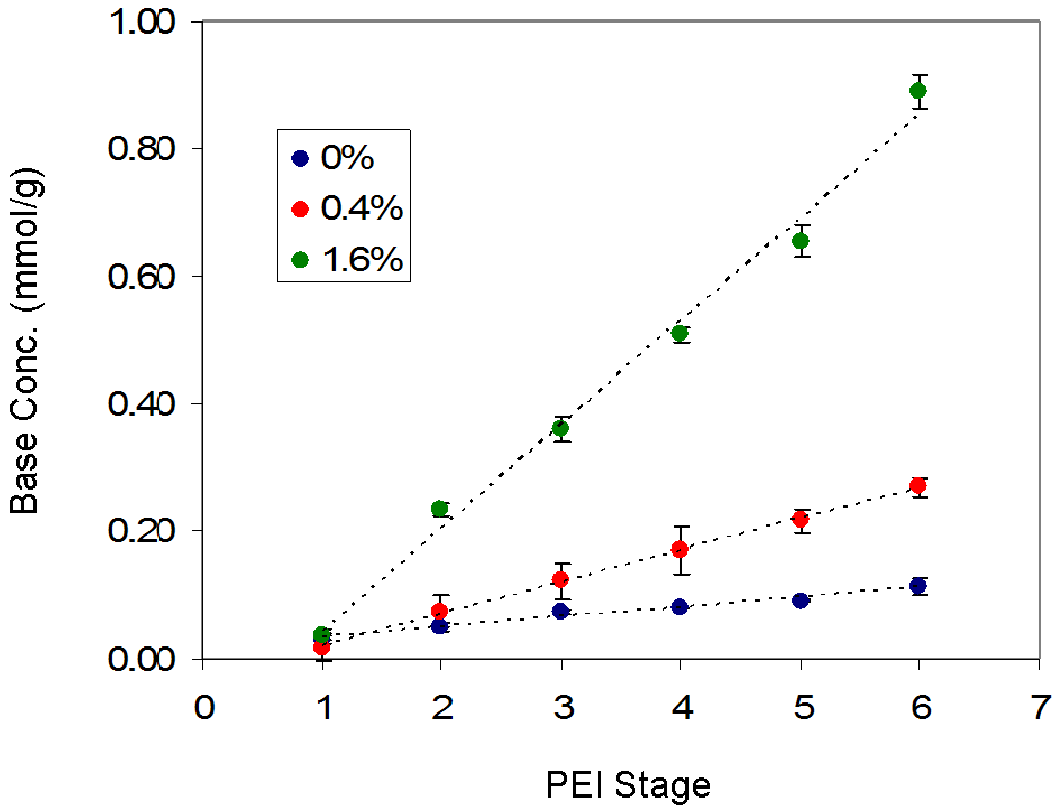

Figure 2. Titrimetric results of PEI/Gantrez PE powders with 0, 0.4, and 1.6 wt % of ethylenediamine added to the Gantrez solution as crosslinker, respectively (based on three individual titrations for each data point).

Ionic LbL assemblies are not always stable to strong acid or strong base. In order to test the stability of the covalent PEI/Gantrez grafts to strong acidic or strong basic condition, the recovered particles were subjected to re-titration after the first titration where strong acid (0.01 M HCl) was used. The grafted particles were collected from the previous titration experiment and treated with excess triethylamine to recover the basic groups. After washing away the triethylamine with large amount of MeOH until the pH

of the eluent became neutral, the grafted particles were dried under vacuum. The resulting grafted particles were than titrated again by the same procedure described in the experimental section. The surface loading of amines did not change significantly even the grafted particles were re-titrated for three times. This shows that the multilayers assembled covalently are stable under strong acid or strong base and the loading of basic surface groups as measured by titration remains constant. It also implies that the surface groups (amines and carboxylates) can be further modified with other functionalities.

Fluorescent Analyses of Dansyl-Labeled PEI/Gantrez - PE Films. A third analytical method used to follow this surface synthetic chemistry involved fluorescence labeling. In this case, covalent tagging of fluorophores on the surface was used to monitor surface growth. In this scheme (Scheme 3), a small percentage of fluorophores with reactive amine groups were added to the PEI solution. The small concentration of added fluorophores would presumably not affect the surface growth. However, because of the sensitivity of fluorescence spectroscopy, enough detectable fluorophores would be attached to the surface for later analysis. In this way, a change in fluorescent intensity of the surface could be used as a second assay of the surface growth profile.

Scheme 3. The procedure for monitoring the LbL growth by fluorescent analyses on surface tagging fluorophores.

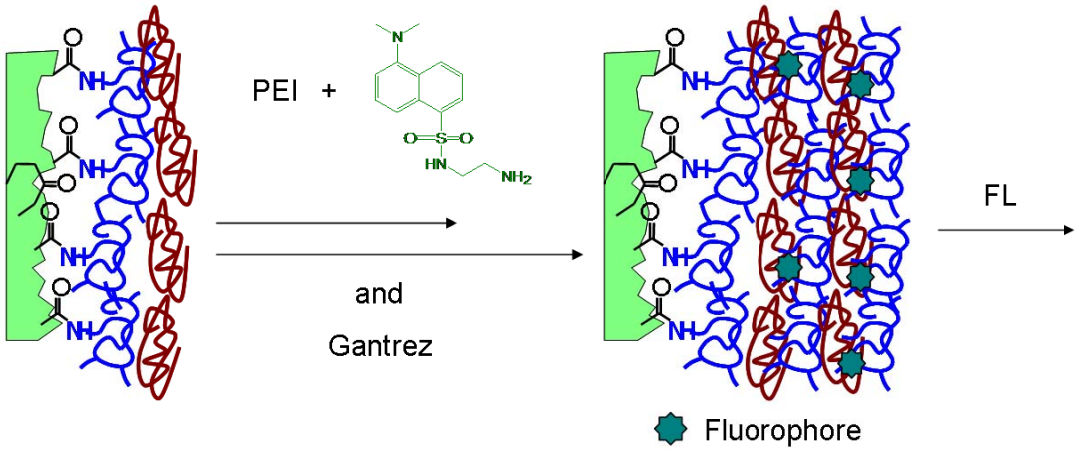

The fluorophore we chose for these labeling studies is *N*-(2-aminoethyl)-5-(*N*,*N*-dimethylamino)naphthalene-1-sulfonamide (dansyl amine, as shown in Scheme 3). There are several reasons we chose dansyl amine for our fluorescent labeling experiments. First, the dansyl group is a well studied fluorophore that is widely used for *N*-terminal derivatization of amino acids and peptides or polymers.[52] It is a sensitive fluorophore with a strong emission around 460 nm (in hexane) when excited with 360 nm light. Second, the fluorescence of dansyl group is sensitive to pH changes. The fluorescence can be quenched if the tertiary amine group is protonated by acid. Such fluorescence quenching has advantages in our work because it means we can probe the accessibility of the functional groups imbedded inside the polymer grafts. Finally, the necessary amine derivative of the dansyl fluorophore can be easily synthesized by reaction of dansyl chloride with ethylenediamine following a reported experimental procedure.[52]

In these fluorescence labeling studies, the covalent LbL assembly procedure was carried out in the same way as in Scheme 2 with the exception that the PEI solution was pre-mixed with dansyl amine (0.2 or 1.0 wt % relative to PEI). Samples of grafted films were saved for each of six grafting stages and the fluorescence of each sample was measured. The fluorescence intensity (λ_{em} 460 nm, λ_{ex} 360 nm) of the resulting (PEI + dansyl amine)/Gantrez PE film versus PEI stage was then plotted in Figure 3. As shown in Figure 3, the fluorescence increased linearly between the stages PEI-2/Gantrez-1 and PEI-6/Gantrez-5 for both dansyl amine concentrations. This relationship revealed the linear growth of the covalent LbL assembly of PEI and Gantrez, a result that was in agreement with the titration results in Figure 2. The PEI-1 stage showed a lower fluorescence compared to the trend line between the PEI-2/Gantrez-1 and PEI-6/Gantrez-5. This is probably a consequence of the limited concentration of activated anhydride group on the oxidized PE surface with which the dansyl amine can react. However, once the Gantrez layer is assembled on the surface, there presumably are more anhydride groups inside the polymer grafts, which are readily available to react with the dansyl amine.

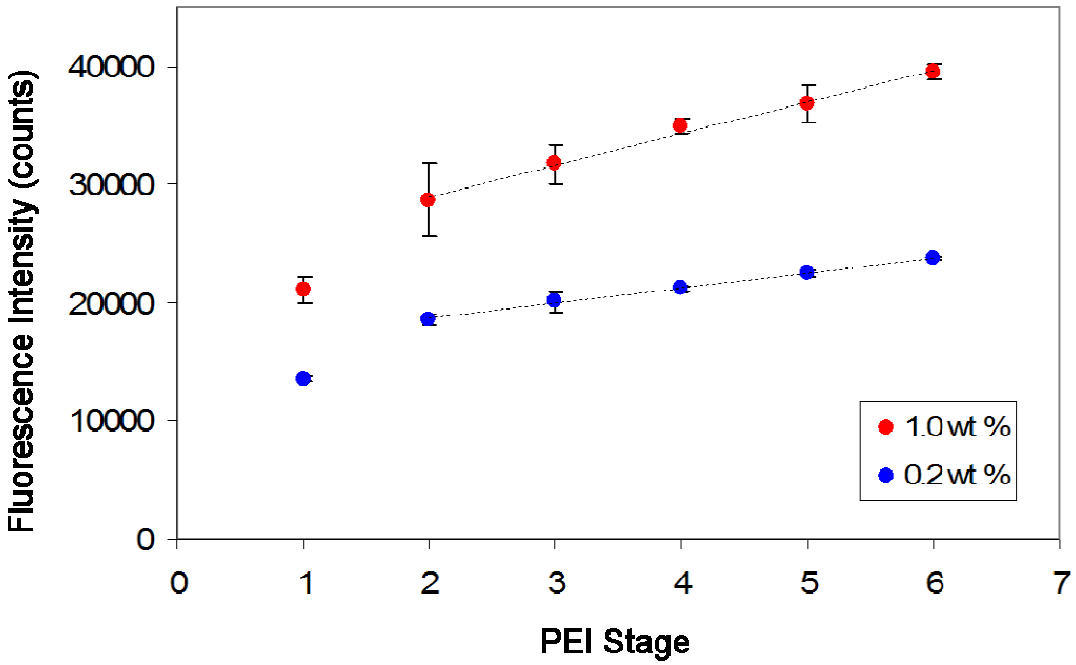

Figure 3. Fluorescence intensity of (PEI + dansyl amine)/Gantrez films in different PEI stages assembled by using PEI solution with 0.2 and 1.0 wt % of dansyl amine relative to PEI, respectively (based on three individual measurements for each data point).

One of the suggested advantages of multilayer covalent assembles is that such covalent multilayers should be more robust under harsh condition because of covalent bonds are more stable to acid and base than ionic bonds where ion exchange can occur. This premise was supported by the studies above that examined the surface by titrimetric analyses. To further establish this premise, the fluorescently labeled PEI/Gantrez grafts assembled by covalent bond formation using a mixture of PEI with 0.2 wt % dansyl amine relative to PEI, and Gantrez in alternating stages were treated with strong acid (1.0 M HCl) or strong base (1.0 M NaOH). These conditions are known to lead to

delamination of ionic LbL grafts. The result is shown in Figure 4. The fluorescence dropped significantly after the acid treatment because protonation of the tertiary amine group on the dansyl group diminished the fluorescence. However, the fluorescence did not completely disappear suggesting that not all the dansyl groups reacted with HCl. Then, on treatment with base, the fluorescence increased to almost the original value due to deprotonation of the tertiary amine salt. This acid/base treatment was repeated two more times without significant changes in the fluorescence intensity of the fluorescently labeled covalent LbL grafts. This further established that the dansyl amine is bonded covalently in these interfaces.

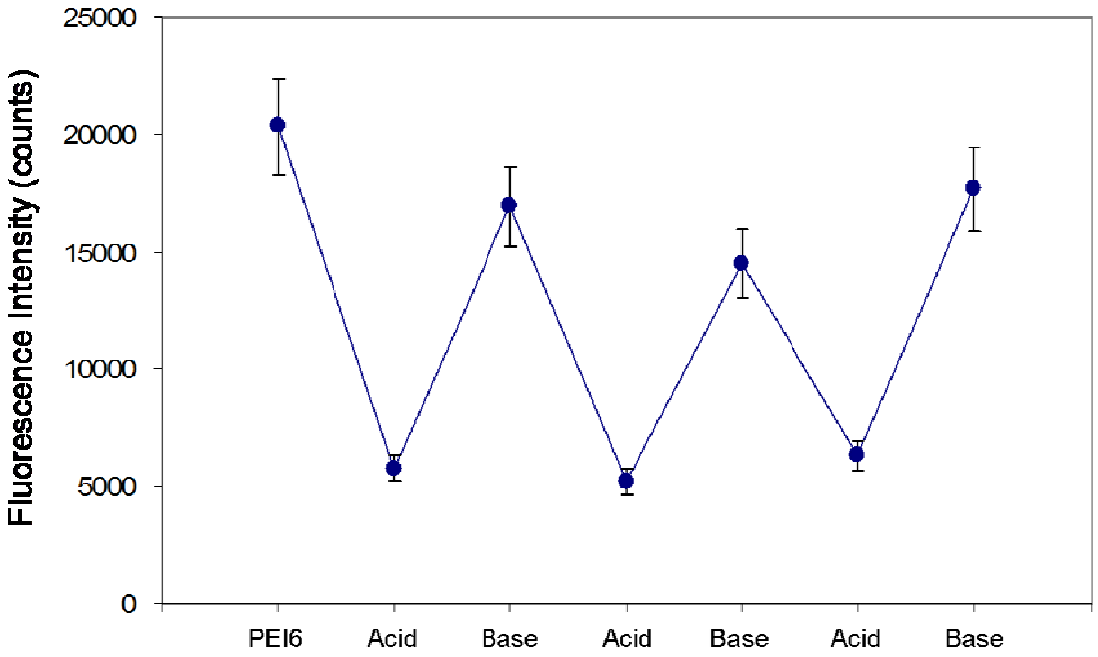

Figure 4. Changes of fluorescence intensity of (PEI + 0.2 wt % dansyl amine)-6/Gantrez-5 films under acid (1.0 M HCl) and basic (1.0 M NaOH) solutions.

Thermogravimetric Analyses of Carbon Black Entrapped PEI/Gantrez - PE Powders. Thermogravimetric analysis (TGA) is a less common tool for analyzing synthetic surface chemistry. However, TGA has been used to analyze the amount of an organic phase on inorganic supports.[40] In this case, we used TGA to monitor formation of PE-carbon black nanocomposite that was formed in conjunction with a covalent LbL grafting process. In these analyses, polyethylene, as well as any organic phase present in the PE-carbon black nanocomposite, is expected to decompose at 500 °C. However, carbon black is stable to up to 1000 °C under a N_2 atmosphere.[53] Thus, gravimetric analysis of the amount of carbon black present in a covalent LbL assembly process at various stages can be used to monitor nanocomposite graft formation. This scheme for monitoring the LbL growth is illustrated in Scheme 4. In this procedure, carbon black nanoparticle is mixed with PEI/CH_2Cl_2 solution. The amine groups of PEI are known to stabilize and disperse carbon black in solution after sonication. Thus, we expected that some carbon black particles would be entrapped in the PEI/Gantrez network during each PEI stage (*cf.* Scheme 2). Presumably the amount of carbon black would be correlated to the amount of PEI. Thus, by analyzing the amount of carbon black in each stage by TGA, a gravimetric growth profile for covalent LbL assembly can be obtained.

Scheme 4. The procedure for monitoring the LbL growth by TGA on carbon black entrapped PEI/Gantrez PE powders.

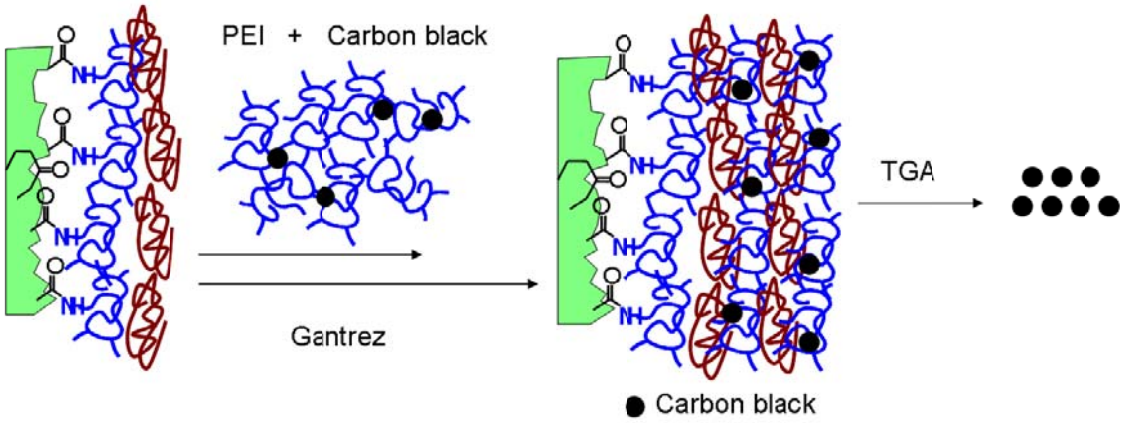

In this gravimetric study of covalent LbL assembly, the synthesis procedure was the same as that used in the fluorescently labeling studies mentioned previously with the exception that the PEI solution was pre-mixed with 5 wt % of carbon black relative to PEI. The grafted PE powder was sonicated under MeOH and washed with large amount of MeOH after each PEI/carbon black treatment stage until no suspended carbon black was visible in the eluent. Then the grafted PE powder was dried under vacuum. The percentage of carbon black entrapped inside the grafts for each stage of the graft was then analyzed by TGA and the results of the carbon black loading versus PEI stage are plotted in Figure 5. The result showed that the percentage of carbon black increased linearly with the PEI stage number. This was true whether simple Gantrez or Gantrez crosslinked with 1.6 wt % of ethylenediamine was used as the electrophile in the covalent LbL process. This result agrees well with titrations and fluorescence studies above. It also suggests that incorporating functional guest molecules or nanoparticles

into the polymer grafts through other interactions such as hydrogen-bonding should be a viable route to the synthesis of covalent LbL nanocomposites.

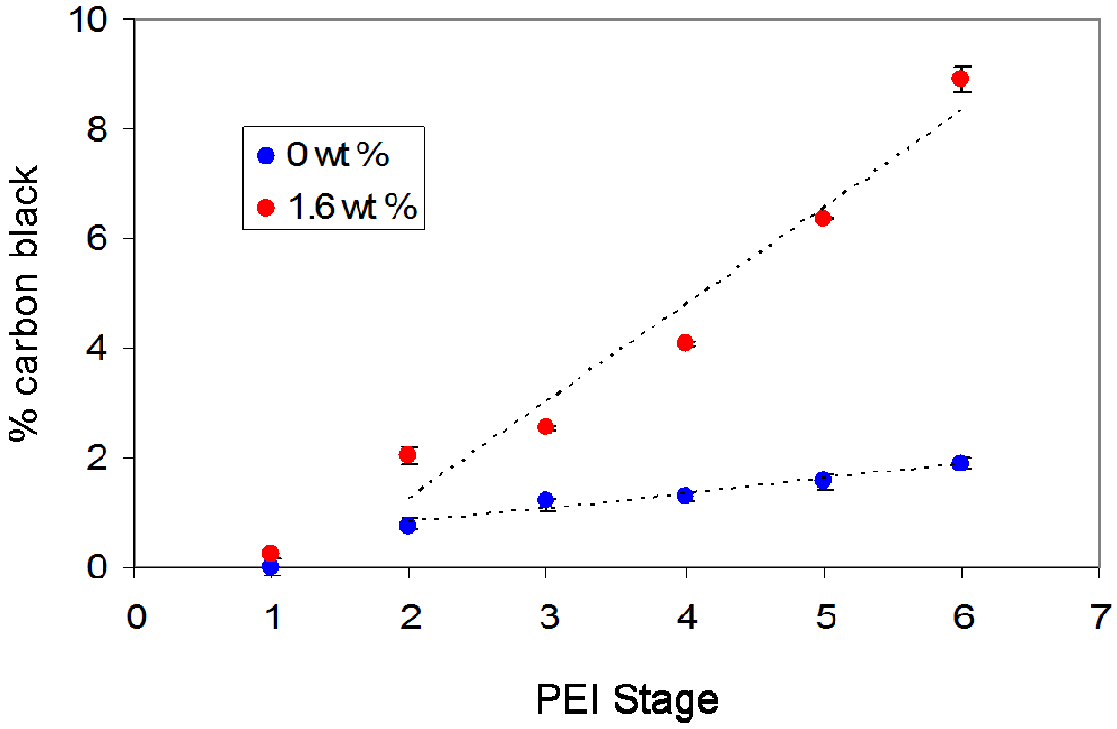

Figure 5. Percentage of carbon black in (PEI + 5 wt % carbon black)/Gantrez PE particles in different PEI stages assembled by using Gantrez solution with 0 and 1.6 wt % of ethylenediamine relative to Gantrez, respectively (based on three individual TGA for each data point).

X-ray Photoelectron Spectroscopy of PEI/Gantrez - PE Films. X-ray photoelectron spectroscopy (XPS) is a useful tool to analyze the element composition in the top 1 to 10 nm of a surface. Although XPS cannot analyze the elemental composition of the multilayers beneath the outermost 10 nm of the surface, it does provide insight

into the process by which these multilayers assemble. Figure 6 shows the percentage of oxygen and nitrogen species for reaction steps that stop with either a PEI- or Gantrez-treatment. Oxygen on these surfaces is mainly a product of Gantrez, $(C_7H_8O_4)_n$. The oxidized PE also contributes some oxygen but is presumably buried below the multilayers at least at later stages in the LbL assembly process. Nitrogen is introduced by the PEI, $(C_4H_5N)_n$. Therefore, based on the relative atom % of oxygen and nitrogen on the surface, we can determine if the surface is either Gantrez-rich or PEI-rich. The results show that a PEI-1 surface has relative low nitrogen atom %, indicating that the surface is not fully covered with PEI. However, after the first Gantrez layer, the oxygen atom % value jumps to a very high level indicating that the surface is mainly Gantrez. Later PEI and Gantrez stages show a periodically changing pattern for both oxygen and nitrogen atom % consistent with the notion that the surface is assembled in the LbL fashion we proposed (*cf.* Scheme 2). Interestingly, the oxygen content in the later Gantrez stage never is as high as it was in Gantrez-1. We interpret this to mean that the multilayer grafts interpenetrate to some extend even within the top 10 nm of the surface. This agrees with the model of LbL assembly proposed first by Decher.[2]

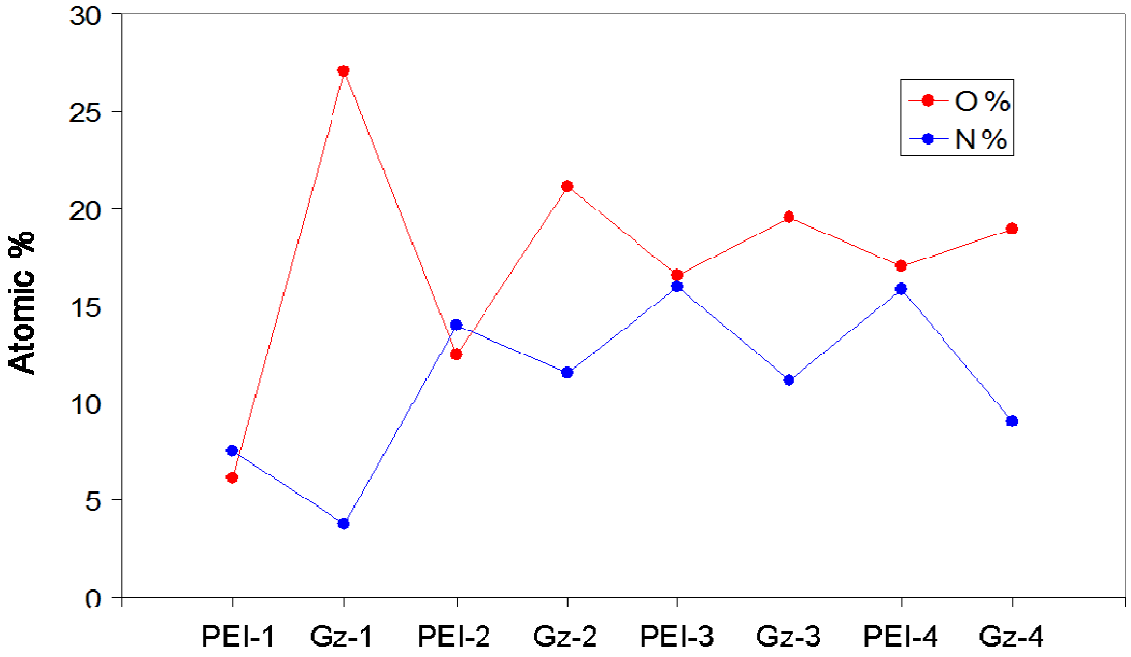

Figure 6. Atomic percentage of oxygen and nitrogen on the surfaces of PEI/Gantrez films in different stages. PEI- or Gz- represents what the most outer layer of the assembled film is.

Conclusions

The results of this chapter show that surface modification of PE substrates using covalent LbL assembly with PEI and Gantrez is a successful route to prepare a surface graft. The procedure is relative easy, fast and reproducible. Characterizations of the resulting substrates carried out by ATR-IR spectrometry, titrimetric analyses, fluorescent analyses, TGA and XPS all are consistent with a covalent assembly process proceeding by nucleophilic and electrophilic reactions. The assembly shows the same linear growth pattern seen for other LbL processes. The covalent multilayer assemblies have been shown to be stable to strong acid or strong base. Most of the surface groups are accessible based on titrimetric analyses. The surface groups can be further modified with other functionalities suggesting that this procedure could be the basis of broader synthetic approaches to functional interfaces.

CHAPTER III

CONDUCTIVE THIN FILMS ON PEI/GANTREZ FUNCTIONALIZED POLYETHYLENE PARTICLES*

Introduction

Electrostatic LbL assembly is proved to be a powerful tool to modify surface during the past two decade.[1] Many materials can be used as a substrate for electrostatic LbL deposition without the need for surface modification, but there is difficulty building layers on polyolefins.[54,55] It is difficult to get water-based coatings to adhere well to polyolefins, such as PE and polypropylene, because of low surface energy and lack of polarity. Corona or plasma treatments can be used to increase the surface energy of polyolefin films.[46-49] Both of these techniques generate polar functionalities on the film surface that will improve wetting and subsequent adhesion of an aqueous coating. Oxidative acid etching is another method that generates hydroxyl and carboxylic acid species to create surface polarity.[56] However, these surface modification techniques only produce monolayer of functionality whose properties change upon surface reorganization. A more recent technique, used here to promote stable LbL film growth and stronger adhesion, is the growth of covalent grafts on polyolefin.[40,57-59] In the present study, a hyperbranched PEI surface was generated on PE particles in a manner similar to that done previously on a silica support.[40] The details are presented in Chapter II. Hyperbranching yields a uniform surface coverage of polyelectrolyte down to the

*Reproduced in part with permission from Kim, Y.-S.; Liao, K.-S.; Jan, C. J.; Bergbreiter, D. E.; Grunlan, J. C. *Chem. Mater.* **2006**, *18*, 2997-3004. Copyright 2006 American Chemical Society.

microscopic level, despite initial growth occurring only sparsely over the PE particle surface. The presence of PEI on the PE particle then facilitates near perfect surface coverage by alternate deposition of CB stabilized with poly(acrylic acid) (PAA) and PEI in a LbL fashion. Untreated PE exhibits very poor acceptance of the LbL film growth under the same conditions, while oxidative acid etching exhibits intermediate behavior. The CB-coated particles so formed produce highly conductive composites when compression molded.

CB-filled polymer composites are useful as thermal resistors,[60,61] chemical sensors,[62,63] electromagnetic interference shielding,[64,65] and electrostatic dissipation layers.[64,66] Such electrically conductive composites are typically prepared using melt mixing[67,68] or solution processing.[69,70] These methods lead to composites with high percolation thresholds because of random CB dispersion. The percolation threshold is the minimum concentration of conductive filler required to generate a conductive pathway that travels through the entire composite film.[71] In many cases, the high CB concentrations (>25 wt %) required to achieve significant electrical conductivity is often accompanied by high mixing viscosity and brittle composite films with extensive porosity due to aggregated filler.[72,73] LbL deposition circumvents high viscosity processing by using dilute mixtures (<1 wt % solids) to deposit layers of CB that are pre-stabilized with PEI and PAA to impart basic and acidic surface chemistry, respectively. The resulting films are thin (<1 μm), flexible, and dense, with a high concentration of CB (>45 wt %).[74] When applied to PEI-treated PE particles, with an average particle size of 1.7 mm, highly conductive composites are produced that have a very small weight

fraction of CB following compaction. Unlike typical composites formed with a random dispersion of CB, a segregated network is generated as the thin conductive shells are pressed together, leading to high conductivity even at very low CB concentration. The segregated network concept relies on a polymer matrix with an exclusionary microstructure.[75] In essence, the conductive filler is given a restricted volume in which to reside that leads to network formation at very low concentration. Larger polymer particles or domain size relative to the conductive particle size yields lower percolation thresholds.[76] A variety of segregated network composites have been produced using polymer blends,[77-81] powders,[76,82,83] and emulsions[84,85] to produce excluded volume during processing. The composites made with CB typically have percolation thresholds from 1.5 to 7.5 wt % and maximum electrical conductivity (plateau of conductivity as a function of CB concentration) from 0.01 to 1 S/cm, with lower percolation thresholds accompanied by reduced maximum conductivity.[77-82,85] In this work, a comparison is made between the untreated PE particle, the oxidative acid etched particle, and the particle that has hyperbranched PEI on its surface. Electron microscopy is used to characterize the three types of particles prior to LbL deposition of CB. The PEI-treated and unmodified PE particles are then compared with respect to LbL film growth using electron microscopy and thermogravimetric analysis (TGA). PE particles containing two to eight bilayers of CB, stabilized with PEI and PAA to provide positive and negative surface charges, were studied. The results indicate that deposition on unmodified or acid etched PE does not produce uniform CB films, and the material that does deposit has variable thickness and poor interfacial adhesion. PEI-grafted PE promotes uniform

deposition of CB thin films as evidenced by gravimetric analyses that show a linear increase in weight per bilayer. Composite films, made using compression molding, exhibited a percolation threshold below 0.01 wt % CB and a maximum electrical conductivity of 0.2 S/cm with a concentration of only 6.2 wt % CB. These segregated network composites have among the lowest percolation threshold ever reported with CB as the conductive filler. This combination of surface functionalization and LbL assembly could be used to deposit other types of conductive material or to impart other properties, such as antimicrobial or flame suppression.

Results and Discussion

Preparation of Carbon Black Coated Layers by LbL Assembly. The details to make PEI/Gantrez grafts on PE particles are presented in Chapter II. Before the CB deposition, the surface morphology of the PEI/Gantrez grafts was imaged by scanning electron microscopy (SEM). The PEI-grafted material has a nanoscale texture on the surface while the neat and oxidized PE have smooth surfaces, as shown in Figure 7. PEI is one of the two polymers used to stabilize CB for the LbL assembly, so the grafted particle has an ideal surface.

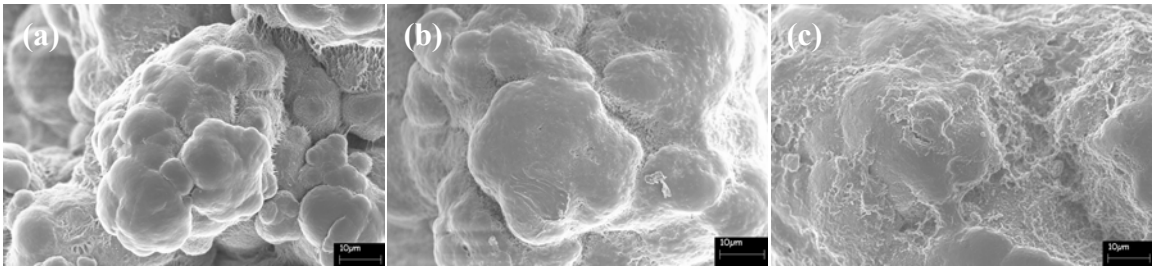

Figure 7. SEM image at 1,000 times magnification of the (a) neat PE; (b) oxidized PE; (c) PEI-grafted PE.

PE is a relatively inert, nonpolar polymer that is largely incompatible with the species used for LbL assembly. As shown in Figure 8, CB deposition is very poor on neat PE after two full deposition cycles (i.e., two bilayers of PEI-CB and PAA-CB). The CB layer covers only a small area of an otherwise clean surface. Oxidized PE is not much better after two bilayers, whereas the PEI-grafted surface is completely coated by CB. After four bilayers the coating area increases significantly for the neat PE, but the coating is non-uniform. Some areas are completely covered by the coating while others are completely clean. It appears that spots coated in the previous step act like nucleation sites for subsequent steps. This phenomenon is more clearly shown once six bilayers are deposited, where the boundary of two coating pieces is observed. Each piece of the coating grows as the number of bilayers increases and eventually links together. After eight bilayers, almost all of the area is covered by the CB coating, but boundaries between initial growth sites persist. In addition to poor growth, the CB exhibits poor

bonding with the neat PE surface as evidenced by the interfacial gaps shown at eight bilayers. Only a small portion of the coating is weakly attached to the surface by van der Waals attractions and can be easily removed with a small amount of force. Some research groups are actually exploiting this behavior to produce free-standing LbL assemblies.[86] Acid oxidation of the surface improves the deposition of CB to some degree. After two bilayers, the oxidized PE shows a surface that is more uniformly speckled with CB than the neat PE particles (see Figure 8). Oxidized PE shows significant improvement over neat PE after four bilayers are deposited. Furthermore, full surface coverage of the oxidized PE particles is achieved with six bilayers. Much like the situation with neat PE, poor bonding between the oxidized PE and the CB thin film is observed. The interfacial gap shown in Figure 8 at eight bilayers is similar to those seen on neat PE, although thin film uniformity is much improved. Lack of completely uniform growth is believed to be due to surface reorganization that eliminates much of the negative surface charge initially produced during the oxidation process.[87]

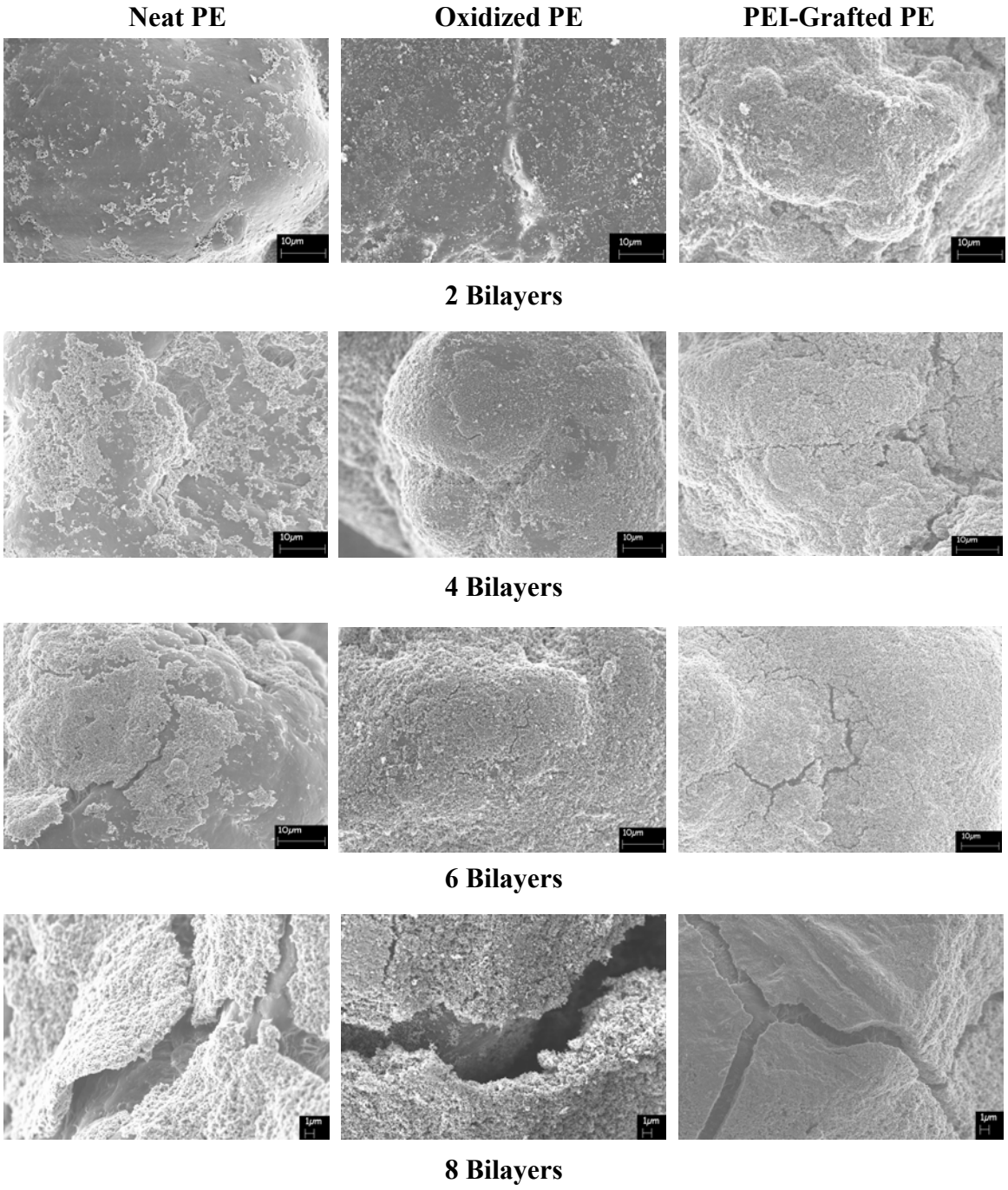

Figure 8. SEM images of neat, acid-oxidized, and PEI-grafted PE particles coated with varying numbers of bilayers of CB stabilized with PAA and PEI.

Only the PEI-grafted powder demonstrates near perfect compatibility with the LbL process. Unlike the neat and oxidized PE, which show poor initial surface coverage, the PEI-grafted surface is completely covered with just two bilayers of PAA-CB/PEI-CB (see Figure 8). Good interfacial adhesion is also evidenced by the lack of an interfacial gap between the CB thin film and grafted PE. With improved adhesion comes an increase in cracking as the deposited film, containing ~45 wt % CB,[74] attempts to relieve stress. The poor adhesion on the neat PE leads to buckling that is not observed on the PEI-grafted PE. The intermediate deposition and adhesion on the oxidized PE exhibit true cracking, but at six bilayers rather than the four needed on the grafted surface. A linear increase in CB concentration with the number of bilayers deposited suggests that cracking does not adversely affect film growth for the PEI-grafted PE. TGA, shown in Figure 9, qualitatively correlates with the SEM images in Figure 8. The CB concentration of the PEI-grafted particles increases linearly as the number of bilayers is increased, exceeding 6 wt % after eight bilayers are deposited. The CB concentration of neat PE is nearly undetectable at two and four bilayers but increases suddenly at six bilayers. The increasing rate from six to eight bilayers is similar to that of the PEI-grafted case. This result suggests that the CB does not achieve good surface coverage until six bilayers, as shown in the SEM images (see Figure 8). Once the CB layer covers a significant fraction of the surface, additional CB layers can be uniformly deposited because the surface of the support is already covered with complementary material. The CB concentration of the oxidized PE falls between that of the grafted and that of the neat

samples. The initial growth is similar to that of the neat PE, but at six bilayers, it becomes more like that of the PEI-grafted PE.

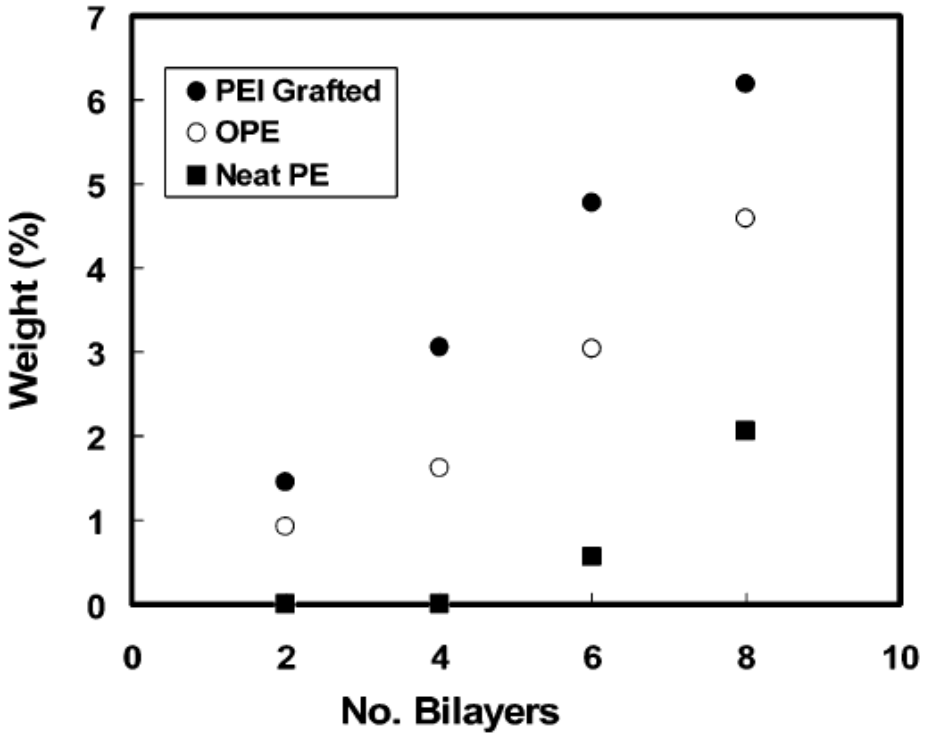

Figure 9. Carbon black concentration as a function of the number of bilayers on PEI grafted, oxidized PE and neat PE particle.

Segregated Network Films Formed by Compact Molding of Carbon Black Coated PE Powders. After deposition, the coated PE powder was compacted at 90 °C for 30 min. Figure 10 shows cross sections of all three films with two and eight bilayers deposited. These images show a segregated network of CB, which is expected to be electrically conductive despite its low concentration of conductive material. During compression, the PE particles lose their roughly spherical shape and become more oblong. The amount of CB, which appears black in these images, correlates well with SEM (see Figure 8) and TGA results (see Figure 9). For neat PE with two bilayers of CB, the network is incomplete because of poor surface coverage. The CB network is much more developed in the film made from oxidized PE and still more enhanced in the film made with PEI-grafted PE. The microstructure shown for two bilayers on PEI-grafted PE is very comparable to that shown for the neat PE with eight bilayers of CB. Electrical conductivity of these films correlates very well with these microstructures, with better developed networks exhibiting higher conductivity.

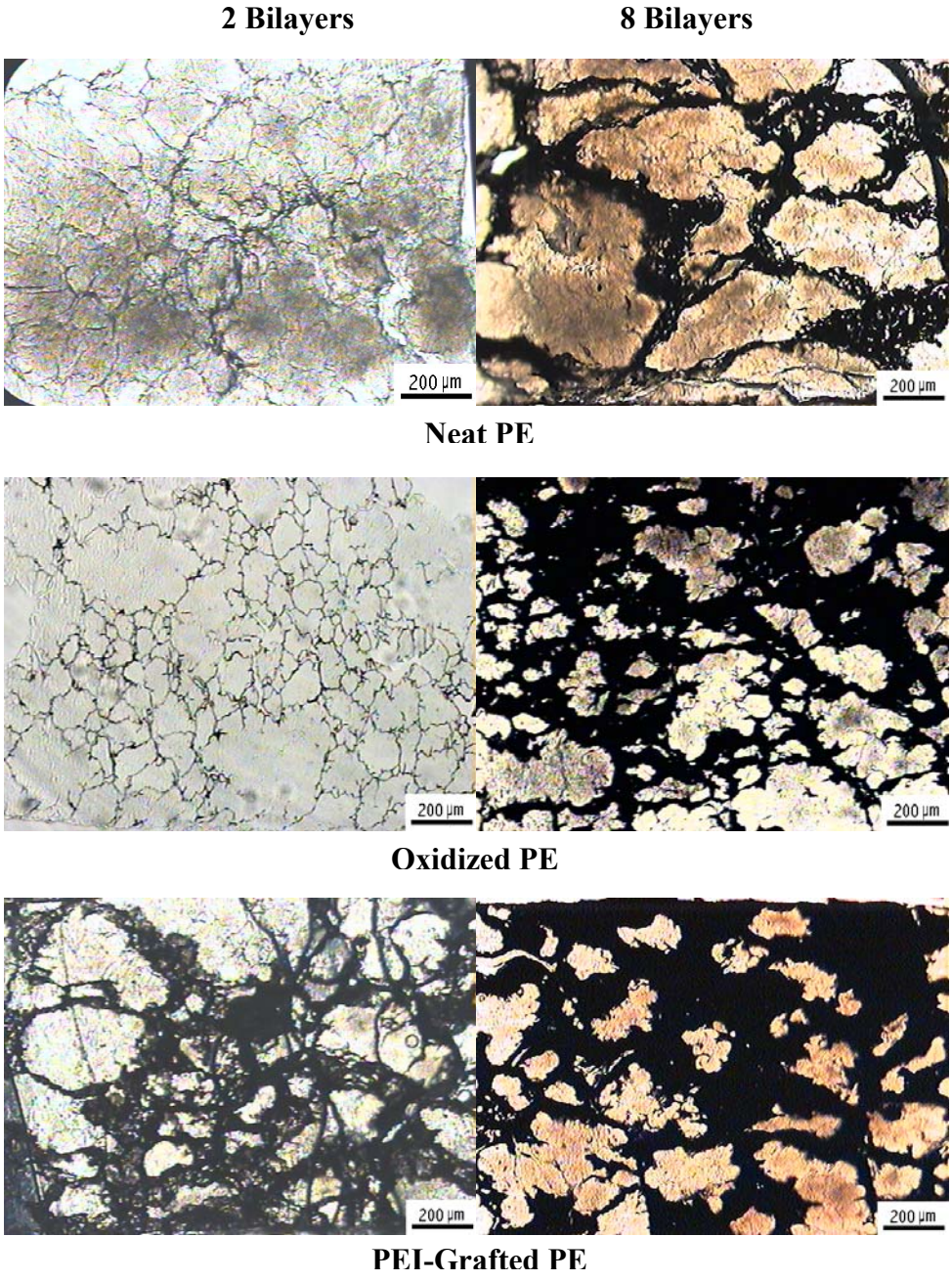

Figure 10. Optical microscope cross sections of compressed films made with neat, acid-oxidized, and PEI-grafted PE particles containing two and eight bilayers of CB stabilized with PAA and PEI.

During compaction, the large PE particles create excluded volume that keeps CB at the boundaries between them. As a result, the CB coatings create a segregated network structure that reduces the percolation threshold. The percolation threshold is the critical concentration of conductive filler required to produce measurable conductivity in an insulating matrix. Previous studies have shown that this concentration can be reduced by up to 1 order of magnitude by creating a segregated network.[77-85] Figure 11a shows the conductivity of compressed films as a function of the number of the bilayers deposited. As expected, films made from PEI-grafted particles exhibit the greatest electrical conductivity. With eight bilayers deposited, conductivity near 0.2 S/cm is achieved. On the basis of TGA results (see Figure 9) this corresponds to a CB concentration of just 6 wt %. Composites made using traditional melt processing required more than 30 wt % of the same high structure CB to obtain a comparable resistivity in HDPE.[88] Films made with neat PE particles do not exhibit measurable conductivity until six bilayers of CB are deposited, and this value (~0.002 S/cm) is more than 1 order of magnitude lower than that of the PEI-grafted film (~0.07 S/cm). The films made from oxidized PE particles show electrical conductivity that is more similar to that of the grafted particles than that of the neat PE, exhibiting measurable conductivity at all bilayers. Despite showing a similar trend of increasing conductivity with number of bilayers, the oxidized particle films are significantly less conductive than the grafted films at all bilayers (see Table 1). The difference in film behavior between oxidized PE and PEI-grafted PE is more pronounced when conductivity is shown as a function of CB concentration.

Table 1. Carbon black concentration and sheet resistance result.

Particle	No. Bilayers	CB Concen. (wt %)	Thickness (mm)	Sheet Resistant (Ω/sq)
Neat	2	N/A	1.45	N/A
	4	N/A	1.64	N/A
	6	0.5737	1.49	3465.99
	8	2.923	1.21	293.13
Oxidzed	2	0.9216	1.69	1308272.89
	4	1.618	1.56	18614.45
	6	3.032	1.54	112.79
	8	4.59	1.47	55.99
Grafted	2	1.455	1.43	672.24
	4	3.05	1.69	168.99
	6	4.778	1.50	92.06
	8	6.1915	1.31	40.13

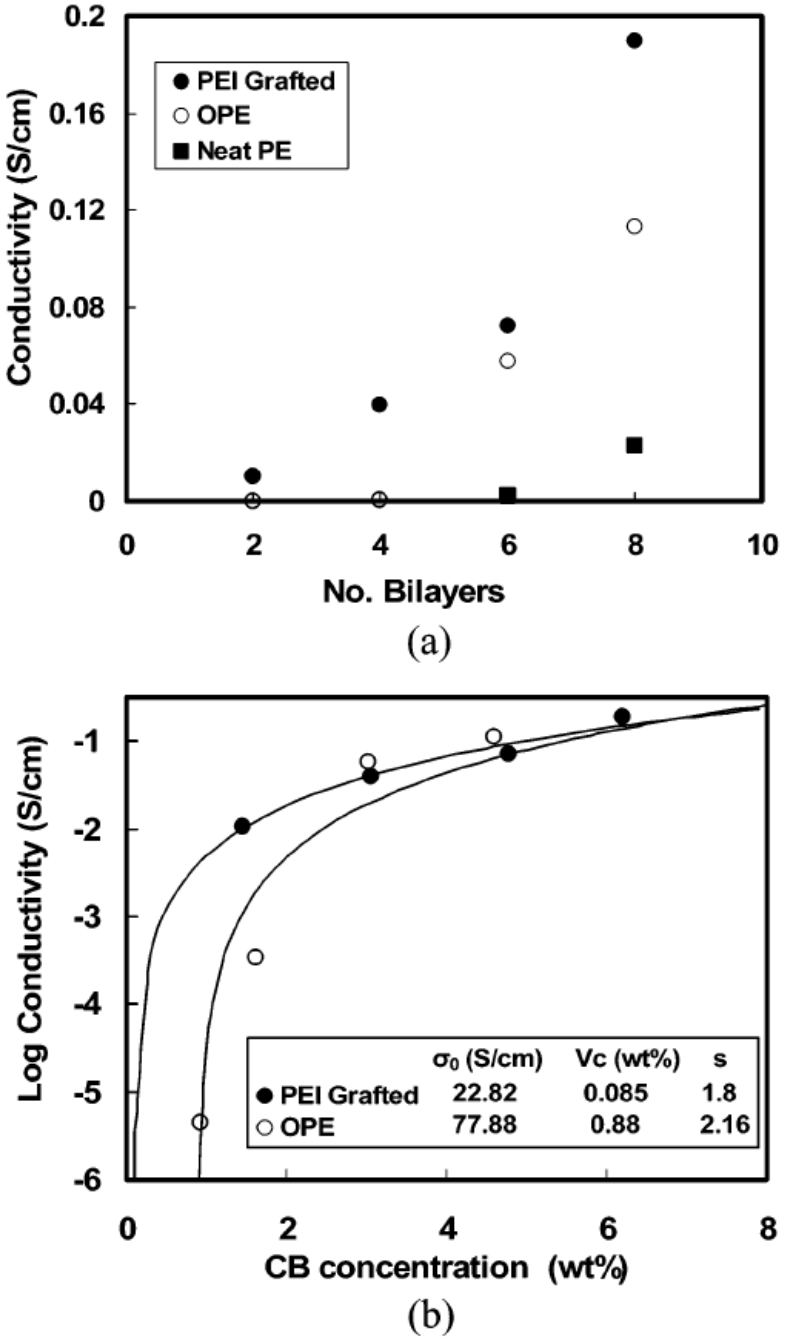

Figure 11. Electrical conductivity as a function of the number of the bilayers (a) and CB concentration (b) for films made by compression molding PE particles following LbL deposition of CB.

Using the TGA data from Figure 9, the number of bilayers in Figure 11a can be converted to CB concentration to generate percolation-style curves for the films made with oxidized and PEI-grafted particles. Figure 11b shows these data fitted with the classical percolation power law[71]

$$\sigma = \sigma_0(V - V_C)^s$$

where σ is the measured conductivity, σ_0 is a scaling factor, V is the volume fraction of CB, Vc is the percolation threshold, and s is the power law exponent. The PEI-grafted PE films have a percolation threshold of 0.085 wt % CB, while the oxidized PE films have a percolation threshold that is 1 order of magnitude higher at 0.88 wt %. Melt processed composite films made with the same CB and PE of the same density show a percolation threshold of 13.5 wt %.[88] It is clear that the segregated network microstructure generated in the compacted films is able to shift the percolation threshold by more than 1 order of magnitude. The order of magnitude difference between the two surface treatments suggests that the deposition is less uniform in the case of the oxidized PE particles, as evidenced by comparing the SEM images in Figure 8. Both systems converge near 3 wt % CB, but this concentration is achieved at four bilayers for the grafted particles and six bilayers for the oxidized particles. This combination of low percolation threshold and relatively high electrical conductivity, especially for the PEI-grafted system, is currently the best reported for a CB-filled polymer composite.

Conclusions

The effects of no treatment, surface oxidation, and covalent grafting of PEI on PE particles were compared with respect to growth and adhesion of CB thin films deposited using LbL assembly. In the absence of surface modification, LbL film growth is patchy and adhesion is very poor. Surface oxidation improves the rate of film growth; however, it still lacked uniformity at small numbers of bilayers, and adhesion remained weak. Grafting multiple layers of PEI to the PE powder surface provided excellent coverage and promoted stable LbL film growth and excellent adhesion. This CB coated powder was compression molded into films, and their conductivity was measured, which revealed a percolation threshold below 0.01 wt % CB for the PEI-grafted system. Electrical conductivity of 0.2 S/cm was achieved with only 6 wt % CB, which is exceptional for a CB-filled PE film. Modification of deposition parameters, such as the ratio of stabilizer to CB, may further increase conductivity and/or reduce the percolation threshold of these films. The use of surface grafting in combination with LbL deposition could be used to impart other useful properties to polyolefin films or particles, including antimicrobial or flame retardant behavior. These initial results demonstrate the ability to use LbL assembly on a substrate that is traditionally incompatible with this water-based technology. It is difficult to quantitatively assess the improvement in thin film adhesion that occurs with surface grafting. Future work will seek to measure interfacial adhesion and evaluate the effects of different grafting techniques and polymers.

CHAPTER IV

DIRECT AMINATION OF MULTIWALL CARBON NANOTUBES*

Introduction

While carbon nanotubes (CNTs) are interesting materials in their own right, functionalized CNTs are of increasing interest as functionalization allows CNTs to be more readily suspended in solvents or to be incorporated into other materials.[89-91] A variety of strategies has been previously used to functionalize CNTs. These strategies include oxidation,[92,93] reductive alkylation,[94] arylation,[95] and graft polymerization chemistry.[96,97] Our group was particularly interested in routes to aminated CNTs as we wanted to use such materials to form ultrathin nanocomposites on surfaces. We expected aminated CNTs to function as the nanoparticle equivalent of a polyaminated dendrimer in either ionic or covalent layer-by-layer assembly chemistry.[14,40,98,99] However, existing synthetic routes to the necessary polyaminated CNTs typically involve harsh oxidations that degrade the CNT and that require several steps.[100] Here we describe an alternative and far simpler reaction where multiwall carbon nanotubes (MWNTs) are simply treated with polyethyleneimine (PEI) in dimethylformamide (DMF) at 50 °C – a straightforward reaction that produces MWNTs with 6-8% by weight PEI. Such aminations have precedence both in the reactions of amines with fullerenes[101] and in similar reactions of amines with MWNTs.[102] In the example here, the use of a readily available polyvalent amine source producing a MWNT product with excess amine groups on these products. The product PEI-grafted MWNTs are readily

protonated and titrated in water and behave as simple amines in amidation chemistry. Details about using this aminated MWNTs to construct ultrarough surface on PE surface by layer-by-layer assembly will be presented in Chapter IV.

Results and Discussion

Direct Amination of MWNTs with Polyethylenimine. The use of functional multiwall carbon nanotubes (MWNTs) as highly anisotropic nanoparticles was a key part of our strategy for the synthesis of surfaces with the desired chemistry and morphology. Since we were successful in earlier covalent layer-by-layer assembly using either polyaminated dendrimers or PEI,[14] we were particularly interested in using aminated carbon nanotubes (CNTs) as reagents to form morphologically complex ultrathin films.

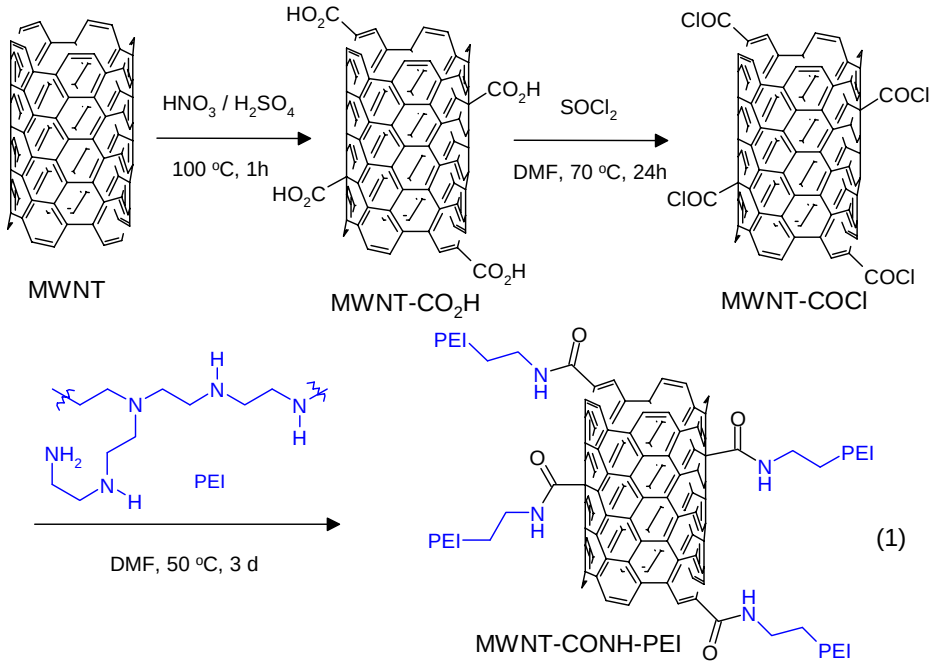
HO2C
CO2H
HO2C
CO2H
HNO3 / H2SO4
100 oC, 1h
SOCl2
DMF, 70 oC, 24h
ClOC
COCl
ClOC
COCl
MWNT
MWNT-CO2H
MWNT-COCl
NH2
PEI
DMF, 50 oC, 3 d
PEI
MWNT-CONH-PEI
(1)

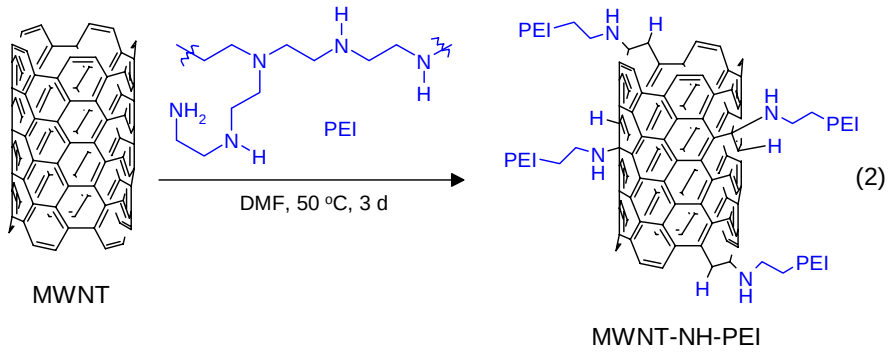
NH2
PEI
DMF, 50 oC, 3 d
PEI
MWNT
MWNT-NH-PEI
(2)

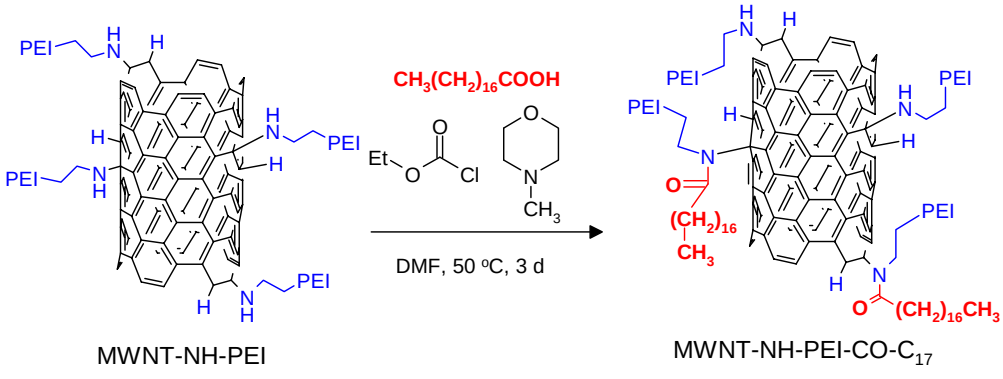
PEI
CH3(CH2)16COOH
Et
O
Cl
N
CH3
DMF, 50 oC, 3 d
MWNT-NH-PEI
MWNT-NH-PEI-CO-C17
(3)

To this end we explored the chemical modification of MWNTs using the two methods shown in eqs. 1 and 2. The first of these methods (eq.1) used a known oxidative degradation process to produce carboxylated MWNTs.[92,100] In order to convert these oxidized MWNTs into a polyvalent amine, the carboxyl groups of these oxidized MWNTs were activated and amidated with PEI to form the functionalized MWNTs (MWNT-CONH-PEI) that could be used in covalent layer-by-layer self-assembly of a nanocomposite. This standard route to polyaminated MWNTs worked but it required several steps and also degraded the MWNTs as shown by Raman spectroscopy (vide infra). Thus, we considered an alternative route to polyaminated MWNTs.

This alternative chemistry chosen involved treatment of MWNTs with PEI in DMF at 50 °C for 3 d to form the PEI grafted species (MWNT-NH-PEI) shown in eq 2. This straightforward chemistry produces MWNTs with 6-8 % by weight PEI. While direct aminations have not been used to graft polymers like PEI onto MWNTs before, aminations of fullerenes[101] and of MWNTs[102] with low molecular weight amines is known. Our work expands on this earlier chemistry using PEI to form a MWNT product functionalized with polyvalent reactive amine groups. The PEI-grafted MWNTs so formed are readily protonated and titrated in water and their amine groups behave like the amines of PEI in amidation chemistry.

Characterization of MWNT-NH-PEI and MWNT-NH-PEI-COC_{17}. Characterization of the products of eq. 2 as PEI grafts included a series of chemical and physical analyses. Thermogravimetric analysis (TGA) under N_2 showed distinct differences between the PEI derivative of the MWNTs and the starting MWNTs. As shown in Figure 12, the as-received MWNTs exhibit a gradual weight loss of 10-15 % over the temperature range 30-950 °C. The MWNT-NH-PEI exhibited a 6-8 % weight loss in the 300-400 ºC temperature range. The TGA results in the 300-400 °C range also showed similar results for either the MWNTs containing PEI prepared using eq. 1 (MWNT-CONH-PEI) or eq. 2 (MWNT-PH-PEI) though the latter material had higher PEI loadings and a larger weight loss. The weight loss in this region was ascribed to loss of the grafted PEI on the MWNT samples. We also found that the amine groups of MWNT-NH-PEI could be converted into amides using an activated octadecanoic acid derivative (eq. 3). The product octadecanoyl derivative of MWNT-NH-PEI (MWNT-NH-PEI-COC_{17}) was also analyzed by TGA and exhibited a more substantial 20-25 % weight loss at a slightly lower temperature than the MWNT-NH-PEI material (Figure 12).

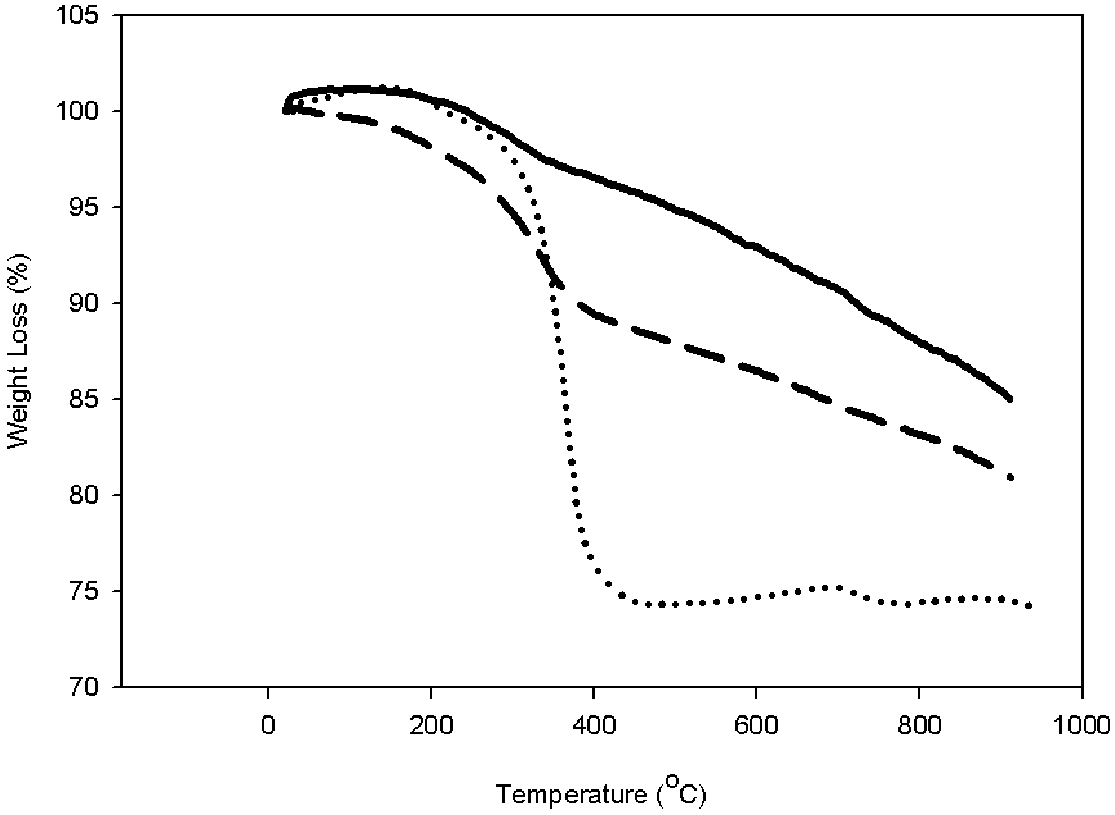

Figure 12. TGA curves for pure MWNTs (—), MWNT-NH-PEI (– – –) and MWNT-NH-PEI-COC_{17} (·····) obtained using a heating rate of 10 ºC min^{-1} under a N_2 atmosphere.

Further evidence for formation of a PEI graft on MWNTs was obtained from titration. In this analysis, a known amount of the MWNT-NH-PEI was added to a known volume of 0.01 M HCl. After sonicating the mixture for 1 h at 25 °C, an aliquot of the resulting HCl solution was titrated to a pH 8.0 endpoint using 0.01 M NaOH with a pH meter. The difference between the original amount of HCl and the amount of HCl titrated corresponds to the loading of titratable amino groups on the MWNT-NH-PEI

(0.3 mequiv of titratable amine groups/g of MWNT-NH-PEI). Separate analysis of pure PEI using the same conditions showed that approximately 20 % of the amine groups of PEI were titrated by this method. As such, the total amine groups on MWNT-NH-PEI were estimated to be *ca*. 1.5 mequiv/g.

Elemental analysis confirmed that PEI had been coupled to the starting MWNTs. Using elemental analysis, we showed the as-received MWNTs contained 98.29 % C. The MWNT-NH-PEI contained 92.56 % C and 2.89 % N which corresponds to *ca*. 8 % by weight grafting of PEI. The octadecanoyl amide product (MWNT-NH-PEI-COC_{17}) contained 89.53 % C and 2.35 % N, consistent with the amidation of some of the PEI amine groups by octadecanoyl groups.

Several spectroscopic analyses of the MWNT-NH-PEI sample were carried out. IR spectroscopy did not provide any useful information for the MWNT-NH-PEI sample but the MWNT-NH-PEI-COC_{17} product did show peaks at 2912 cm^{-1} and 2869 cm^{-1} consistent with C-H stretches associated with the octadecanoyl moieties. Raman spectroscopy showed the expected peaks for the D band at 1290 cm^{-1} and for the G band at 1580 cm^{-1} for both the pure MWNTs and the MWNT-NH-PEI. These spectra also showed no detectable sidewall degradation in these samples in contrast to a sample of oxidized MWNTs (Figure 13). The D/G band ratio in the Raman spectra for the MWNTs starting materials was 1.39, while the D/G band ratio of the MWNT-NH-PEI was 1.42 indicating that PEI grafting did not measurably affect the overall integrity of the MWNT sidewalls. The Raman spectra of MWNT-CONH-PEI derived from MWNT oxidation had a D/G band ratio of 1.53. Thus, while oxidation of MWNTs can be used

to graft PEI onto MWNTs,[92] our results suggest that direct amination with PEI is a far milder and a preferable procedure in that more PEI is incorporated with minimal degradation of the MWNTs.

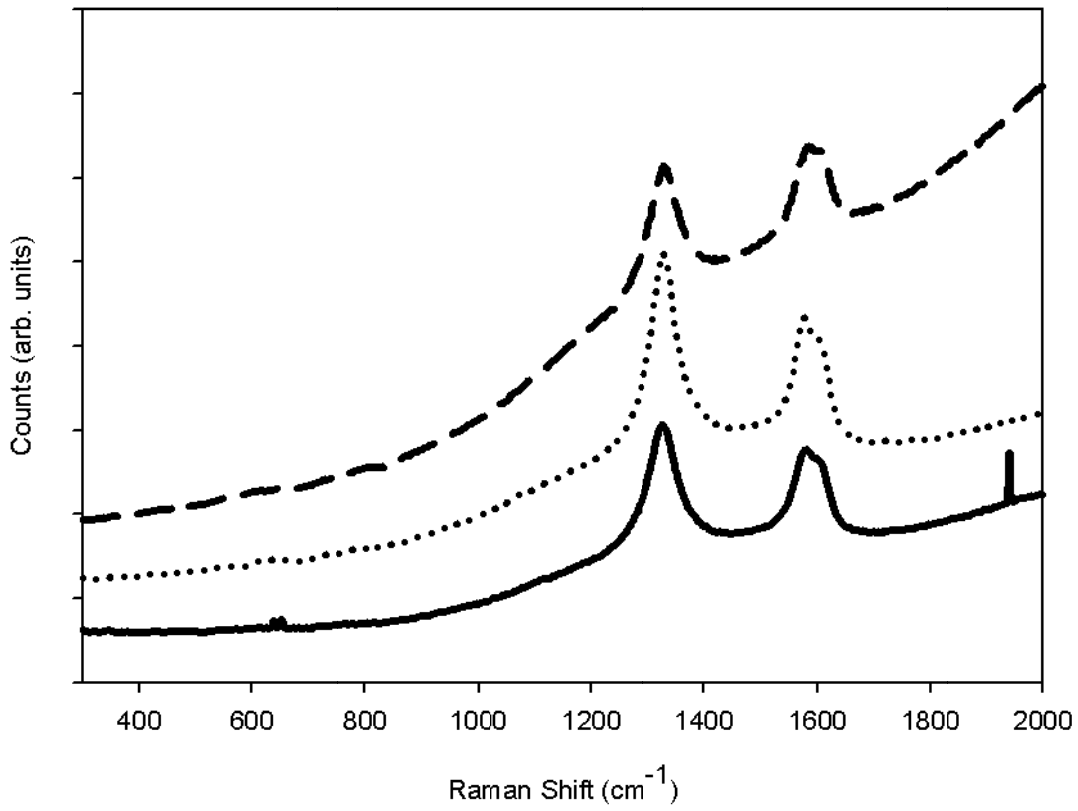

Figure 13. Raman spectra (633 nm excitation) of pure MWNTs (—), MWNT-NH-PEI (– –) and oxidized MWNT-CONH-PEI (·····).

The ^{1}H NMR spectrum of MWNT-NH-PEI suspended in D_2O (Figure 14) showed two broad peaks with chemical shifts of 3.38 and 1.52 δ which were attributed to the grafted PEI. A ^{1}H NMR spectrum of MWNT-NH-PEI-COC_{17} in $CDCl_3$ (Figure 15)

showed four additional peaks centered at 2.08, 1.64 1.24 and 0.86 δ which were attributed to protons in octadecanoyl amide. Broad PEI peaks were also present at 3.49 δ. Integration of the PEI protons and the protons of the octadecanoyl group in this latter sample yielded a 1:2 ratio, consistent with the ratio of 1:1.7 calculated from the increased hydrogen content in the elemental analysis of MWNT-NH-PEI-COC_{17}.

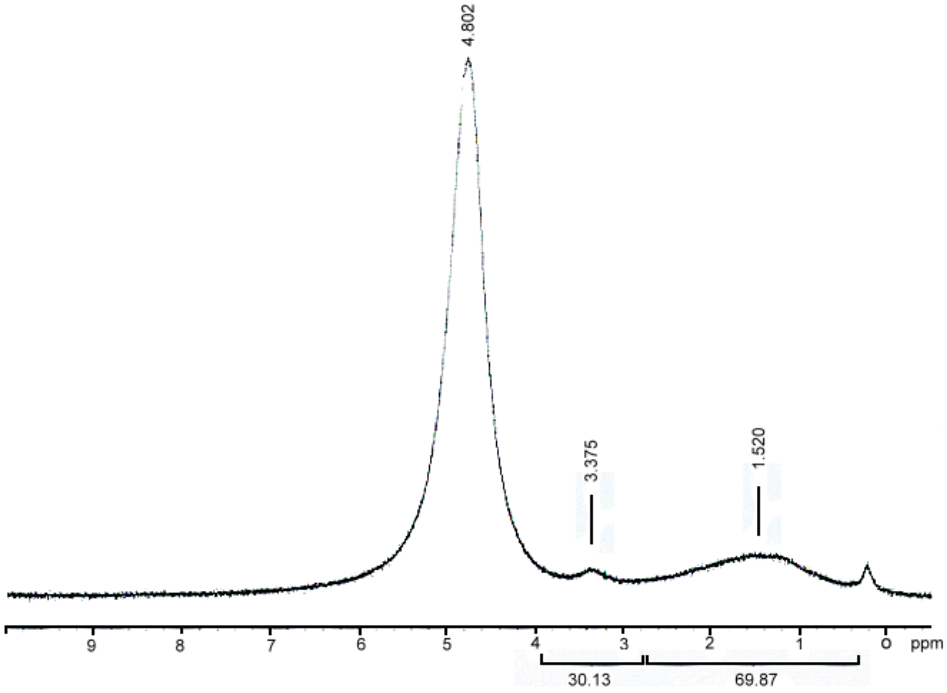

Figure 14. ^{1}H NMR spectrum of MWNT-NH-PEI suspended in D_2O.

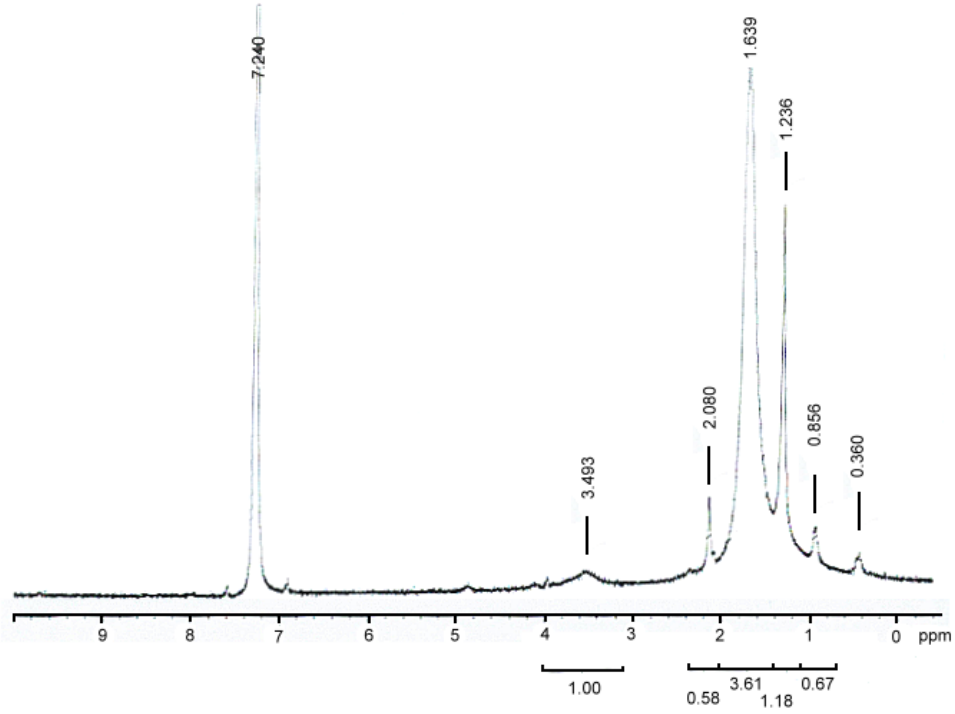

Figure 15. ^{1}H NMR spectrum of MWNT-NH-PEI-COC_{17} in $CDCl_3$.

Solid state MAS (3 kHz spinning rate) ^{1}H NMR of MWNT-NH-PEI (Figure 16) showed two distinctive peaks. One very broad peak extended from 70 to -20 δ. A second sharper peak spanned the 9.5 to -8.4 δ region. The sharper peak did not change shape even without spinning, suggesting that the protons responsible for that peak are isotropic with a more liquid-like environment. These protons may be PEI chains further from the MWNTs that are conformationally more mobile. Measurements of T_1 showed that the protons in the 9.5 to -8.4 δ region exhibit different relaxation rates, which may reflect distance dependent spin-lattice relaxations of these PEI protons and the MWNTs.

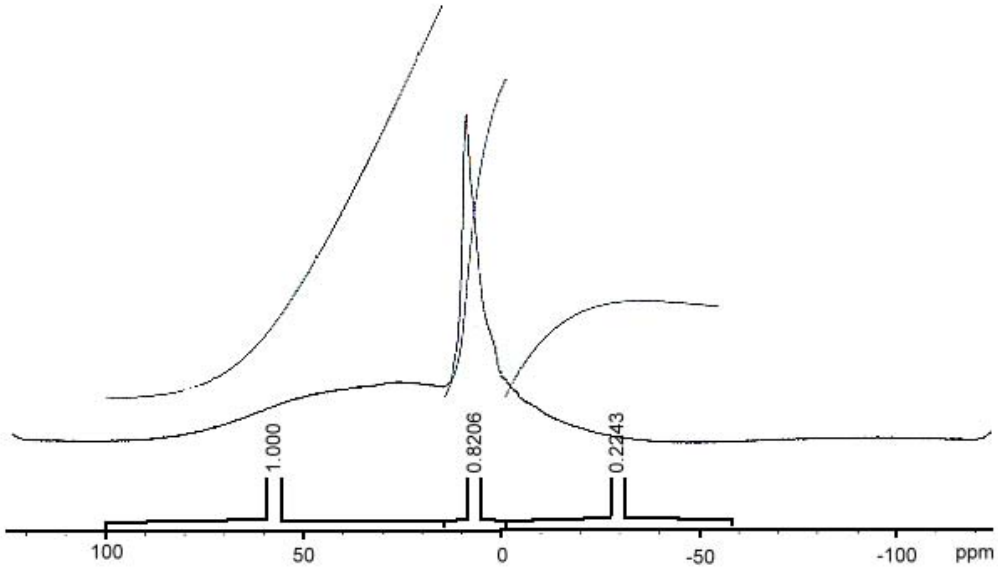

Figure 16. Solid state MAS (3 kHz spinning rate) ^{1}H NMR of MWNT-NH-PEI.

Interestingly, the PEI functionalized MWNTs exhibited increased dispersibility in solvents – an important property to enable their use in covalent LbL self-assembly with Gantrez. The dispersibility of MWNT-NH-PEI was demonstrated by comparing their behavior in solvent to the starting as-received MWNTs. In these comparisons, the MWNT samples were suspended in a solvent by sonication for 30 min, resulting in a suspension, and their temporal stability monitored visually. As seen in Figure 17, the starting unfunctionalized MWNTs dispersed in water precipitate within seconds. In contrast, the MWNT-NH-PEI dispersion in water (pH < 7) did not exhibit any visible changes for over 1 year. The dispersibility of MWNT-NH-PEI in water was found to be pH dependent. At pH 12 (0.01 M NaOH) where the graft amino groups would be

present as free amine groups, the MWNT-NH-PEI material began to settle after only one day. We ascribe this difference to the acid-base properties of the PEI attached to the MWNTs. The cationic ammonium groups expected to be present in the PEI grafts on

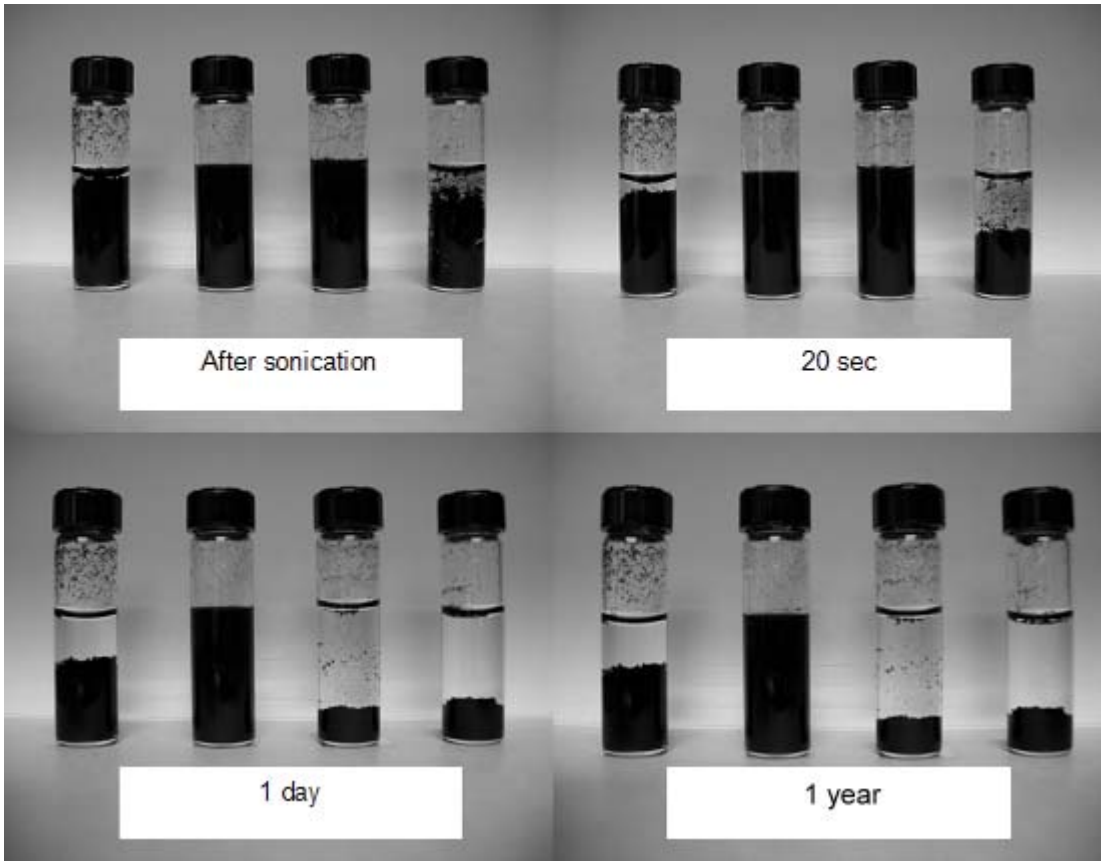

Figure 17. Samples (from left to right) of pure MWNTs in water, MWNT-NH-PEI in water (pH 7), MWNT-NH-PEI in 0.01 M NaOH solution, and MWNT-NH-PEI after thermolysis of the PEI graft in water immediately after sonication or after standing for the indicated times.

MWNT-NH-PEI at pH < 7 facilitate dispersion of MWNT-NH-PEI in water. A MWNT-NH-PEI sample that was heated to 400 °C under N_2 showed dispersibility like that of the starting MWNTs, consistent with the TGA analysis that suggested thermolysis of PEI occurs < 400 °C.

The MWNT-NH-PEI samples readily disperse in polar organic solvents such as methanol and DMF and stayed in suspension for more than one day – a time that greatly exceeds the reaction time for either LbL assembly process we used to form thin film nanocomposite grafts on PE. We also noted that the amidation product, MWNT-NH-PEI-COC_{17}, cannot be dispersed in water but could be dispersed in nonpolar organic solvents. Dispersions of MWNT-NH-PEI-COC_{17} in solvents such as hexane, tetrahydrofuran and ethyl acetate were stable for at least an hour.

The MWNTs before and after amination were also analyzed by transmission electron microscopy (TEM). Representative TEM images of both the as-received and aminated MWNTs are shown in Figure 18. While the starting commercial material was very polydisperse, the nanotubes were generally highly anisotropic with a length/width ratio that was generally above 1000. The aminated MWNTs had similar properties. Although the functionalization appears to break up the nanotubes to some extent.

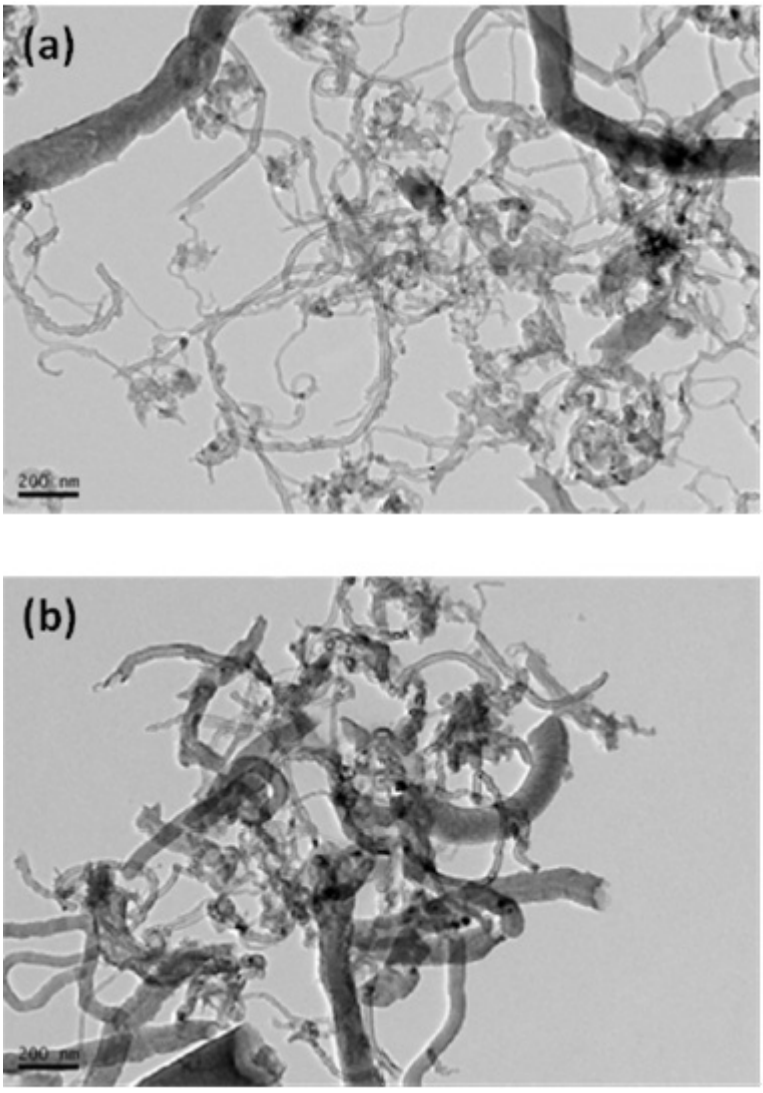

Figure 18. TEM images of the MWNTs before (a) and after (b) modification by PEI. The tubes show aspect ratios of >100:1 and in many cases are bundled. Consistent with the Raman spectra, the functionalization appears to break up the nanotubes to some extent.

Conclusions

Direct amination of MWNTs with PEI is a convenient and simple method leading to highly functionalized product that contains 6-8 % by weight PEI based on elemental analysis and thermal gravimetric analysis. The total amine groups on MWNT-NH-PEI are estimated to be *ca.* 1.5 mmol/g based on titration. The Raman spectroscopy suggests that the direct amination is a far milder procedure for grafting PEI than oxidation followed by amidation. The MWNT-NH-PEIs formed in this way produce stable emulsions in water below pH 9 and can be derivatized to form alkylated MWNTs that are dispersible in organic media. Thus, the free amine groups of MWNT-NH-PEI can be used as chemical linkers for forming ultrathin nanocomposites on surfaces or immobilizing other compounds on the MWNTs.

CHAPTER V

SUPERHYDROPHOBIC SURFACES FORMED USING LAYER-BY-LAYER SELF-ASSEMBLY WITH AMINATED MULTIWALL CARBON NANOTUBES*

Introduction

The wetting behavior of solid surfaces by a liquid is a very important property for surface chemistry. In recent years, superhydrophobic and self-cleaning surfaces have attracted significant interest not only because of their potential applications,[103-107] but also because of a renewed interest and new insights into the fundamental aspects of wetting behavior[108-112] that has been inspired by superhydrophobic living organisms in nature such as lotus leaves[113,114] and water-striders (legs).[115] Artificial superhydrophobic surfaces are most commonly fabricated in one of two general ways: first, they can be produced by creating hierarchical micro/nanostructures on hydrophobic substrates[116,117] or, second, they can be prepared by chemically modifying a micro/nanostructured surface with molecules of low surface free energy.[118-120] It is known that deposition of anisotropic nanoparticles is a simple way to construct a rough surface with micro/nanostructures.[121-124] Given the broad success of layer-by-layer (LbL) syntheses and our own interest in covalent LbL self-assembly of polymers,[14,40,44,99] we have explored the possibility of applying such approaches using functionalized anisotropic nanoparticles as components for the construction of superhydrophobic interfaces on polyethylene (PE).

---

*Reproduced in part with permission from Liao, K.-S.; Wan, A.; Batteas, J. D.; Bergbreiter, D. E. *Langmuir,* **2008,** *24,* 4245-4253.

LbL self-assembly processes based on ionic, hydrogen bonding, or covalent interactions are widely used strategies for surface modification.[3,4,6] In such processes, thin nanocomposite films are assembled on a surface by alternately depositing mutually attractive molecules or particles. In the most common case, these mutually attractive species are positively and negatively charged polymers. In this chemistry, a "bilayer" is formed by depositing a cationic polymer onto an anionic polymer bound to a surface. Subsequent alternating additions of more cationic and anionic polymers produce additional "bilayers". This process is performed again and again until the grafted thin film so formed reaches the desired thickness or the surface has the desired properties. The work described below includes an example of this chemistry using alternating depositions of aminated multiwall carbon nanotubes and poly(acrylic acid). This work also demonstrates that a covalent LbL self-assembly of an electrophilic polyanhydride-containing polymer and these same nucleophilic aminated multiwall carbon nanotubes is comparable in efficiency to an ionic LbL self-assembly process. Both the ionic and covalently assembled films formed in these processes exhibit superhydrophobic character after final modification with hydrophobic octadecanoyl groups. However, the covalently assembled thin films are more chemically robust.

Covalent LbL self-assembly has been described previously by the our lab and others.[7] These prior studies include studies of assembly using a polyaminated or polyhydroxylated dendrimer with a polyanhydride polymer[14] and assembly of azide- and alkyne-containing polymers by Cu(I)-mediated [3+2] cycloaddition ("Click" chemistry).[41,44] We have also investigated covalent LbL self-assembly of the

nucleophilic polyethylenimine (PEI) with either an electrophilic chlorotriazine[40] or an electrophilic poly(methyl vinyl ether-*alt*-maleic anhydride) (Gantrez) polymer[99] on inorganic (silica) or organic (PE) surfaces. Like electrostatic or hydrogen bond based LbL self-assembly, these covalent assembly processes are experimentally simple and lead to functional interfaces that can be further modified to produce a desired surface property. Extending such processes to include syntheses of ultrathin nanocomposites using anisotropic nanoparticles as nucleophilic or electrophilic components provides a route to tailoring new materials with interesting surface properties. Covalently assembled surfaces are of interest as they could have better chemical durability than ultrathin nanocomposites formed ionically. The work described below has accomplished this goal. As described below, we have successfully produced ultrathin nanocomposites on PE films based on the incorporation of aminated multiwall carbon nanotubes (MWNTs) as either a basic or nucleophilic nanoparticle with poly(acrylic acid) or Gantrez as an acidic or electrophilic component in an ionic or covalent LbL self-assembly process. The ultrathin nanocomposite grafts on PE so formed have superhydrophilic or, after acylation with the mixed anhydride formed from ethyl chloroformate and octadecanoic acid, superhydrophobic character. The details of the chemical assembly and surface characteristics are described herein.

Results and Discussion

Covalent Layer-by-Layer Self-Assembly of Gantrez and MWNT-NH-PEI on PE Substrate. The process of covalent step-by-step assembly of MWNT-NH-PEI and Gantrez used here is analogous to the process we used in our previous work for covalent LbL assembly.[99] This process is shown in Scheme 5.

Scheme 5. Procedure for covalent LbL self-assembly of Gantrez/MWNT-NH-PEI on PEI grafted oxidized PE films (4) and further acylation with a mixed anhydride prepared from ethyl chloroformate and octadecanoic acid (5).

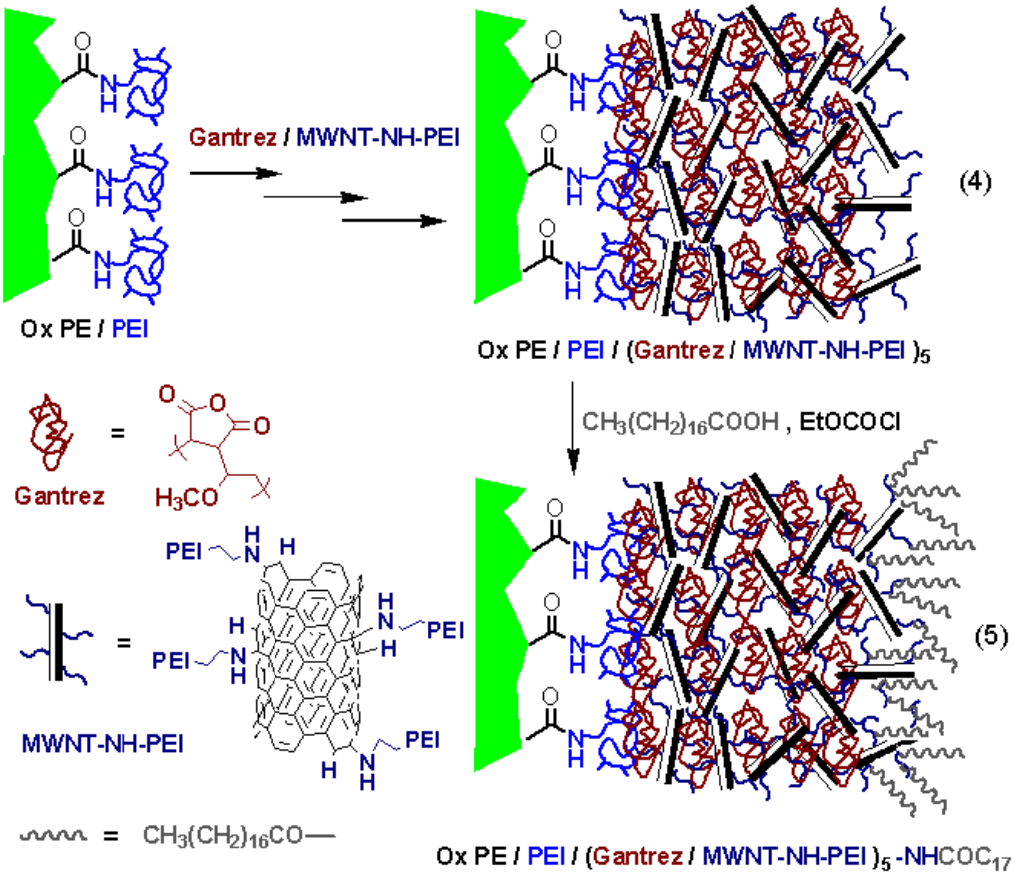

This assembly process on films yielded visibly uniform coverage with films that become darker after each bilayer deposition for the first five bilayers. To more conveniently monitor the growth of this covalent assembly process, we carried out the assembly process on PE powders, which can be more easily analyzed thermogravimetrically. TGA of (Gantrez/MWNT-NHPEI)$_x$ PE powders (Figure 19) showed a linear increase of MWNT content after each bilayer deposition. These data show that this covalent LbL assembly process of aminated MWNT nanoparticles and Gantrez has the same trend of growth as that seen in our prior covalent LbL processes that used PEI and Gantrez.[99] However, unlike the PEI/Gantrez chemistry which formed relatively smooth surfaces, a PE film modified in a covalent LbL process with (Gantrez/MWNT-NH-PEI)$_x$ nanocomposite grafts has a very rough surface. This rough polar surface is also superhydrophilic with $\Theta_a < 10°$. It is known that a superhydrophilic surface can sometimes be transformed into a superhydrophobic surface by chemical attachment of hydrophobic groups.[122,123] Gratifyingly, this proved to be true in this case, too. When PE films with (Gantrez/MWNT-NH-PEI)x nanocomposite grafts were allowed to react with a mixed anhydride prepared from ethyl chloroformate and octadecanoic acid, the resulting acylated films all exhibited superhydrophobic character ($\Theta_a = 165°$) whether the PE films were grafted with a single-bilayer nanocomposite or with a five-bilayer nanocomposite. The only notable difference was that a PE film with a five-bilayer nanocomposite graft exhibited a self-cleaning property with a water sliding angle of less than 5°. As shown in Figure 20, when the grafted PE film with a five-bilayer covalent graft is tilted 5°, the water droplet easily rolls off the surface.

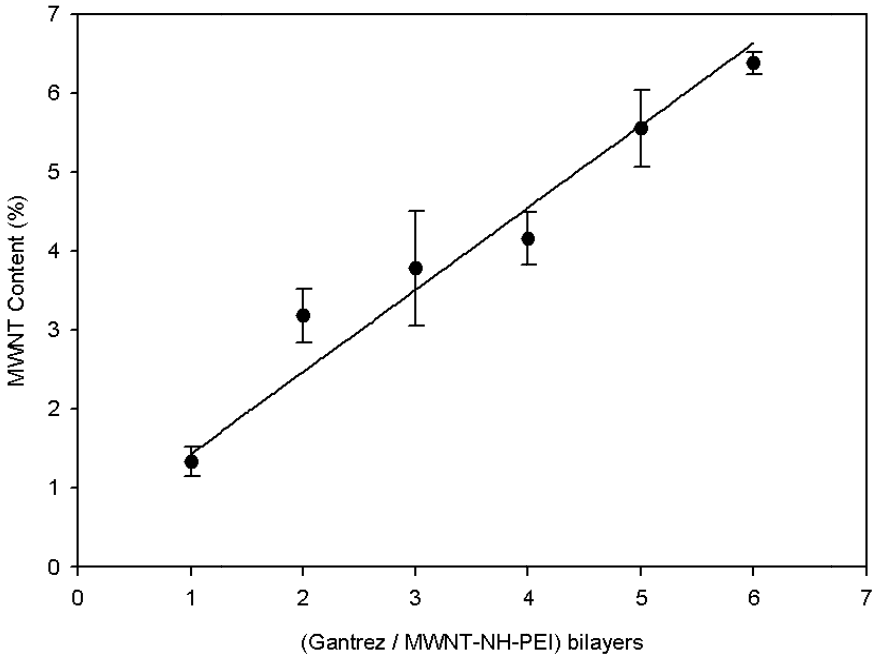

Figure 19. MWNT content of (Gantrez/MWNT-NH-PEI)$_x$ PE powders measured by TGA.

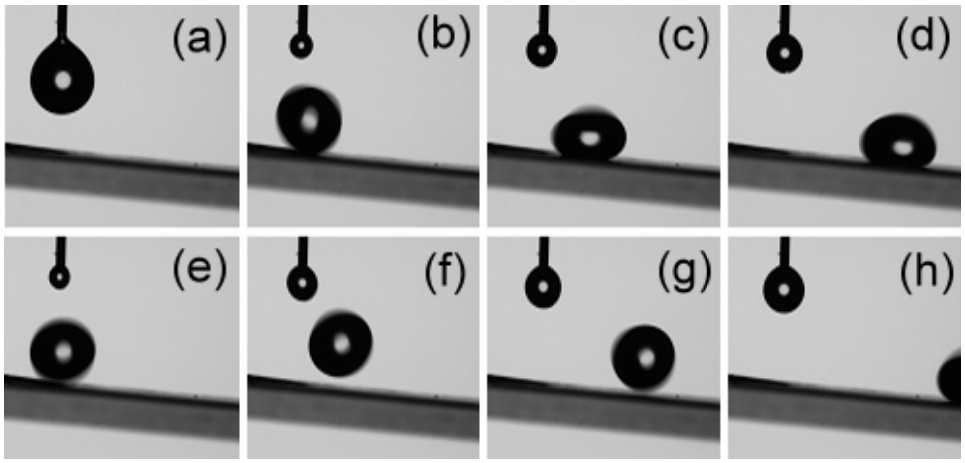

Figure 20. Water sliding behavior of a superhydrophobic film prepared by covalent assembly: (a) to (d) first water droplet rolling off the surface, (e) to (h) another water droplet. The stage is tilted 5° and the interval between each frame is 33 ms.

Ionic Layer-by-Layer Self-Assembly of MWNT-NH-PEI with PAA on PE Films. As noted above, LbL assembly does not require covalent bond formation. Indeed, it was expected that the polybasic MWNT-NH-PEI nanoparticles could also self-assemble in an ionic LbL process with an acidic polymer as shown in Scheme 6.

Scheme 6. Procedure for ionic LbL self-assembly of PAA/MWNT-NH-PEI on PEI grafted oxidized PE films (6) and further acylation with a mixed anhydride prepared from ethyl chloroformate and octadecanoic acid (7).

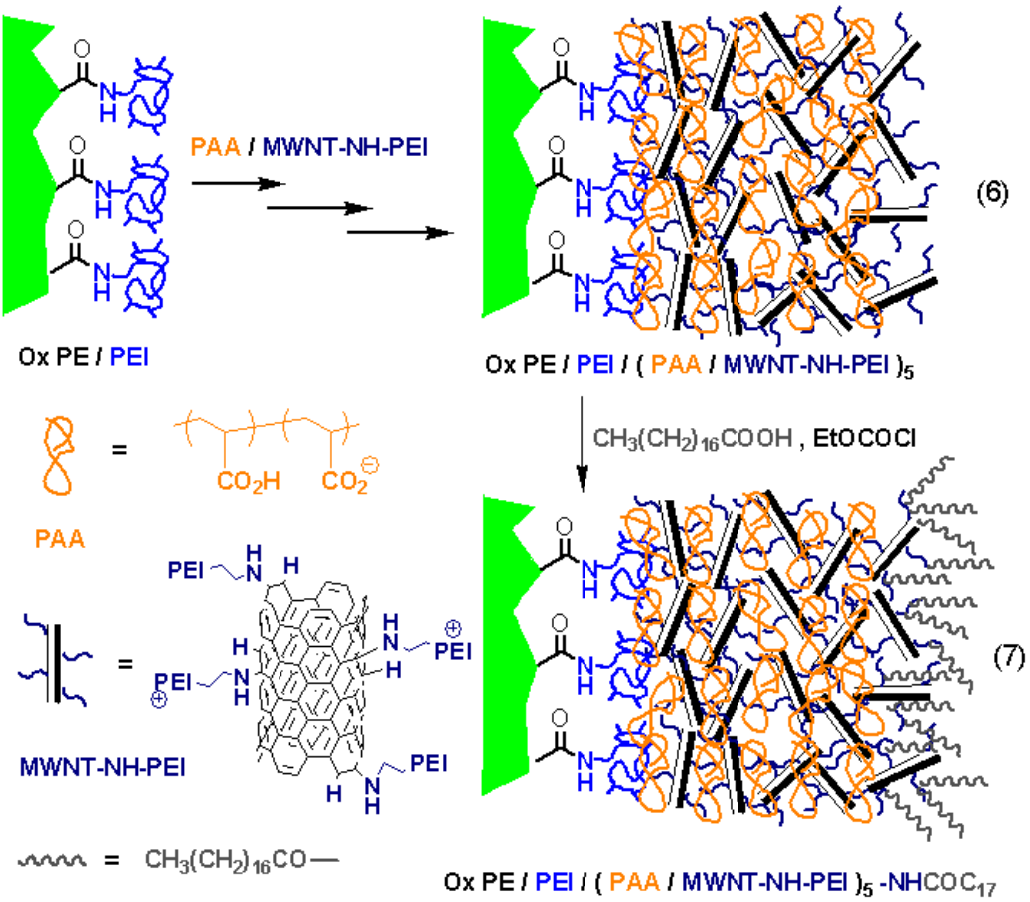

This proved to be the case, and ionic LbL self-assemblies were successfully prepared on an oxidized PE film that was covalently primed with a PEI layer (the same starting material used for the covalent LbL assembly shown in Scheme 5). The resulting grafted surfaces were also superhydrophilic with water contact angles of <10°. To test if the surface superhydrophobicity seen above was unique to the product formed by covalent LbL self-assembly, films containing these ionic LbL self-assembly nanocomposite grafts prepared using poly(acrylic acid) and the MWNT-NH-PEI nanoparticles were acylated with the mixed anhydride prepared from ethyl chloroformate and octadecanoic acid. These resulting surfaces too were superhydrophobic (Θ_a = 155°) after acylation. The ionic LbL self-assembly did however differ from the covalently grafted surface in that the ionically grafted films showed water pinning behavior. This is shown in Figure 21 where the water droplet has a high contact angle yet it is still pinned to the surface even when the film is tilted 180°.

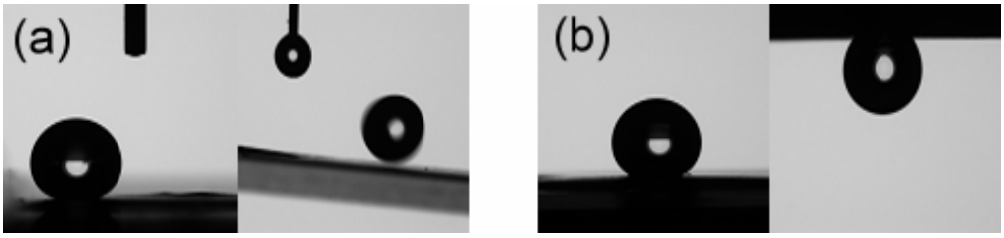

Figure 21. The surface assembled by a covalent LbL process followed by acylation (a) is superhydrophobic ($\Theta_a \sim 165^o$) and exhibits a water sliding angle < 5^o while the surface assembled by an ionic LbL self assembly process followed by acylation (b) is still superhydrophobic ($\Theta_a \sim 155^o$) but exhibits water pinning.

Chemical Stability Test of (Gantrez/MWNT-NH-PEI)$_5$-NHCOC$_{17}$ and (PAA/MWNT-NH-PEI)$_5$-NHCOC$_{17}$ PE Films. A goal of the covalent LbL self-assembly process was to prepare nanocomposite grafts that are chemically durable. This goal was achieved as the covalent amide linkages rendered the nanocomposite graft stable even under strongly acidic conditions where the ionically assembled nanocomposite grafts delaminated. As shown in Figure 22, the five-bilayer films made by either covalent or ionic LbL self-assembly showed similar surface coverage based on the darkness of both films. However, shaking with 1 M HCl for 24 h followed by a short period of sonication (0.5 h) removed much of the nanocomposite graft from the ionically grafted film, while the covalently assembled graft remained robustly bound to the surface and showed no visible changes.

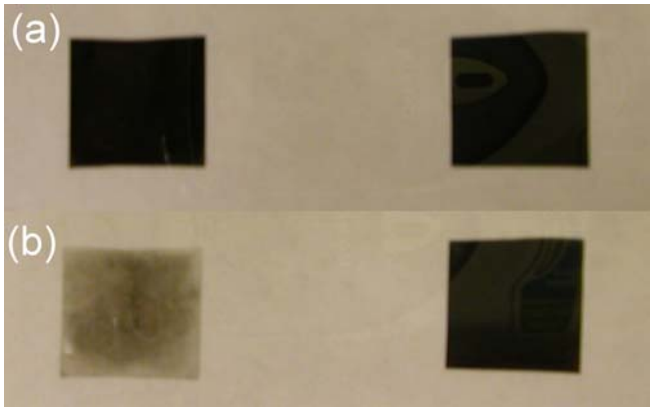

Figure 22. Results of a durability test of a 5-bilayer ionic (left) or a 5-bilayer covalent (right) LbL self-assembly nanocomposite grafted films. Samples (1 cm^2) of the grafted films were placed in 1M HCl for 24 h and treated by sonication for 0.5 h. The photographs are films (a) before the treatment and (b) after the treatment.

Experiments also showed large differences in the advancing contact angle for films after the HCl treatment and sonication. The covalently modified surface became less hydrophobic with its contact angle dropping from ~160° to ~100°. However, the ionically assembled grafted film's contact angle dropped from ~150° to ~30° under the same conditions. While the large dropping of Θ_a (~120°) of the ionically assembled film is mainly because of the delamination of grafted materials, it cannot be the reason for the moderate dropping of Θ_a (~60°) of the covalently assembled film because the film showed no delamination optically after the HCl treatment and sonication. Further analysis of the acid-treated film by AFM showed a large decrease of surface roughness (from ~300 nm to ~100 nm based on a 20 μm × 20 μm sized image), which may contribute to the moderate decrease of Θ_a. To understand the reorganization of the relatively soft polymer composites under acid condition is still an important issue for future studies.

Atomic Force Microscopy Studies and Confocal Raman Imaging. To better understand the character of these nanocomposite grafts, the surface morphology of the starting film, the ionically assembled LbL graft, and the covalently assembled LbL graft was examined by AFM (Figure 23). The initial oxidized PE surface showed the typical fibrillar structure expected for PE films (Figure 23a). Upon sequential LbL self-assembly, large clusters of MWNT-NH-PEI/Gantrez are found on the surface, with generally increasing roughness up to the fifth bilayer. Water drops placed on a sample with one bilayer graft exhibited a relatively large sliding angle of > 90°, indicating significant adhesion between the surface and the water. The AFM images suggest that

this may be due to the incomplete coverage of the underlying surface by the first graft bilayer. As seen in Figure 23b, large regions of oxidized PE remain exposed on the surface. Those regions of oxidized PE contain carboxylic acid groups that can form hydrogen bonds with water. However, after depositing additional bilayers, the fiber like oxidized PE surface was buried (Figure 23c-f). The sliding angle of these samples with additional graft bilayers decreased suddenly and was only ~5°-10° after 3 bilayers. Topographic AFM images showed that the initial oxidized PE film had a root-mean-square (rms) roughness of ~58 nm. After five covalent LbL self-assembly steps, the rms roughness of the (Gantrez/MWNT-NH-PEI)$_5$-NHCOC$_{17}$ PE film increased to ~306 nm (based on a 20 μm × 20 μm sized image). A second sample, (Gantrez/PEI)$_5$-NHCOC$_{17}$ PE film, which was prepared using a covalent LbL assembly process using PEI in place of MWNT-NH-PEI, had a contact angle of 100° and a rms roughness of only ~97 nm, indicating that the MWNTs play an important role in the formation of an ultrarough surface. The ionically assembled (PAA/MWNT-NH-PEI)$_5$-NHCOC$_{17}$ PE film sample also had a large rms roughness of ~310 nm (based on a 20 μm × 20 μm sized image), showing that ionic LbL self-assembly produces grafts with a level of roughness that is similar to that seen in covalent LbL self-assembly of Gantrez and MWNT-NH-PEI.

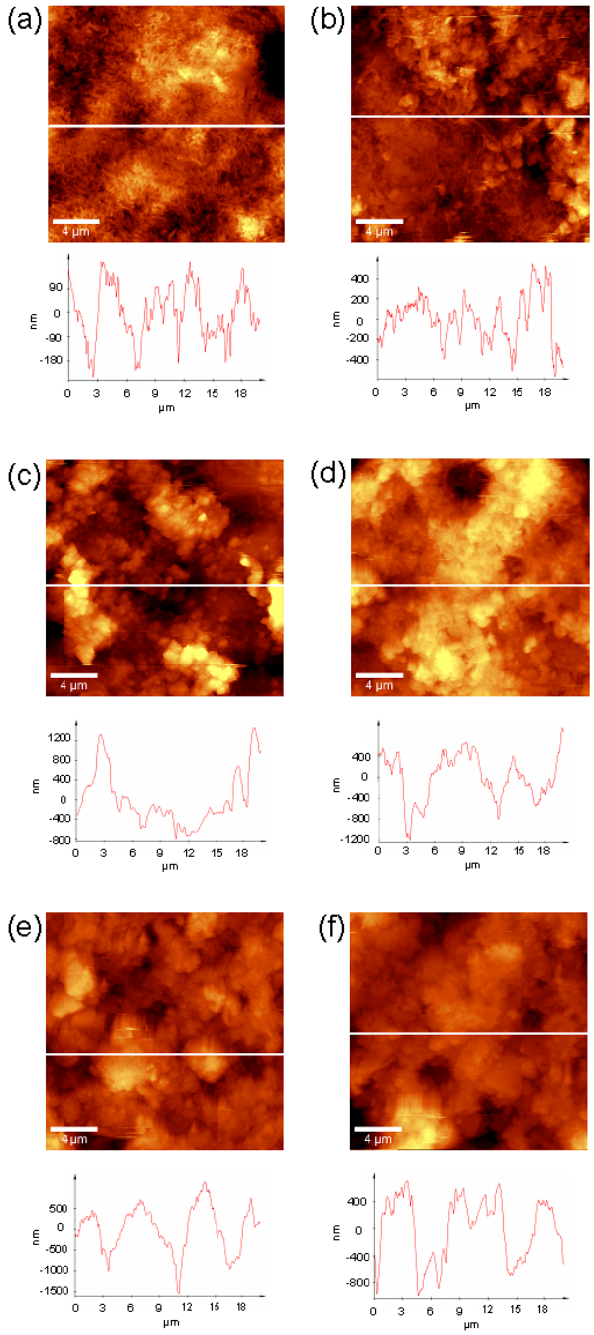

Figure 23. A series of tapping mode AFM topographic images of covalent LbL self-assembled (Gantrez/MWNT-NH-PEI)$_x$-NHCOC$_{17}$ PE films with different numbers of bilayers (x = 1, 2, 3, 4, 5): (a) oxidized PE film, (b) 1 bilayer, (c) 2 bilayers, (d) 3 bilayers, (e) 4 bilayers, and (f) 5 bilayers.

Spatial variations in the MWNT coverage were examined by confocal Raman microspectroscopy. The Raman spectrum of the (Gantrez/MWNT-NH-PEI)$_5$-NHCOC$_{17}$ PE film showed a D band and G band of MWNTs at 1354 and 1584 cm^{-1}, respectively, and also a 2D band at 2710 cm^{-1} (Figure 24c). Horizontal and vertical Raman mapping based on the intensities of the G band and D band indicated that MWNTs were distributed throughout the sample (Figure 24a and 24b). High-resolution Raman images taken with a 100×, 0.9 NA objective were convoluted with the significant height variations over the sample of nearly 800 nm, which moves materials in and out of the focal plane of the image. This was confirmed by images taken with a 20×, 0.45 NA objective which has a larger focal volume and shows that the tubes are distributed fairly uniformly throughout the samples.

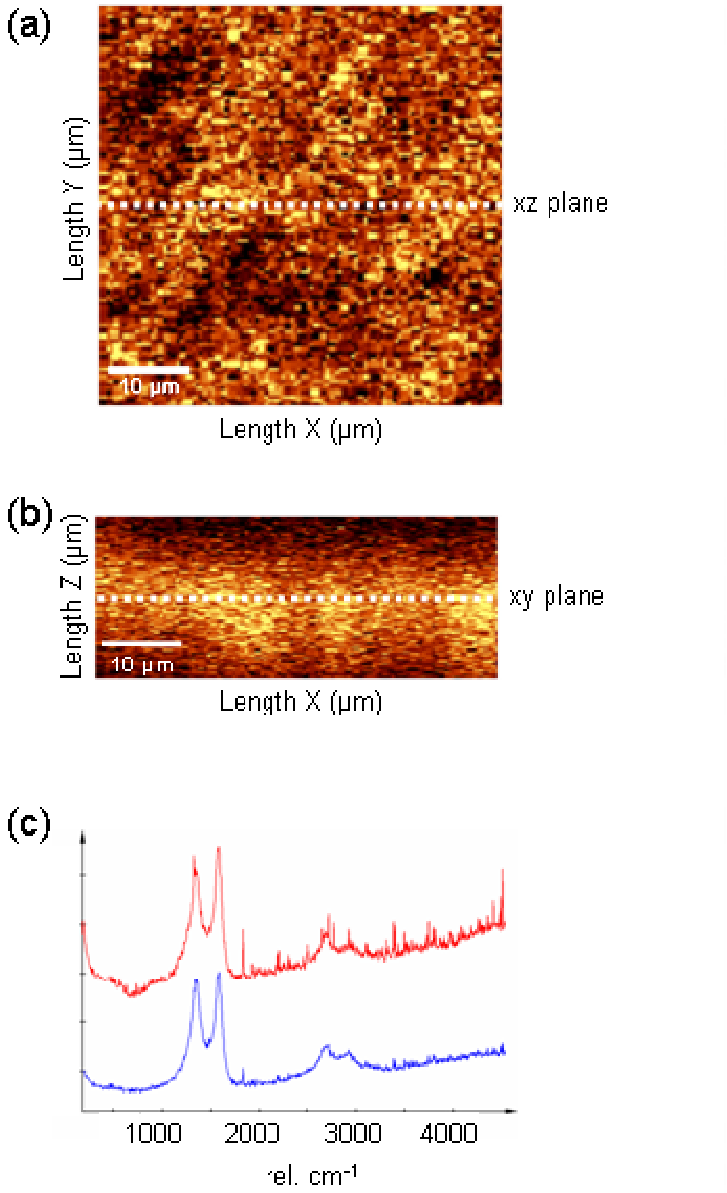

Figure 24. Raman spectrum of the (Gantrez/MWNT-NH-PEI)$_5$-NHCOC$_{17}$ PE film and relative Raman images in the spectrum range of 1050 to 1700 cm^{-1}. (a) Raman image in the X-Y plane. (b) Raman image in X-Z plane. (c) Integrated average Raman spectrum obtained from the image (red) as compared to that of a pure MWNT sample (blue).

Conclusions

Superhydrophobic PE films can be formed either from ionic LbL self-assembly of MWNT-NH-PEIs and poly(acrylic acid) or from covalent LbL self-assembly of MWNT-NH-PEIs and Gantrez when the final graft is acrylated with a mixed anhydride prepared from ethyl chloroformate and octadecanoic acid. While the ionically assembled nanocomposite graft is labile under acidic conditions, the covalently assembled graft is more chemically robust. A variety of analyses show that the MWNTs are distributed uniformly in the product grafts. AFM shows that these self-assembly processes that couple anisotropic MWNTs with Gantrez or poly(acrylic acid) produce ultrarough surfaces. The self-cleaning property of the superhydrophobic surface combined with the properties of MWNTs may bring novel applications in the future.

CHAPTER VI

SOLUTE RESPONSIVE WETTABILITY AT FUNCTIONAL SURFACES FORMED BY COVALENT LAYER-BY-LAYER SELF-ASSEMBLY

Introduction

'Smart' surfaces[125-127] respond to external stimuli such as pH, temperature, or solvent and are of interest in many applications. However, while large changes in permeability, wettability or reactivity would be of most interest, the observed changes vary in magnitude. Large differences in wettability or permeability are seen with ionizable surface grafts.[14,128,129] Varied effects are seen for thermally responsive surfaces containing species like poly(*N*-isopropylacrylamide) (PNIPAM) that have lower critical solution temperature (LCST) behavior.[130-137] For example, we only saw small changes in the I_1/I_3 ratio for fluorescence of a PEG-pyrene-labeled thermoresponsive surface.[138] In addition, while Hofmeister effects at interfaces are known,[139-141] easily prepared surfaces with significant Hofmeister-like anion-responsive wettability have little precedence. This is surprising given the extensive studies of such effects and the sharp and visually obvious phase transitions seen for polymers like PNIPAM at their LCST.[126,142-144] Here we describe nanocomposite PNIPAM-containing surfaces that exhibit large reversible changes in solute responsive wettability.

Responsive surfaces with significant, reversible, reproducible wettability changes can be prepared by covalent layer-by-layer (LbL) grafting chemistry.[14,145] In prior work, condensation of an electrophilic anhydride-containing polymer with a polyvalent amine-containing dendrimer or MWNT (multiwall nanotubes) led to covalent nanocomposite grafts. Such grafts with pH-responsive groups exhibited pH-responsive wettability. Nanocomposites with surface roughness prepared this way could be chemically modified to be superhydrophobic or superhydrophilic. Here we describe nanocomposite grafts whose hydrophobic or hydrophilic character changes in response to solute concentration without chemical derivatization. This involves stepwise covalent grafting alternately using first a NIPAM and *N*-acryloxysuccinimide (PNIPAM-*c*-PNASI) copolymer and then an aminated silica nanoparticle suspension. This covalent LbL process ultimately leads to a thin film PNIPAM-containing nanocomposite (Scheme 7).

Results and Discussion

Scheme 7. Covalent LbL self-assembly of a PNIPAM-*c*-PNASI/aminated silica nanoparticle/PNIPAM graft on a PEI modified PE film.

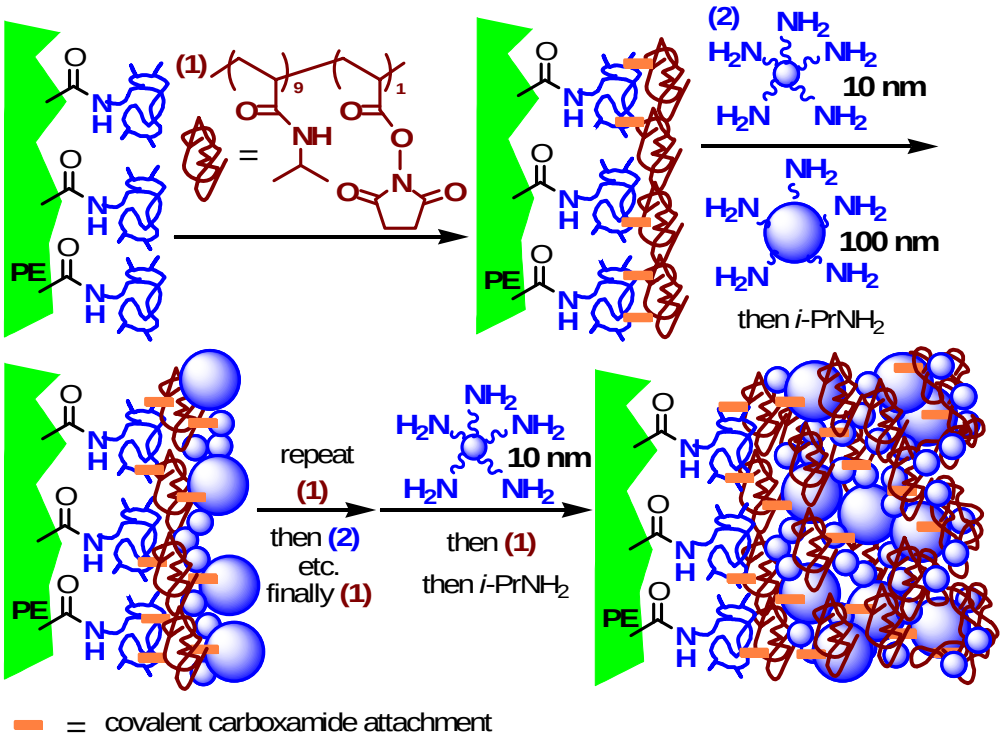

Preparing the PNIPAM-c-PNASI/Aminated Silica Nanoparticle/PNIPAM Grafts by Covalent Layer-by-Layer Self-Assembly. This synthesis uses a readily prepared electrophilic copolymer, PNIPAM-*c*-PNASI (M_n = 30,000 Da), as a reagent. The NASI groups in this polymer are known to react quantitatively with amines to form acrylamides. In the first step, the amine groups of a polyvalent aminated surface derived from the reaction of an activated, oxidized polyethylene with polyethyleneimine (PEI)[99] were allowed to react with PNIPAM-*c*-PNASI. While PNIPAM-*c*-PNASI covalently

binds to the surface, spatial constraints preclude complete consumption of the NASI groups of PNIPAM-*c*-PNASI leaving unreacted NASI groups that can react in a second step with amine groups of amine-functionalized 10- and 100-nm diameter silica nanoparticles. As shown in Scheme 7, this reaction produces an amine-rich surface. While this surface could be used as is for further grafting, we treated this surface with excess *i*-$PrNH_2$ to convert unreacted NASI groups into NIPAM groups. The covalent LbL assembly then continued with further stages of PNIPAM-*c*-PNASI/10- and 100-nm aminated silica nanoparticle/*i*-$PrNH_2$ treatment. After 7 stages, the surface was capped with PNIPAM-*c*-PNASI and treated with excess *i*-$PrNH_2$ to form the PNIPAM-*c*-PNASI/aminated silica nanoparticle/PNIPAM graft on a PEI modified PE film. These grafts contain carboxamides based on peaks at 1670 cm^{-1} and 1640 cm^{-1} as well as a Si-O peak at around 1100 cm^{-1} in the ATR-IR spectrum (Figure 25). The absorption intensity of both the carboxamide and Si-O peaks increased as the number of deposition bilayers increased. The resulting surface was further characterized by AFM (Figure 26) and had an average surface roughness of ~200 nm on a 1 μm^2 scale. The 100-nm nanoparticles are discernable at the surface of the film and define the local surface roughness. Although it is difficult to observe the 10-nm nanoparticles in the AFM image, some discussions in the literature and some preliminary work suggests it is crucial to have both 100-nm and 10-nm nanoparticles in the dipping mixture in order to create high surface roughness.[119]

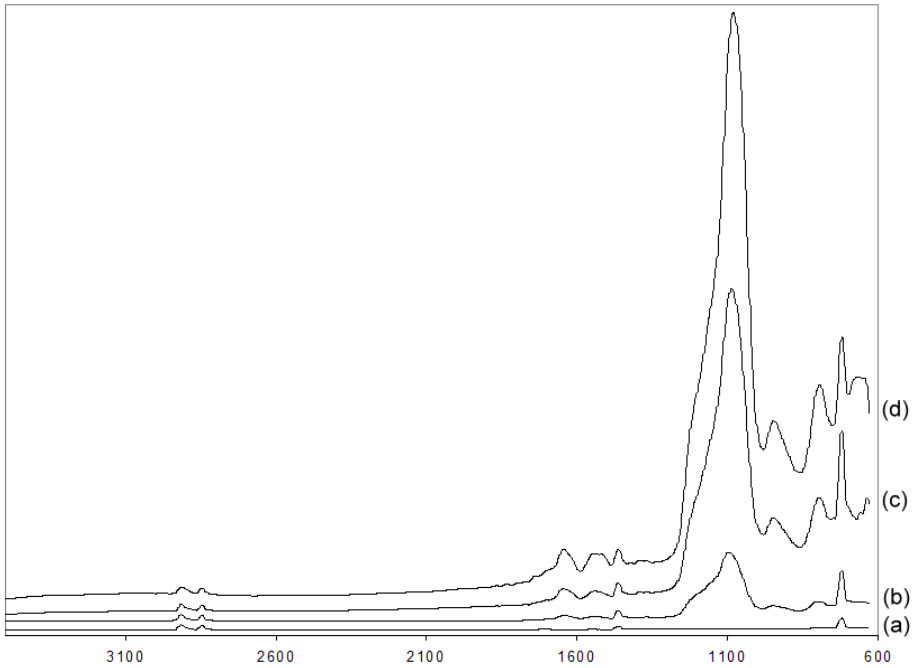

Figure 25. ATR-IR spectra of (a) oxidized PE and PE_{oxid}-(PNIPAM-*c*-PNASI/aminated silica nanoparticles)$_x$ –PNIPAM surface which (b) x = 2; (c) x = 4; (d) x = 6.

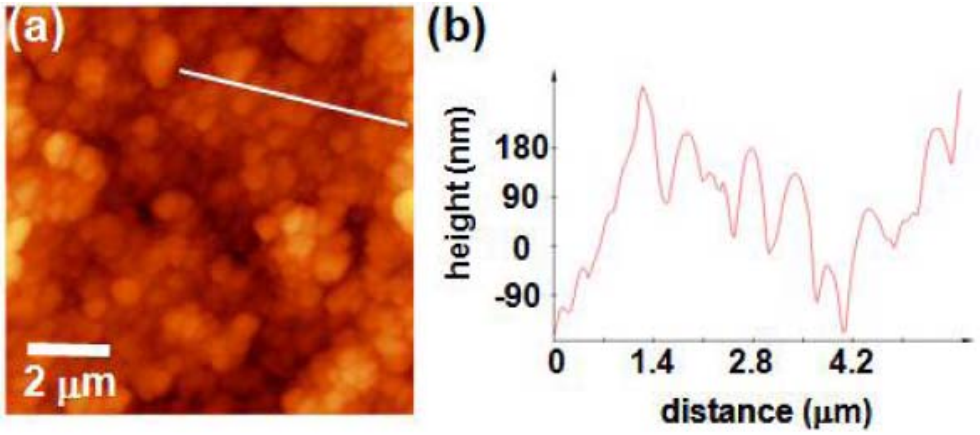

Figure 26. (a) Tapping mode AFM image (10 µm x 10 µm) of a PE_{oxid}-(PNIPAM-*c*-PNASI/aminated silica nanoparticle)$_7$/PNIPAM surface. The nanoparticles are discernable at the surface of the film and define the local surface roughness. (b) Cross-section along the line marked in (a).

Solute Responsive Wettability. The graft surfaces prepared by covalent LbL assembly of PNIPAM-*c*-PNASI and aminated silica nanoparticles exhibit a time dependent wettability. As shown in Figure 27, when a water droplet was added to the graft surface, the static contact angles (Θ) decreased rapidly in the first five seconds because of the surface reorganization. Later, the Θ values decreased more slowly (about 1º min^{-1}) because of the water evaporation (Figure 28). In order to compare solute responsive wettability for different salt solutions, all photographs were taken after 6 minutes, at which point the Θ values were measured.

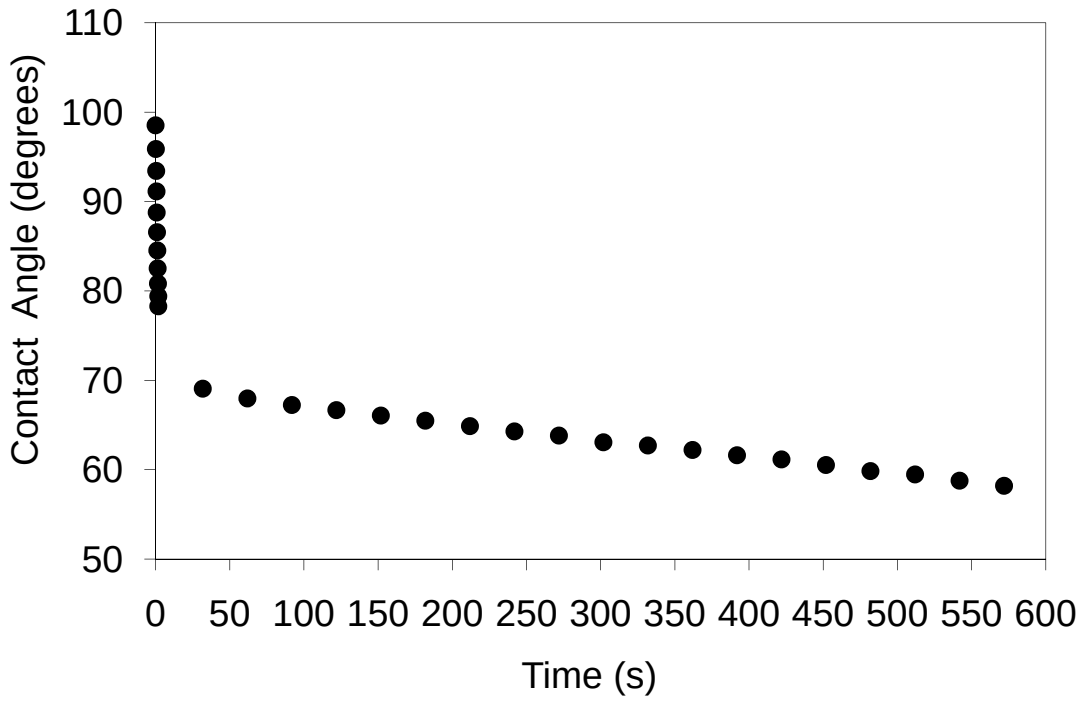

Figure 27. Θ values of a PE_{oxid}-(PNIPAM-*c*-PNASI/aminated silica nanoparticle)$_7$/ PNIPAM surface measured with water as a function of time.

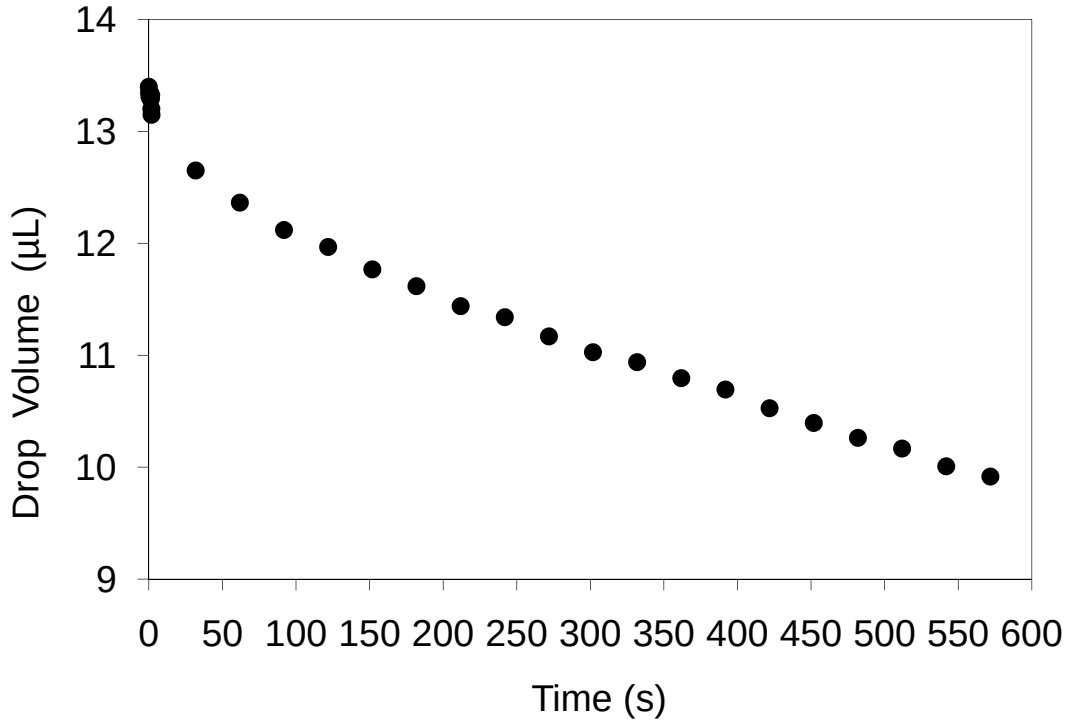

Figure 28. Water drop volume on a PE_{oxid}-(PNIPAM-*c*-PNASI/aminated silica nanoparticle)$_7$/ PNIPAM surface measured as a function of time.

The graft surfaces prepared by covalent LbL assembly of PNIPAM-*c*-PNASI and aminated silica nanoparticles are the first examples of a surface to exhibit wettability that is dependent on the concentration and identity of a solute salt. With water, the static contact angle (Θ) of a PNIPAM-*c*-PNASI/aminated silica nanoparticle grafted surface was 60º while with 1.4 M Na_2SO_4 (a Hofmeister kosmotrope) the Θ value was 125º. This 65º change in contact angle with water versus 1.4 M Na_2SO_4 was much larger than the ΔΘ seen using these same solutions on glass, unfunctionalized PE, oxidized PE, or a

PEI/Gantrez graft on PE that was grafted with PNIPAM.[131] Those surfaces had smaller ΔΘ values of 8º, 4º, 7º, and 15º.

Procedures using both 100-nm and 10-nm nanoparticles in the assemble mixture were shown to be crucial for successful assembly of covalent LbL grafts with large ΔΘ. Procedures using only 100-nm or only 10-nm nanoparticle mixture in the covalent LbL deposition didn't generate surfaces with the large ΔΘ observed previously (30 to 40º compared to 65º with water vs. 1.4 M Na_2SO_4). Also, the surface made with capping a bilayer of 10-nm aminated silica nanoparticles/PNIPAM-*c*-PNASI has a larger ΔΘ (65º) than one made without capping (45º). This result agreed with the study by Rubner group. Their study concluded that the hierarchical roughness generated by assembling nanoparticles with two different scales is necessary to fabricate superhydrophobic surface.[119]

The errors inherent in studying water contact angles and the modest changes seen in solute responsive wettability with other PNIPAM grafts usually preclude an extensive study of solute responsiveness with grafts. In contrast, the large solute responsive wettability of these PE_{oxid}-(PNIPAM-*c*-PNASI/aminated silica nanoparticle)$_7$-PNIPAM surfaces allowed us to examine the concentration dependence of wettability changes with solute anions. The results of these studies (Figure 29) parallel results seen in solution-state studies though there were some differences. First, Na_2CO_3, a generally strong kosmotrope,[143] only has a modest effect on wettability of these graft surfaces. We speculate that this is a result of the basicity of this solution which produces $–NH_2$ groups at the surface that would otherwise be present as $–NH_3^+$ groups in less basic solutions.

Second, aqueous solutions of sodium thiocyanate, a chaotropic anion known to exhibit salting in behavior for PNIPAM,[142] hydroxymethylcellulose[146] and other macromolecules[147] with LCST behavior, exhibits salt-enhanced wetting wherein a 1.2 M NaSCN solution has a lower contact angle than H_2O, 0.1 M NaSCN, or 2.0 M NaSCN. Salt-enhanced wetting is also seen for NaI though the differences in the latter case are closer to the error in contact angle measurements.

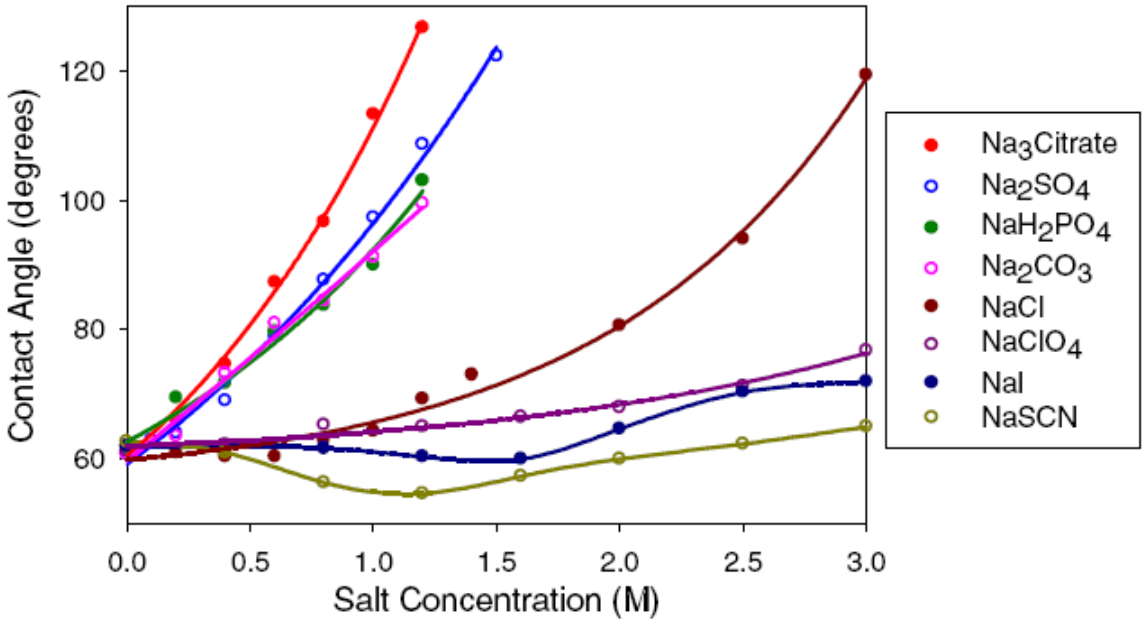

Figure 29. Θ values of a PE_{oxid}-(PNIPAM-*c*-PNASI/aminated silica nanoparticle)$_7$/ PNIPAM surface measured with solutions of various sodium salts as a function of salt concentration. Each data point is the average of three individual measurements and has an error of ± 2º.

The effects of solutes on surface wettability are reversible. As shown is Figure 30, when a film prepared as shown in Scheme 7 had its Θ analyzed using pure water, the Θ value was 58º. The surface was washed with THF, dried and then analyzed using 1.4 M Na_2SO_4 solution, the Θ value was 127º. If that same surface was washed with distilled water, washed with THF, dried, and reanalyzed using water, it had a Θ of 58º, the same contact angle seen for a film that had never been exposed to Na_2SO_4. The contact angles with water or 1.4 M Na_2SO_4 didn't change significantly during the time frame of multiple measurements (about 3 weeks). It proves that the film is stable under ambient conditions and still retains its reversible wettability. However, the film did show some degradation after extend period of measurements using various salt solutions. After ca. 100 cycles using various salt solutions, THF, and water, the ΔΘ values (1.4 M Na_2SO_4 vs. H_2O) gradually decreased to ca. 50º. We suspect that salt ions, especially the chaotropic ones, may change the interaction between polymer grafts and nanoparticles. The reorganization between polymer grafts and nanoparticles may cause the decrease of surface roughness. The reorganization has happened in our previous covalent LbL assembly of MWNT-NH-PEI with Gantrez. The surface lost its superhydrophobicility after 24 h treatment of strong acid because of the decrease of surface roughness (Chapter V).

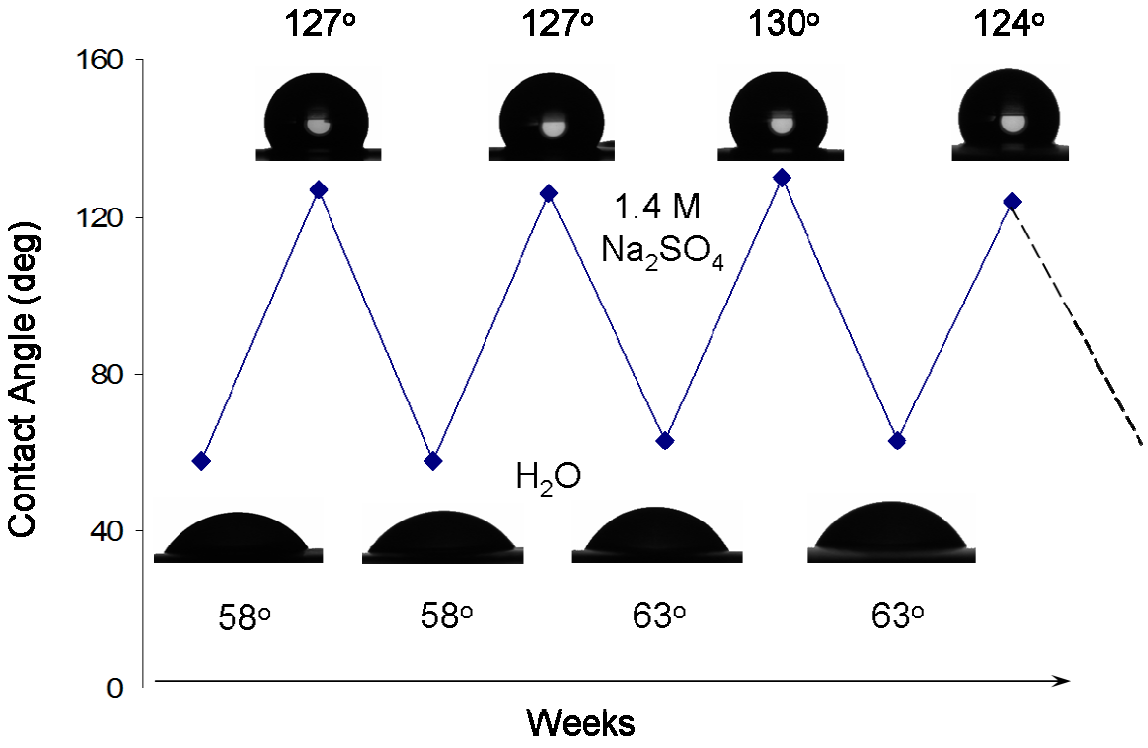

Figure 30. Θ values of a PE_{oxid}-(PNIPAM-*c*-PNASI/aminated silica nanoparticle)$_7$/ PNIPAM surface measured with water and 1.4 M Na_2SO_4 solutions during the time frame of multiple measurements (about 3 weeks).

In solution state studies, cations have small effects on LCSTs. The effects of cations on Θ measured using aqueous solutions containing varying concentrations of sulfate salts (Figure 31) show cations can have a significant effect on ΔΘ. Preliminary studies using cations with Cl^- anions show similar behavior but since the ΔΘ seen with Cl^- is modest, it is difficult to reliably investigate the effects of changing Cl^- concentrations.

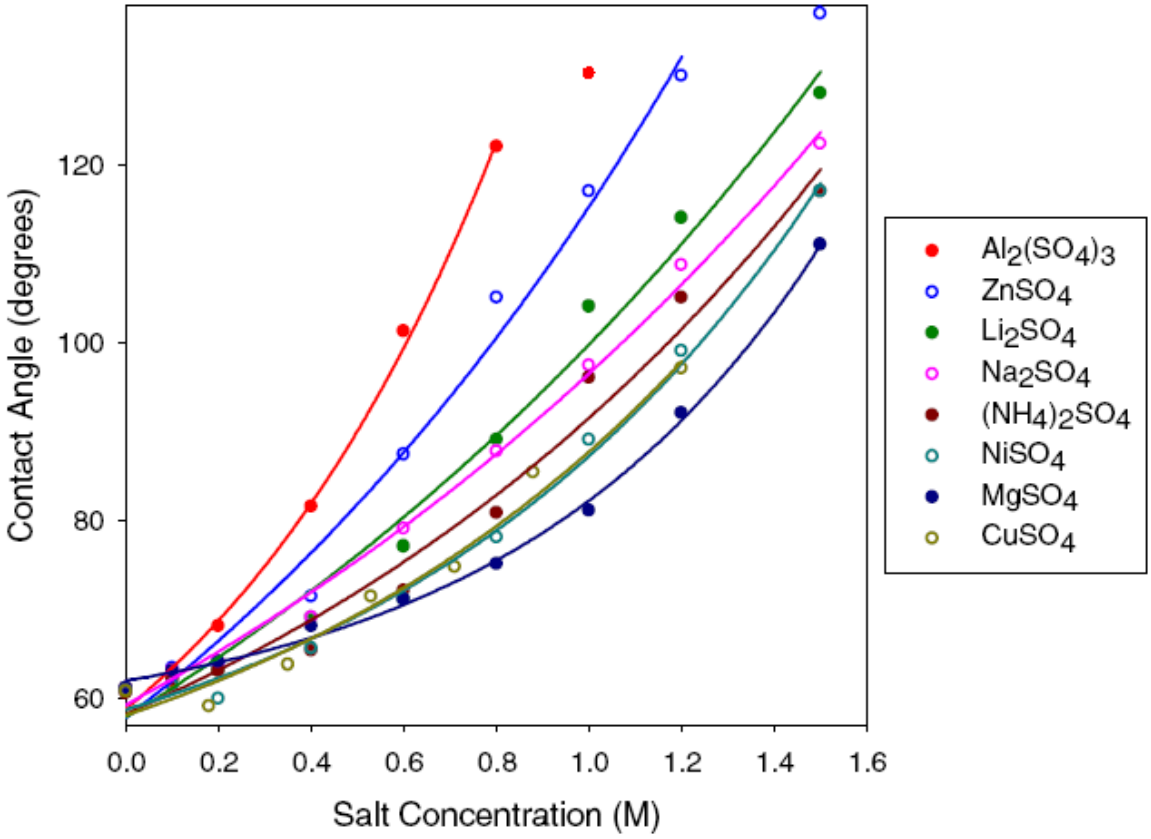

Figure 31. Θ values for a PE_{oxid}-(PNIPAM-*c*-PNASI/aminated silica nanoparticle)$_6$/ PNIPAM surface measured with solutions of various sulfate salts as a function of salt concentration. Each data point is the average of three individual measurements and has an error of ± 2º.

Dynamic Contact Angle Measurements. When a small water drop encounters a solid surface, a droplet is formed that consists of a sphere of water sectioned by the surface at a discrete, measurable contact angle (Θ). If a droplet on a surface is carefully withdrawn from the droplet with a syringe, the droplet decreases in volume and contact angle, maintaining the same contact area with the surface until it begins to recede. It

recedes with a constant contact angle, Θ_r, characteristic of the surface chemistry and topography. If a droplet on a surface is carefully added to the droplet with a syringe, the droplet volume and contact angle increase, and again, the same contact area is maintained until the droplet begins to advance. It does so at a constant advancing contact angle, Θ_a, which is also characteristic of the surface chemistry and topography. There are arguments that static contact angle (Θ) is less meaningful and only designates a metastable angle somewhere between Θ_a and Θ_r.[109] Therefore, dynamic contact angle measurements were also carried out on the resulting responsive film. Θ_a and Θ_r were recorded as water was added to or withdrawn from a 13 μL water droplet, which was pre-deposited on the resulting surface 2 minutes before the measurement.

To measure the Θ_r, we carefully withdrew the water from the droplet with a syringe. The droplet decreased in volume and contact angle gradually, maintaining the same contact area with the surface. Interestingly, we didn't observe any receding events even when the essentially the entire water droplet was withdrawn by the syringe. Therefore, the Θ_r is 0°. The same event happened when we withdrew all the solution from the droplet of a 1.2 M Na_2SO_4. A thin, smooth layer of Na_2SO_4 salt remained on the surface after the water in the salt solution evaporated.

To measure the Θ_a, we carefully added the water to the droplet with a syringe. The droplet increased in volume and contact angle gradually, maintaining the same contact area with the surface until the droplet begins to advance. The effects of anions on Θ_a measured using aqueous solutions containing varying concentrations of sodium salts are shown in Figure 32. For chaotropic anions such as NaSCN, the trends were similar to

the trends shown in Figure 29. Salt-enhanced wetting occurred wherein a 0.6 M (NaSCN) solution had a lower Θ_a (68°) than in water (76°). However, for kosmotropic anions such as sodium citrate, Na_2SO_4, NaH_2PO_4 and NaCl, the results were very different than the results shown in Figure 29. Instead of gradual increase of Θ as the salt concentration increased, the increase of Θ_a followed a sigmoidal curve with inflection points from around 0.6 M (sodium citrate) to 1.2 M (NaCl). Nonetheless, the solute responsive wettability of the prepared surface based on Θ_a values still followed the Hofmeister series.

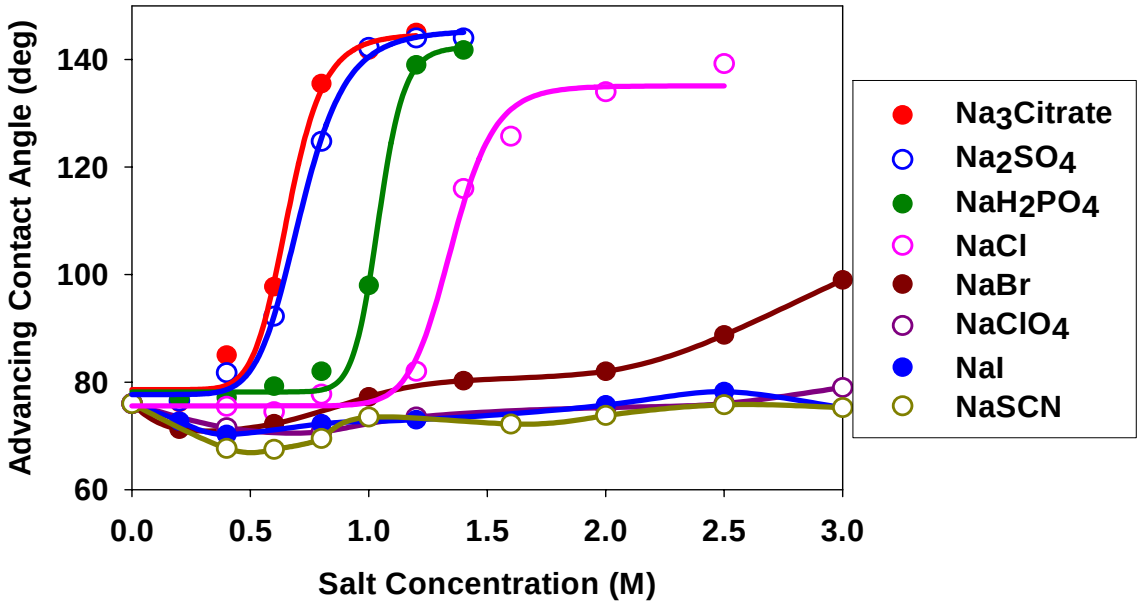

Figure 32. Θ_a values of a PE_{oxid}-(PNIPAM-*c*-PNASI/aminated silica nanoparticle)$_7$/ PNIPAM surface measured with solutions of various sodium salts as a function of salt concentration. Each data point is the average of three individual measurements and has an error of ± 2º.

Atomic Force Microscopy Studies. AFM measurements of the PE_{oxid}-(PNIPAM-*c*-PNASI/aminated silica nanoparticle)$_6$-PNIPAM surfaces show visible changes in surface texture when moving from one solute to the next (Figure 33). In air the surfaces are rough and the larger ca. 100 nm silica particles dominate the surface morphology. Upon immersion in water, the film is observed to swell with a noted decrease in surface roughness from ca. 287 nm rms to ca. 170 nm rms. The introduction of Na_2SO_4 results in an increase in roughness along with the corresponding dramatic increase in water contact angle. When this solution is exchanged for NaSCN, the surface roughness again decreases. This illustrate the surfaces are reconfigurable in different solute conditions and that the changes in water contact angle are likely due to combination of change in surface roughness along with swell and intercalation of the solute ions into the PNIPAM surface.

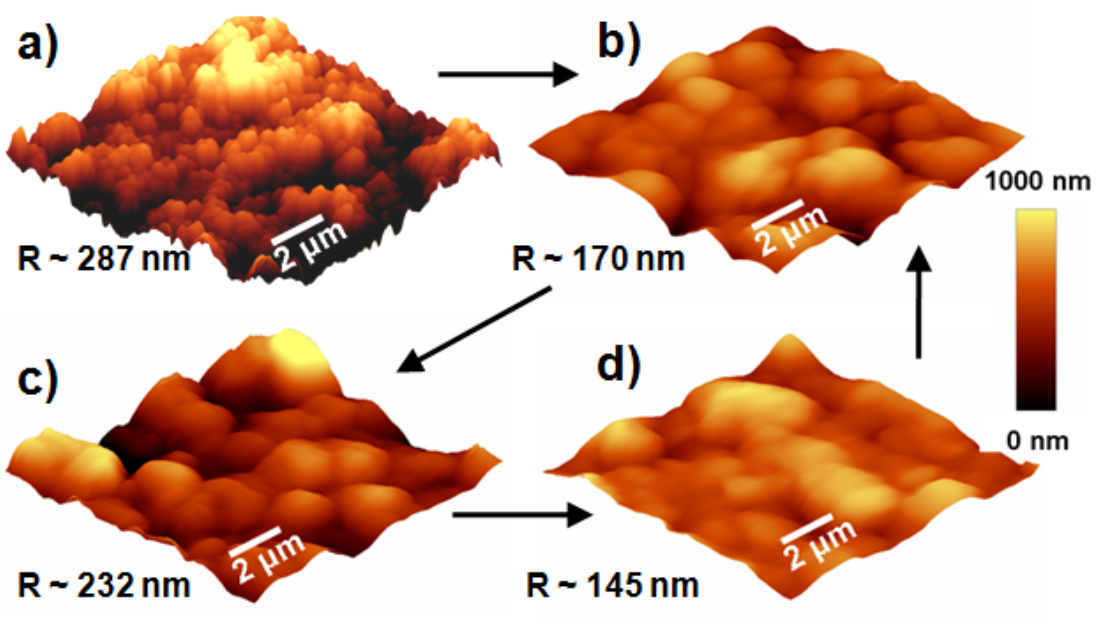

Figure 33. Tapping mode AFM images of PE_{oxid}-(PNIPAM-c-PNASI/aminated silica nanoparticles)$_7$ –PNIPAM obtained in (a) air (b) water (c) 1.4 M Na_2SO_4 and (d) 1.2 M NaSCN. Returning to water yields to a similar structure to (b). The average RMS roughness of the surface in each environment is listed below each figure.

Conclusions

Responsive surfaces with significant, reversible, reproducible wettability changes can be prepared by covalent LbL grafting chemistry using PNIPAM-*c*-PNASI and aminated silica nanoparticles. A 65º $\Delta\Theta$ value was observed with water vs. 1.4 M Na_2SO_4, which is much larger than the $\Delta\Theta$ seen using these same solutions on other non-functional surfaces. The prepared film shows a high surface roughness of ~300 nm, which contributes to the large solute responsive $\Delta\Theta$ values. The solute responsive wettability of the prepared surface generally follows the Hofmeister series in both anions and cations. The receding contact angles (Θ_r) of the graft surface are 0° with both water and Na_2SO_4 solutions. The advancing contact angles (Θ_a) of the graft surface are similar to the static contact angles (Θ) for chaotropic anions. However, for kosmotropic anions, the Θ_a values followed a sigmoidal curve rather than increased gradually. The surfaces are reconfigurable in different solute conditions and that the changes in water contact angle are likely due to combination of change in surface roughness along with swell and intercalation of the solute ions into the PNIPAM surface. The significant, reversible, reproducible wettability changes give us a new and easy way to probe the changes on surfaces. It may be used as a platform for fundamental studies such as protein-surface interactions, or applications such as anti-fouling materials.

CHAPTER VII

EXPERIMENTAL SECTION

Materials and General Methods. All reagents and solvents were obtained from commercial sources and used without further purification unless specified. Water was obtained from a Milli-Q water purification system. PE films or powder used here were Fortiflex HDPE J60-800-178 which has a density of 0.96 g/cm^3. The thickness of PE films was 3-mil. The PE powder had an average particle size of 1.7 mm with a very broad size distribution. ^{1}H NMR spectra were obtained on Varian Inova 300, Mercury 300, or Inova 500 spectrometers at 300 or 500 MHz. ^{13}C NMR spectra were obtained on Varian Inova 300, Mercury 300, or Inova 500 spectrometers at 75 or 125 MHz. ^{1}H and ^{13}C NMR spectroscopy chemical shifts are reported in ppm referenced to tetramethylsilane, or residual solvent peaks respectively.

Oxidation of PE Powder. The PE powder was extracted for 12 h with CH_2Cl_2 in a Soxhlet apparatus and dried at reduced pressure. The PE powder was then oxidized using $CrO_3/H_2SO_4/H_2O$ (1:1:2 by weight) at 90 °C for 1 h, washed with water and acetone, and allowed to air-dry. The oxidized PE powder was then extracted for 12 h with CH_2Cl_2 in a Soxhlet apparatus and dried at reduced pressure.

Preparation of PEI/Gantrez Hyperbranched Grafts on Oxidized PE Powder. Oxidized PE powder (10 g) was first activated by treatment with a mixture of ethyl chloroformate (5 mL) and *N*-methylmorpholine (5 mL) in 60 mL of *N,N*-dimethylformamide for 15 min. Next, the powder was isolated by filtration, solution

washed with CH_2Cl_2, and allowed to air-dry. The activated PE powder was then placed into a 60 mL solution of CH_2Cl_2 and PEI (branched, M_n = 10 000; 1.5 g) for 1 h. After isolating the PE by filtration and washing it with CH_2Cl_2 and MeOH, the PEI treated PE powder was placed into a solution of triethylamine (10 mL) and of MeOH (60 mL) for 5 min to ensure that any surface ammonium salts were neutralized. The aminated PE was again isolated by filtration, washed with MeOH, and allowed to air-dry. This PEI-treated PE powder was then placed into 60 mL of tetrahydrofuran (THF) solution of poly(methyl vinyl ether-alt-maleic anhydride) (Gantrez, M_n = 1,130,000; 1.5 g) containing ethylenediamine (28 μL) for 1 h, isolated by filtration, washed with THF, and allowed to air-dry. The Gantrez-treated PE powder could then be placed into the PEI solution to reform a nucleophilic aminated surface. This cycle of PEI treatment followed by Gantrez treatment was repeated five times to obtain the PEI-6/Gantrez-5 PE powder.

Characterization of the PEI/Gantrez Grafts on PE Substrates. Attenuated total reflection-infrared (ATR-IR) spectroscopy was used to confirm growth of the PEI/Gantrez graft on the PE surface. A Bruker Tensor 27 series FT-IR, with a Pike MIRacle ATR accessory at an angle of 45° using a ZnSe crystal, was used. In these spectra, the integrated intensity of the amide peak (1640-1650 cm^{-1}) and carboxylate peak (1550-1560 cm^{-1}) is shown to increase in comparison with the intensity of the underlying bulk polymer C-H absorption (2910 and 2850 cm^{-1}). Titrimetric analysis was carried out by first suspending a weighed amount of the PEI/Gantrez PE powder in a 0.01 M HCl solution and shaking the mixture for 1 h. An aliquot of the resulting HCl solution was titrated with a 0.01 M NaOH solution. In this way, the amount of HCl

consumed by basic groups (amine and carboxylate) on the PEI/Gantrez PE powder could then be determined. The average numbers of millimoles of basic groups of PE powder for PEI-1, PEI-2/Gantrez-1, PEI-3/Gantrez-2, PEI-4/Gantrez-3, PEI-5/Gantrez-4, and PEI-6/Gantrez-5 PE powder were 0.0380, 0.2332, 0.3613, 0.5089, 0.6545, and 0.8896 mmol/g of powder, respectively.

Preparation of *N*-(2-aminoethyl)-5-(*N*,*N*-dimethylamino)naphthalene-1-sulfonamide. The synthesis is carried out following a literature procedure.[52] To a solution of ethylenediamine (5.20 mL, 77.1 mmol) in THF (150 mL) at 0°C was added dropwise dansyl chloride (2.08 g, 7.71 mmol) in THF (200 mL). The reaction was stirred at 0°C for 4 h, and 1 N $HCl_{(aq)}$ (18 mL) was added. The THF was evaporated and the aqueous layer was extracted with CH_2Cl_2 (4 × 100 mL). The combined organic layer was dried with $MgSO_4$. The solvent was removed at reduced pressure using a rotary evaporator to leave a pale yellow-green oil. The crude product was purified by chromatography (CH_2Cl_2) and recrystalized from ethanol to give the product in the form of light-green needles (1.70 g, mp 149-151°C, yield 75%). ^{1}H-NMR (300 MHz, $CDCl_3$) : δ 8.51 (d, 1 H, *J* = 8.4 Hz, ArH); 8.29 (d, 1 H, *J* = 8.4 Hz, ArH); 8.22 (d, 1 H, *J* = 8.4 Hz, ArH); 7.51 (m, 2 H, ArH); 7.15 (d, 1 H, *J* = 7.6 Hz, ArH); 2.90 (m, 8 H, $N(CH_3)_2$ and SO_2NHCH_2); 2.68 (m, 2 H, CH_2NH_2).

Fluorescent Analyses of Dansyl-Labeled PEI/Gantrez - PE Films. Fluorescence spectra were recorded using an ISA JOBIN YVON-SPEX fluorolog-3 spectrofluorometer. All the analyses used a λ_{ex} of 360 nm and a λ_{em} of 460 nm.

Thermogravimetric Analysis of Carbon Black Entrapped PEI/Gantrez - PE Powders. Thermogravimetric analyses (TGA) were carried out using a Netzsch TG 209C TGA instrument using a nitrogen atmosphere over a temperature range from 30 °C to 950 °C at a heating rate of 10 °C /min.

Carbon Black Film Deposition by LbL Self-Assembly. PE powder was alternately immersed into aqueous mixtures containing 0.25 wt % CB and 0.05 wt % PEI or PAA. The initial immersion in each mixture was for 5 min followed by 1 min immersions to deposit additional bilayers. Following each immersion the powder was filtered to remove water and excess material. For the PEI-grafted PE powder, the CB-PAA mixture was used first because it was already covered by PEI, but normally CB-PEI would be deposited first. After the deposition was complete, the coated powder was vacuum-dried for more than 24 h to remove residual moisture. Once dried, the powder was compacted in an aluminum mold at 90 °C for 30 min with a pressure of 150 kg/cm^2. The resulting films are 1.5 mm thick.

Characterization of the Carbon Black Coating. The concentration of carbon black on the PE surface was determined using a Netzsch TG 209C TGA in a nitrogen atmosphere operated from 25 to 900 °C at a rate of 10 °C/min. The conductivities of the compacted films were measured by a home-built four-point-probe system.

Direct Amination of MWNTs with Polyethylenimine. MWNTs (2 g) and polyethylenimine (10 g) were mixed in 100 mL of DMF. Sonication for 30 min and stirring at 50 ºC for 3 d formed the product, MWNT-NH-PEI. The resulting suspension was filtered through a 0.20 μm nylon membrane and the precipitate was washed with 1

M HCl, 1 M NaOH, water and methanol to remove any excess PEI. After drying, 1.9 g of the product was obtained. The ^{1}H NMR spectrum (obtained from a Varian Mercury-300) of MWNT-NH-PEI suspended in D_2O showed three broad peaks with chemical shifts of 3.49, 3.38 and 1.52 δ. Solid state MAS (3 kHz spinning rate) ^{1}H NMR (obtained from a Varian Avance-400) of MWNT-NH-PEI showed two distinctive peaks. One very broad peak extended from 70 to -20 δ. A second sharper peak spanned from 9.5 to -8.4 δ.

Titration of MWNT-NH-PEI. A known amount of the MWNT-NH-PEI was added to a 20 mL of 0.01 M HCl. After sonicating the mixture for 1 h at 25 °C, an aliquot (5 mL) of the resulting HCl solution was titrated to a pH 8.0 endpoint using 0.01 M NaOH with a pH meter. The difference between the original amount of HCl and the amount of HCl titrated corresponded to the loading of titratable amino groups on the MWNT-NH-PEI and was 0.3 mequiv of titratable amine groups/g. The MWNT-NH-PEI in HCl was basified with excess amount of 1 M NaOH solution. The resulting suspension was filtered through a 0.20 μm nylon membrane and the precipitate was washed with water to remove any NaOH and dried. A titration of the resulting MWNT-NH-PEI was carried out again by the same procedure described above and the loading of titratable amino groups on the MWNT-NH-PEI is still 0.3 mequiv of titratable amine groups/g.

Acylation of MWNT-NH-PEI with Octadecanoic Acid. A mixed anhydride of octadecanoic acid prepared from 0.5 g of the acid using ethyl chloroformate and *N*-methylmorpholine in DMF was used to acylate 0.2 g of the MWNT-NH-PEI. This

reaction involved sonication for 30 min and stirring at 50 ºC for 2 days. The product MWNT-NH-PEI-COC_{17} (0.2 g) was again isolated by filtration using a 0.20 μm nylon membrane and the MWNT products were washed with ethyl acetate, tetrahydrofuran and hexanes before drying. Attenuated total reflection-infrared (ATR-IR) spectroscopy was used to confirm that acylation occurred using a Bruker Tensor 27 series FT-IR, with a Pike MIRacle ATR accessory at an angle of 45 . with a ZnSe crystal. These spectra showed distinctive peaks at 2912 cm^{-1} and 2869 cm^{-1}. The ^1H NMR spectrum (obtained from a Varian Mercury-300) of MWNT-NH-PEI-COC_{17} in $CDCl_3$ showed seven broad peaks centered at 3.49, 3.38, 2.08, 1.64, 1.52, 1.24 and 0.86 δ.

Thermogravimetric Analysis of MWNTs, MWNT-NH-PEI and MWNT-NH-PEI-COC_{17}. TGA was carried out using a Netzsch TG 209C TGA instrument in a nitrogen atmosphere over a temperature range from 30 °C to 950 °C at a heating rate of 10 °C /min. The additional weight loss of MWNT-NH-PEI and MWNT-NH-PEI-COC_{17} as compared to MWNTs between 300-400 ºC is 6-8 % and 20-25 %, respectively.

Raman Spectra of MWNTs, MWNT-NH-PEI and MWNT-CONH-PEI. The Raman spectroscopy was carried out using 632 nm laser excitation. A JY Horiba LabRam-IR system with an InGaAs diode array JY IGA-3000 detector was used. It showed the expected peaks for the D band at 1290 cm-1 and for the G band at 1580 cm-1 for all three samples. The D/G band ratio calculated from the Raman spectra of MWNTs, MWNT-NH-PEI and MWNT-CONH-PEI were 1.39, 1.42 and 1.53, respectively.

Dispersibility Test of MWNTs and MWNT-NH-PEI in Aqueous Solutions. Samples of pure MWNTs in water (pH 7), MWNT-NH-PEI in water (pH 7), MWNT-NH-PEI in 0.01 M NaOH solution, and MWNT-NH-PEI after thermolysis of the PEI graft in water (pH 7) were prepared. Suspensions prepared after 30 min of sonication were then analyzed with pictures taken just after sonication ended, after 20 seconds, after 1 day and after 1 year, respectively.

Covalent Layer-by-Layer Self-Assembly of MWNT-NH-PEI with Gantrez on PE Substrates. An oxidized PE substrate (film or powder) was first activated by treatment with a mixture of ethyl chloroformate and N-methylmorpholine in DMF for 15 min. The activated PE substrate was isolated by filtration, washed with CH_2Cl_2, and allowed to air-dry. The activated PE substrate was then placed into a CH_2Cl_2 solution of PEI (2.5 wt %) and shaken for 30 min. The product aminated PE substrate was isolated by filtration, washed with MeOH, and allowed to air-dry. This PEI treated PE substrate was then placed into a THF solution of Gantrez (10 wt %) for 30 min, isolated by filtration, washed with THF, and allowed to air-dry. The Gantrez treated PE substrate was placed into a MeOH suspension of MWNT-NH-PEI (1.0 wt %) and shaken for 30 min. The aminated PE substrate was again isolated by filtration, washed with MeOH, and allowed to air-dry. This MWNT-NH-PEI treated PE substrate could then be placed into the Gantrez solution again. This cycle of Gantrez treatment followed by MWNT-NH-PEI treatment was repeated five times to obtain the $(Gantrez/MWNTNH\text{-}PEI)_5$ PE substrate. Characterization of the $(Gantrez/MWNTNH\text{-}PEI)_x$ (x = 1-6) PE powders was carried out by TGA using a Netzsch TG 209C TGA instrument in a nitrogen atmosphere

over a temperature range from 30 to 950 °C at a heating rate of 10 °C/min. The average percentages of the residues of the (Gantrez/MWNTNH-PEI)$_1$ to (Gantrez/MWNT-NH-PEI)$_6$ PE powders based on three individual measurements were 1.34 ± 0.18, 3.19 ± 0.34, 3.78 ± 0.72, 4.16 ± 0.33, 5.56 ± 0.48, and 6.38 ± 0.14%, respectively. Characterization of the (Gantrez/MWNT-NH-PEI)$_x$ (x = 1-5) PE films was carried out by ATR-IR spectroscopy. In these spectra, the integrated intensity of the amide peak (1640-1650 cm^{-1}) and carboxylate peak (1550-1560 cm^{-1}) increased in comparison with the intensity of the underlying bulk polymer C-H absorption (2910 and 2850 cm^{-1}).

Ionic Layer-by-Layer Self-Assembly of MWNT-NH-PEI with PAA on PE Films. The PEI treated PE film obtained by the procedure described above was placed into a MeOH/water (1:1) solution of poly(acrylic acid) (PAA, 1.0 wt %, adjusted pH to 4 by using NaOH) and shaken for 30 min. The anionic PE film was washed with water and allowed to air-dry. This PAA treated PE film was placed into a water suspension of MWNT-NH-PEI (1.0 wt %, adjusted pH to 9 by using HCl) and shaken for 30 min. The cationic PE film was washed with water and allowed to air-dry. This MWNT-NH-PEI treated PE film could then be placed into the PAA solution again. This cycle of PAA treatment followed by MWNT-NH-PEI treatment was repeated five times to obtain the (PAA/MWNT-NH-PEI)$_5$ PE film. Characterization of the (PAA/MWNT-NH-PEI)$_5$ PE film was carried out by ATR-IR spectroscopy. Similar peak intensities in the amide region (1640-1650 cm^{-1}) and carboxylate region (1550-1560 cm^{-1}) in comparison with those of the (Gantrez/MWNT-NH-PEI)$_5$ PE film were seen.

Acylation of Gantrez/MWNT-NH-PEI or PAA/MWNT-NH-PEI PE Films with Octadecanoic Acid. A mixed anhydride of octadecanoic acid prepared by reaction of 0.5 g of the acid with ethyl chloroformate and *N*-methylmorpholine in DMF was used to acrylate either the $(Gantrez/MWNT\text{-}NH\text{-}PEI)_x$ (x = 1-5) or $(PAA/MWNT\text{-}NH\text{-}PEI)_5$ PE films. The reaction was carried out at 50 °C for 24 h. The films were washed with THF and MeOH and allowed to air-dry. The success of acylation was seen in the ATR-IR spectra of the product which showed higher intensity absorptions in the C-H absorption region (2910 and 2850 cm^{-1}) in comparison with unreacted films.

Contact Angle Measurements. Static water contact angles were measured on a KSV CAM 200 optical goniometer with an automatic single liquid dispenser at ambient temperature. The average water droplet size was about 13 μL. The static contact angles of $(Gantrez/MWNT\text{-}NH\text{-}PEI)_x$ (x = 1-5) PE films were 149, 154, 166, 158, and 165° (with error bar of ± 2° based on three measurements), respectively. Photographs of the water sliding behavior of a five bilayer superhydrophobic film prepared by covalent assembly were taken by using the same goniometer with the rate of 30 frames/s. The stage was tilted by 5°.

Chemical Stability Test of $(Gantrez/MWNT\text{-}NH\text{-}PEI)_5\text{-}NHCOC_{17}$ and $(PAA/MWNT\text{-}NH\text{-}PEI)_5\text{-}NHCOC_{17}$ PE Films. Samples (1 cm^2) of the grafted films were placed in 1 M HCl for 24 h and treated by sonication for 0.5 h. After this treatment, the films were washed with acetone and dried under N_2. Photographs (Figure 7) were taken before and after the acid treatment followed by sonication. Experiments also showed large differences in the advancing contact angle for films after 24 h. The

covalently modified surface became less hydrophobic with its contact angle dropping from ~160° to ~100°. However, the ionically assembled grafted film's contact angle dropped from ~150° to ~30° under the same conditions.

Atomic Force Microscopy Studies. The surface topography and roughness of the samples were characterized by atomic force microscopy in the tapping mode using a commercial atomic force microscope (Alpha300 S, WITec, Germany) which combines a confocal (Raman and fluorescence) microscope (CM) and an atomic force microscope. Ultrasharp silicon atomic force microscopy (AFM) tips (VISTA probes, NanoScience Instruments, Phoenix, AZ) with nominal tip radii of <10 nm, a lever resonance frequency of ~300 kHz, and a force constant of ~40 N/m were utilized. To determine the representative roughness of the surface, 10 1 μm × 1 μm AFM topographic images were taken at random positions on each sample and the value of the root-mean-square (rms) roughness was obtained.

Confocal Raman Imaging. Raman spectra and images were acquired with the same instrument described above, including a piezoelectric scan table, a microscope objective (100×, NA = 0.9 and 20×, NA = 0.45, Nikon), and a Peltier cooled charge-coupled device (CCD) detector (Andor). An air-cooled argon-ion laser at 488 nm was focused onto the samples. The Raman spectra were obtained at 4 cm^{-1} resolution with a 0.2 s integration time. Confocal Raman images were acquired based on the integrated G band and D band intensities in the frequency range between 1050 and 1700 cm^{-1}. The laser intensity was kept as low as possible during the experiment to minimize thermal damage caused by the laser.

Synthesis of *N*-acryloxysuccinimide. This monomer was prepared from acrolyl chloride and *N*-hydroxysuccinimide following a literature procedure.[148]

Synthesis of Poly(*N*-acryloxysuccinimide). This polymer was prepared following a literature procedure.[149] A solution of *N*-acryloxysuccinimide (8.0 g, 47 mmol) and 2,2'-azobisisobutylnitrile (40 mg, 0.24 mmol) in 200 mL of benzene was degassed under positive pressure of N_2 for 1 h. Then the solution was heated to 60° and stirred for 24 h. The resulting mixture was allowed to cool to room temperature. The white precipitate of polymer product which formed was collected by filtration and washed with benzene and THF and dried under vacuum to yield 7.8 g (99 %) of the desired polymer. ^{1}H NMR (*d*-DMSO) δ 2.05 (bs, 2H), 2.80 (bs, 4H), 3.13 (bs, 1H). ATR-IR (powder) 1813, 1782, 1734, 1204, 1068, 648 cm^{-1}. The polymer was also analyzed by gel permeation chromatography in THF. In a typical analysis, 15.0 mg of the polymer was dissolved in 5 mL of degassed THF and the analysis was carried out using a Viscotek I-MBMMW-3078 mixed bed column using a Viscotek GPC instrument. This GPC analysis used multiple detectors, including a Model VE 3580 RI detector and OmniSEC software. M_n (GPC) = 30,000 Da.

Synthesis of Poly(*N*-isopropylacrylamide)-*c*-Poly(*N*-acryloxysuccinimide) A solution of isopropylamine (1.8 mL, 21.5 mmol) in 20 mL of DMF was added to a solution of poly(*N*-acryloxysuccinimide) (4.0 g, 24 meq NASI) in 80 mL of DMF. The resulting solution was stirred at room temperature for 18 h during which time some precipitate formed. The mixture was filtered to remove the precipitate. The 100 mL of the supernatant solution was then added drop-by-drop to 2 L of ether at room

temperature to precipitate the copolymer. The precipitate of the desired copolymer was then isolated by filtration and redissolved in 100 mL of THF and again reprecipitated in 2 L of hexanes. This process was repeated 2 times, yielding 2.6 g (92 %) of the polymer. The mole ratio of NIPAAm and NASI groups in the copolymer was analyzed by ^{1}H NMR spectroscopy. Based on the ratio of the integrals for the broad singlet at δ 1.12 (NIPAM –CH(CH_3)$_2$ groups) and the peak at δ 2.61 (NASI –C(=O)CH_2-), this ratio was 1 : 9.

Syntheses of Aminated Silica Nanoparticles (10 nm or 100 nm in Diameter). These materials were prepared following a literature procedure.[40] In a typical procedure, 5 g of silica nanoparticles (10 nm or 100 nm in diameter) were first cleaned by placing them in 100 mL of 5 % hydrochloric acid at room temperature overnight. The silica nanoparticles were then recovered by filtration, washed with water, and dried under vacuum. The dried silica nanoparticles were then added to a 10 % solution of 3-aminopropyltriethoxysilane in 100 mL toluene. This mixture was heated to reflux overnight. The product aminated silica nanoparticles were isolated by filtration, washed with THF and MeOH then dried under vacuum. Titrimetric analysis of the aminated silica nanoparticles was carried out by first suspending a weighed amount of aminated silica nanoparticles in a 0.01 M HCl solution and shaking the mixture for 1 h. An aliquot of the resulting HCl solution was titrated with a 0.01 M NaOH solution to a pH 9 endpoint. In this way, the amount of HCl consumed by basic groups on the aminated silica nanoparticles could then be determined. These aminated silica nanoparticles had amine loadings of 0.74 mmol (10 nm) and 0.19 mmol (100 nm) of base/g, respectively.

Covalent Layer-by-Layer Self-Assembly of PNIPAM-*c*-PNASI with Aminated Silica Nanoparticles (10 nm and 100 nm) on PE Films. Following a literature procedure,[99] an oxidized PE film was first activated by treatment with a mixture of ethyl chloroformate and *N*-methylmorpholine in DMF for 15 min. The activated PE film was removed from the solution of excess ethyl chloroformate and then rinsed with DMF. The activated PE film was then placed into a DMF solution of PEI (2.5 wt %) and this mixture was shaken for 30 min at room temperature. The product aminated PE film was removed from the PEI solution and washed with DMF. This PEI-treated PE film was placed into a DMF solution of PNIPAM-*c*-PNASI (20 wt %) for 30 min, removed from the polymer solution and washed with DMF. The polymer treated PE film was placed in a 20 mL DMF suspension of aminated silica nanoparticles (10 and 100 nm particles, 0.5 wt % each and 0.5 vol % of triethylamine) and shaken for 30 min. The aminated silica treated PE film was again removed from the aminated silica nanoparticles suspension, washed with DMF, and placed into a DMF solution of isopropylamine (10 vol %) and shaken for 5 min. This step was designed to convert any unreacted NASI groups to amides. This isopropylamine-treated PE film was again removed from the isopropylamine solution and then washed with DMF. This isopropylamine treated PE film could then be placed into the PNIPAM-*c*-PNASI solution again. This cycle of aminated silica nanoparticles treatment followed by PNIPAM-*c*-PNASI treatment was repeated 1 to 6 times to obtain the Ox-PE / PEI / PNIPAM-*c*-PNASI / [SiO_2-NH_2 (10 nm + 100 nm) / PNIPAM-*c*-PNASI]$_x$ (x = 1 to 6). The resulting polymer treated PE films were treated with one more cycle of aminated

silica nanoparticles (10 nm particles only, 1.0 wt % and 0.5 vol % of triethylamine) and PNIPAM-*c*-PNASI, followed by isopropylamine treatment to yield the final Ox-PE / PEI / PNIPAM-*c*-PNASI / [SiO_2-NH_2 (10 nm + 100 nm) / PNIPAM-*c*-PNASI]$_x$ (x = 1 to 6) / [SiO_2-NH_2 (10 nm) / PNIPAM-*c*-PNASI]$_1$ surfaces. The surfaces prepared in this manner were subjected to a final immersion in water followed by washing with THF then drying under nitrogen. The static contact angles with 1.4 M Na_2SO_4 for Ox-PE / PEI / PNIPAM-*c*-PNASI / [SiO_2-NH_2 (10 nm + 100 nm) / PNIPAM-*c*-PNASI]$_x$ (x = 1 to 6) / [SiO_2-NH_2 (10 nm) / PNIPAM-*c*-PNASI]$_1$ surfaces were 90°, 116°, 125°, 130°, 140°, and 146°, respectively. The static contact angles with water for Ox-PE / PEI / PNIPAM-*c*-PNASI / [SiO_2-NH_2 (10 nm + 100 nm) / PNIPAM-*c*-PNASI]$_x$ (x = 1 to 6) / [SiO_2-NH_2 (10 nm) / PNIPAM-*c*-PNASI]$_1$ surfaces were 50°, 60°, 54°, 60°, 58°, and 62°, respectively.

Covalent Layer-by-Layer Self-Assembly of PNIPAM-*c*-PNASI with Aminated Silica Nanoparticles (10 nm only) on PE Films. An oxidized PE film was first activated by treatment with a mixture of ethyl chloroformate and *N*-methylmorpholine in DMF for 15 min. The activated PE film was removed from the solution of excess ethyl chloroformate and then rinsed with DMF. The activated PE film was then placed into a DMF solution of PEI (2.5 wt %) and this mixture was shaken for 30 min at room temperature. The product aminated PE film was removed from the PEI solution and washed with DMF. This PEI-treated PE film was placed into a DMF solution of PNIPAM-*c*-PNASI (20 wt %) for 30 min, removed from the polymer solution and washed with DMF. The polymer treated PE film was placed in a 20 mL

DMF suspension of aminated silica nanoparticles (10 nm particles, 1.0 wt % and 0.5 vol % of triethylamine) and shaken for 30 min. The aminated silica treated PE film was again removed from the aminated silica nanoparticles suspension, washed with DMF, and placed into a DMF solution of isopropylamine (10 vol %) and shaken for 5 min. This step was designed to convert any unreacted NASI groups to amides. This isopropylamine-treated PE film was again removed from the isopropylamine solution and then washed with DMF. This isopropylamine treated PE film could then be placed into the PNIPAM-*c*-PNASI solution again. This cycle of aminated silica nanoparticles treatment followed by PNIPAM-*c*-PNASI treatment was repeated 1 to 6 times to obtain the Ox-PE / PEI / PNIPAM-*c*-PNASI / [SiO_2-NH_2 (10 nm) / PNIPAM-*c*-PNASI]$_x$ (x = 1 to 6) surfaces. The surfaces prepared in this manner were subjected to a final immersion in water followed by washing with THF then drying under nitrogen. The static contact angles with 1.4 M Na_2SO_4 for Ox-PE / PEI / PNIPAM-*c*-PNASI / [SiO_2-NH_2 (10 nm) / PNIPAM-*c*-PNASI]$_x$ (x = 1 to 6) surfaces were 90°, 92°, 105°, 106°, 83° and 113°, respectively. The static contact angles with water for Ox-PE / PEI / PNIPAM-*c*-PNASI / [SiO_2-NH_2 (10 nm) / PNIPAM-*c*-PNASI]$_x$ (x = 1 to 6) surfaces were 50°, 67°, 46°, 52°, 57° and 50°, respectively.

Covalent Layer-by-Layer Self-Assembly of PNIPAM-*c*-PNASI with Aminated Silica Nanoparticles (100 nm only) on PE Films. An oxidized PE film was first activated by treatment with a mixture of ethyl chloroformate and *N*-methylmorpholine in DMF for 15 min. The activated PE film was removed from the solution of excess ethyl chloroformate and then rinsed with DMF. The activated PE film

was then placed into a DMF solution of PEI (2.5 wt %) and this mixture was shaken for 30 min at room temperature. The product aminated PE film was removed from the PEI solution and washed with DMF. This PEI-treated PE film was placed into a DMF solution of PNIPAM-*c*-PNASI (20 wt %) for 30 min, removed from the polymer solution and washed with DMF. The polymer treated PE film was placed in a 20 mL DMF suspension of aminated silica nanoparticles (100 nm particles, 1.0 wt % and 0.5 vol % of triethylamine) and shaken for 30 min. The aminated silica treated PE film was again removed from the aminated silica nanoparticles suspension, washed with DMF, and placed into a DMF solution of isopropylamine (10 vol %) and shaken for 5 min. This step was designed to convert any unreacted NASI groups to amides. This isopropylamine-treated PE film was again removed from the isopropylamine solution and then washed with DMF. This isopropylamine treated PE film could then be placed into the PNIPAM-*c*-PNASI solution again. This cycle of aminated silica nanoparticles treatment followed by PNIPAM-*c*-PNASI treatment was repeated 1 to 6 times to obtain the Ox-PE / PEI / PNIPAM-*c*-PNASI / $[SiO_2\text{-}NH_2$ (100 nm) / PNIPAM-*c*-PNASI$]_x$ (x = 1 to 6) surfaces. The surfaces prepared in this manner were subjected to a final immersion in water followed by washing with THF then drying under nitrogen. The static contact angles with 1.4 M Na_2SO_4 for Ox-PE / PEI / PNIPAM-*c*-PNASI / $[SiO_2\text{-}NH_2$ (100 nm) / PNIPAM-*c*-PNASI$]_x$ (x = 1 to 6) surfaces were 90°, 94°, 91°, 82°, 75° and 94°, respectively. The static contact angles with water for Ox-PE / PEI / PNIPAM-*c*-PNASI / $[SiO_2\text{-}NH_2$ (100 nm) / PNIPAM-*c*-PNASI$]_x$ (x = 1 to 6) surfaces were 50°, 51°, 41°, 46°, 25° and 54°, respectively.

Preparation of PNIPAM Grafted (Gantrez/PEI)$_4$-PE Surface by Atom Transfer Radical Polymerization. The graft polymerization is based on a literature procedure.[131] A (Gantrez/PEI)$_4$-PE film (1.5 cm × 3 cm) (see procedure for the preparation of PEI/Gantrez hyperbranched grafts on oxidized PE**)** was first immersed into a CH_2Cl_2 solution (10 mL) containing bromoisobutyryl bromide (1.0 mL) and pyridine (1.0 mL) at room temperature for 12 h to covalently bind bromoisobutyryl initiator groups to the PE. The product PE film was then removed from this reaction solution and washed with acetone and dried under N_2. A graft polymerization of PNIPAM was then carried out by immersing the PE film with the covalently bound bromoisobutyryl initiator into a degassed solution of *N*-isopropylacrylamide (1.25 g, 11.0 mmol) in a 1:1 (v/v) mixture of H_2O and MeOH (5 mL) containing CuBr (0.032 g, 0.23 mmol) and 1,10-phenanthroline (0.12 g, 0.67 mmol). The graft polymerization was allowed to proceed overnight. Then the PNIPAM grafted PE film was washed first with 50 mL of water and 50 mL of MeOH, and then dried under N_2. The PNIPAM grafts on the PE surface were analyzed by ATR-IR. These grafts contain carboxamides based on peaks at 1670 cm^{-1} and 1640 cm^{-1} in the ATR-IR spectrum.

ATR-IR Spectroscopy. ATR-IR spectroscopy was used to confirm growth of the aminated silica nanoparticles / PNIPAM-*c*-PNASI graft on the PE surface. A Bruker Tensor 27 series FT-IR, with a Pike MIRacle ATR accessory at an angle of 45° using a ZnSe crystal, was used in these analyses.

Contact Angle Measurements. Static water contact angles (Θ) were measured on a KSV CAM 200 optical goniometer with an automatic single liquid dispenser at

ambient temperature. The average water droplet size was about 13 μL. Photographs were taken until the droplet was no longer spreading (usually within 6 min), at which point the contact angles were measured by the CAM 200 software. Dynamic advancing angles (Θ_a) and receding angles (Θ_r) were recorded as water was added to or withdrawn from a 13 μL water droplet, which was pre-deposited on the surface 2 minutes before the measurement. Θ_a values were also recorded as water was added to a 13 μL water droplet, which was pre-deposited on the surface 1, 3, 5 or 10 minutes before the measurement. These Θ_a values showed no difference compared to the one that was recorded after 2 minutes.

Atomic Force Microscopy. The surface of PE_{oxid}-(PNIPAM-*c*-PNASI/aminated silica nanoparticles)$_6$ –PNIPAM was characterized by atomic force microscopy in tapping mode using a commercial AFM (Alpha300 S, WITec, Germany). Images were collected using ultrasharp silicon AFM tips (VISTA probes, NanoScience Instruments, Phoenix, Arizona) with nominal tip radii of < 10 nm, a lever resonance frequency of ~ 300 kHz and a force constant of ~ 40 N/m. The tip was modified with octadecyltrichlorosilane (OTS) prior to the measurement to minimize the adhesion between the tip and the polymer surface. To coat the tips, they were immersed in a $NH_4OH/H_2O_2/H_2O$ solution (vol. ratio: 1:1:4) for 1 minute, rinsed with water, acetone and dried with N_2 flow. The tip was then immersed in a solution of 1 μm OTS/ 10 ml hexane for 30 seconds, rinsed with hexane, ethanol, water, acetone, and dried with N_2 flow. To follow changes in morphology under varying solute conditions, the samples were scanned in the following order: ambient air, high purity water, 1.4 M Na_2SO_4, 1.2

M NaSCN, and then again in high purity water. Between each solute condition the samples were rinsed with water, THF, and dried with N_2 flow. In each condition the representative root-mean-square (rms) roughness of the surface was determined from the average of a series of 2.5 μm x 2.5 μm regions at random positions.

CHAPTER VIII

SUMMARY

LbL assembly based on ionic interactions has proven to be a versatile route for surface modification and construction of ultrathin nanocomposites for the last two decades. Covalent LbL assembly based on facile 'click' covalent bond formation is an effective alternative, especially for the applications where a more robust ultrathin films or nanocomposites is desired. The subject of this dissertation focuses on the design of three different covalent LbL assemblies and their applications on conductive thin films, superhydrophobic surfaces, and solute responsive surfaces, respectively.

Surface modification of PE substrates using covalent LbL assembly with PEI and Gantrez is a successful route to prepare a surface graft. The procedure is relative easy, fast and reproducible. The assembly shows the same linear growth pattern seen for other LbL processes. The covalent multilayer assemblies have been shown to be stable to strong acid or strong base. Grafting multiple layers of PEI/Gantrez to the PE powder surface provided excellent coverage and promoted stable LbL film growth and excellent adhesion. This carbon black (CB) coated powder was compression molded into films, and their conductivity was measured, which revealed a percolation threshold below 0.01 wt % CB for the PEI-grafted system. Electrical conductivity of 0.2 S/cm was achieved with only 6 wt % CB, which is exceptional for a CB-filled PE film.

Direct amination of MWNTs with PEI is a convenient and simple method leading to highly functionalized product that contains 6-8 % by weight PEI. The total

amine groups on MWNT-NH-PEI are estimated to be *ca.* 1.5 mmol/g based on titration. The free amine groups of MWNT-NH-PEI can be used as chemical linkers for forming ultrathin nanocomposites on surfaces. Superhydrophobic PE films can be formed either from ionic LbL self-assembly of MWNT-NH-PEIs and poly(acrylic acid) or from covalent LbL self-assembly of MWNT-NH-PEIs and Gantrez when the final graft is acrylated with a mixed anhydride prepared from ethyl chloroformate and octadecanoic acid. While the ionically assembled nanocomposite graft is labile under acidic conditions, the covalently assembled graft is more chemically robust. AFM shows that these self-assembly processes that couple anisotropic MWNTs with Gantrez or poly(acrylic acid) produce ultrarough surfaces.

Responsive surfaces with significant, reversible, reproducible wettability changes can be prepared by covalent LbL grafting chemistry using PNIPAM-*c*-PNASI and aminated silica nanoparticles. A 65º $\Delta\Theta$ value was observed with water vs. 1.4 M Na_2SO_4, which is much larger than the $\Delta\Theta$ seen using these same solutions on other non-functional surfaces. The prepared film shows a high surface roughness of ~300 nm, which contributes to the large solute responsive $\Delta\Theta$ values. The surfaces are reconfigurable in different solute conditions and that the changes in water contact angle are likely due to combination of change in surface roughness along with swell and intercalation of the solute ions into the PNIPAM surface.

REFERENCES

(1)Decher, G.; Hong, J.-D.; Schmitt, J. *Macromol. Chem. Macromol. Symp.* **1991**, *46*, 321-327.

(2)Decher, G. *Science* **1997**, *277*, 1232-1237.

(3)Bertrand, P.; Jonas, A.; Laschewsky, A.; Legras, R. *Macromol. Rapid Commun.* **2000**, *21*, 319-348.

(4)Decher, G.; Schlenoff, J. B. *Multilayer Thin Films-Sequential Assembly of Nanocomposites Material ;* Wiley-VCH: Weinheim, Germany 2003.

(5)Hammond, P. *Adv. Mater.* **2004**, *16*, 1271-1293.

(6)Ariga, K.; Hill, J. P.; Ji, Q. *Phys. Chem. Chem. Phys.* **2007**, *9*, 2319-2340.

(7)Quinn, J. F.; Johnston, A. P. R.; Such, G. K.; Zelikin, A. N.; Caruso, F. *Chem. Soc. Rev.* **2007**, *36*, 707-718.

(8)Bergbreiter, D. E.; Tao, G.; Franchina, J. G.; Sussman, L. *Macromolecules* **2001**, *34*, 3018-3023.

(9)Kumanotani, J. *Prog. Org. Coat.* **1997**, *34*, 135-146.

(10)Otto, V. *J. Polym. Sci., Part A: Polym. Chem.* **2000**, *38*, 4327-4335.

(11)Kolb, H. C.; Finn, M. G.; Sharpless, K. B. *Angew. Chem. Int. Ed.* **2001**, *40*, 2004-2021.

(12)Liu, Y.; Bruening, M. L.; Bergbreiter, D. E.; Crooks, R. M. *Angew. Chem. Int. Ed. Engl.* **1997**, *36*, 2114-2116.

(13)Liu, Y.; Zhao, M.; Bergbreiter, D. E.; Crooks, R. M. *J. Am. Chem. Soc.* **1997**, *119*, 8720-8721.

(14)Zhao, M.; Liu, Y.; Crooks, R. M.; Bergbreiter, D. E. *J. Am. Chem. Soc.* **1999**, *121*, 923-930.

(15)Dai, J.; Sullivan, D. M.; Bruening, M. L. *Ind. Eng. Chem. Res.* **2000**, *39*, 3528-3535.

(16)Major, J. S.; Blanchard, G. J. *Langmuir* **2001**, *17*, 1163-1168.

(17)Major, J. S.; Blanchard, G. J. *Chem. Mater.* **2002**, *14*, 2567-2573.

(18)Major, J. S.; Blanchard, G. J. *Chem. Mater.* **2002**, *14*, 2574-2581.

(19)Major, J. S.; Blanchard, G. J. *Chem. Mater.* **2002**, *14*, 4320-4327.

(20)Serizawa, T.; Nanameki, K.; Yamamoto, K.; Akashi, M. *Macromolecules* **2002**, *35*, 2184-2189.

(21)Serizawa, T.; Nakashima, Y.; Akashi, M. *Macromolecules* **2003**, *36*, 2072-2078.

(22)Serizawa, T.; Matsukuma, D.; Nanameki, K.; Uemura, M.; Kurusu, F.; Akashi, M. *Macromolecules* **2004**, *37*, 6531-6536.

(23)Puniredd, S. R.; Srinivasan, M. P. *Langmuir* **2005**, *21*, 7812-7822.

(24)Zhang, F.; Jia, Z.; Srinivasan, M. P. *Langmuir* **2005**, *21*, 3389-3395.

(25)Zhang, F.; Srinivasan, M. P. *Colloids Surf., A* **2005**, *257-258*, 509-514.

(26)Puniredd, S. R.; Srinivasan, M. P. *J. Colloid Interface Sci.* **2007**, *306*, 118-127.

(27)Puniredd, S. R.; Srinivasan, M. P. *Ind. Eng. Chem. Res.* **2007**, *46*, 464-471.

(28)Tian, Y.; He, Q.; Tao, C.; Li, J. *Langmuir* **2006**, *22*, 360-362.

(29)Liang, Z.; Wang, Q. *Langmuir* **2004**, *20*, 9600-9606.

(30)Liang, Z.; Cabarcos, O. M.; Allara, D. L.; Wang, Q. *Adv. Mater.* **2004**, *16*, 823-827.

(31)Liang, Z.; Dzienis, K. L.; Xu, J.; Wang, Q. *Adv. Funct. Mater.* **2006**, *16*, 542-548.

(32)Buck, M. E.; Zhang, J.; Lynn, D. M. *Adv. Mater.* **2007**, *19*, 3951-3955.

(33)Chan, E. W. L.; Lee, D. C.; Ng, M. K.; Wu, G.; Lee, K. Y. C.; Yu, L. *J. Am. Chem. Soc.* **2002**, *124*, 12238-12243.

(34)Lee, D. C.; Chang, B. J.; Morales, G. M.; Jang, Y. A.; Ng, M. K.; Heller, S. T.; Yu, L. *Macromolecules* **2004**, *37*, 1849-1856.

(35)Park, M. K.; Lee, D. C.; Liang, Y.; Lin, G.; Yu, L. *Langmuir* **2007**, *23*, 4367-4372.

(36)Tong, W.; Gao, C.; Mohwald, H. *Macromol. Rapid Commun.* **2006**, *27*, 2078-2083.

(37)Ma, Y.; Qian, L.; Huang, H.; Yang, X. *J. Colloid Interface Sci.* **2006**, *295*, 583-588.

(38)Chen, J.; Luo, G.; Cao, W. *Macromol. Rapid Commun.* **2001**, *22*, 311-314.

(39)Zhang, Y.; Yang, S.; Guan, Y.; Cao, W.; Xu, J. *Macromolecules* **2003**, *36*, 4238-4240.

(40)Bergbreiter, D. E.; Simanek, E. E.; Owsik, I. *J. Polym. Sci., Part A: Polym. Chem.* **2005**, *43*, 4654-4665.

(41)Such, G. K.; Quinn, J. F.; Quinn, A.; Tjipto, E.; Caruso, F. *J. Am. Chem. Soc.* **2006**, *128*, 9318-9319.

(42)Such, G. K.; Tjipto, E.; Postma, A.; Johnston, A. P. R.; Caruso, F. *Nano Lett.* **2007**, *7*, 1706-1710.

(43)Vestberg, R.; Malkoch, M.; Kade, M.; Wu, P.; Fokin, V. V.; Sharpless, K. B.; Drockenmuller, E.; Hawker, C. J. *J. Polym. Sci., Part A: Polym. Chem.* **2007**, *45*, 2835-2846.

(44)Bergbreiter, D. E.; Chance, B. S. *Macromolecules* **2007**, *40*, 5337-5343.

(45)Kato, K.; Uchida, E.; Kang, E.-T.; Uyama, Y.; Ikada, Y. *Prog. Polym. Sci.* **2003**, *28*, 209-259.

(46)Hougen, L. R. *Nature* **1960**, *188*, 577-578.

(47)Carley, J. F.; Kitze, P. T. *Polym. Eng. Sci.* **1978**, *18*, 326-334.

(48)Morra, M.; Occhiello, E.; Gila, L.; Garbassi, F. *J. Adhes.* **1990**, *33*, 77 - 88.

(49)Nihlstrand, A.; Hjertberg, T.; Johansson, K. *Polymer* **1997**, *38*, 3581-3589.

(50)Russell, K. E. *Prog. Polym. Sci.* **2002**, *27*, 1007-1038.

(51)Ruckenstein, E.; Li, Z. F. *Adv. Colloid Interface Sci.* **2005**, *113*, 43-63.

(52)Ren, B.; Gao, F.; Tong, Z.; Yan, Y. *Chem. Phys. Lett.* **1999**, *307*, 55-61.

(53)Cataldo, F. *Fullerenes, Nanotubes, Carbon Nanostruct.* **2002**, *10*, 293 - 311.

(54)Delcorte, A.; Bertrand, P.; Wischerhoff, E.; Laschewsky, A. *Langmuir* **1997**, *13*, 5125-5136.

(55)Greene, G.; Tannenbaum, R. *Appl. Surf. Sci.* **2004**, *233*, 336-342.

(56)Blais, P.; Carlsson, D. J.; Csullog, G. W.; Wiles, D. M. *J. Colloid Interface Sci.* **1974**, *47*, 636-649.

(57)Bergbreiter, D. E. *Prog. Polym. Sci.* **1994**, *19*, 529-560.

(58)Tao, G.; Gong, A.; Lu, J.; Sue, H. J.; Bergbreiter, D. E. *Macromolecules* **2001**, *34*, 7672-7679.

(59)Bergbreiter, D. E.; Boren, D.; Kippenberger, A. M. *Macromolecules* **2004**, *37*, 8686-8691.

(60)Brodeur, S. A.; Huebner, W.; Runt, J. P.; Newnham, R. E. *J. Mater. Res.* **1991**, *6*, 175-182.

(61)Wan, Y.; Wen, D. *Smart Mater. Struct.* **2004**, *13*, 983-989.

(62)Koscho, M. E.; Grubbs, R. H.; Lewis, N. S. *Anal. Chem.* **2002**, *74*, 1307-1315.

(63)Kim, Y. S.; Ha, S.-C.; Yang, Y.; Kim, Y. J.; Cho, S. M.; Yang, H.; Kim, Y. T. *Sens. Actuators, B* **2005**, *108*, 285-291.

(64)Klason, C.; McQueen, D. H.; Kubat, J. *Macromol. Symp.* **1996**, *108*, 247-260.

(65)Das, N. C.; Chaki, T. K.; Khastgir, D.; Chakraborty, A. *Adv. Polym. Technol.* **2001**, *20*, 226-236.

(66)Kale, V.; Moukwa, M. *J. Electrost.* **1996**, *38*, 239-248.

(67)Lee, G. J.; Suh, K. D.; Im, S. S. *Polym. Eng. Sci.* **1998**, *38*, 471-477.

(68)Feller, J. F.; Linossier, I.; Levesque, G. *Polym. Adv. Technol.* **2002**, *13*, 714-724.

(69)Tang, H.; Chen, X.; Luo, Y. *Eur. Polym. J.* **1996**, *32*, 963-966.

(70)Schueler, R.; Petermann, J.; Schulte, K.; Wentzel, H.-P. *J. Appl. Polym. Sci.* **1997**, *63*, 1741-1746.

(71)Kirkpatrick, S. *Rev. Mod. Phys.* **1973**, *45*, 574-588.

(72)Grunlan, J. C.; Gerberich, W. W.; Francis, L. F. *J. Mater. Res.* **1999**, *14*, 4132-4135.

(73)Souza, F. G.; Sena, M. E.; Soares, B. G. *J. Appl. Polym. Sci.* **2004**, *93*, 1631-1637.

(74)Jan, C. J.; Walton, M. D.; McConnell, E. P.; Jang, W.-S.; Kim, Y. S.; Grunlan, J. C. *Carbon* **2006**, *44*, 1974-1981.

(75)Kusy, R. P. *J. Appl. Phys.* **1977**, *48*, 5301-5305.

(76)Malliaris, A.; Turner, D. T. *J. Appl. Phys.* **1971**, *42*, 614-618.

(77)Sumita, M.; Sakata, K.; Hayakawa, Y.; Asai, S.; Miyasaka, K.; Tanemura, M. *Colloid Polym. Sci.* **1992**, *270*, 134-139.

(78)Breuer, O.; Tchoudakov, R.; Narkis, M.; Siegmann, A. *J. Appl. Polym. Sci.* **1997**, *64*, 1097-1106.

(79)Foulger, S. H. *J. Polym. Sci., Part B: Polym. Phys.* **1999**, *37*, 1899-1910.

(80)Thongruang, W.; Balik, C. M.; Spontak, R. J. *J. Polym. Sci., Part B: Polym. Phys.* **2002**, *40*, 1013-1025.

(81)Feng, J.; Chan, C.-M.; Li, J.-X. *Polym. Eng. Sci.* **2003**, *43*, 1058-1063.

(82)Yacubowicz, J.; Narkis, M.; Benguigui, L. *Polym. Eng. Sci.* **1990**, *30*, 459-468.

(83)Bouchet, J.; Carrot, C.; Guillet, J.; Boiteux, G.; Seytre, G.; Pineri, M. *Polym. Eng. Sci.* **2000**, *40*, 36-45.

(84)Wang, Y.; Anderson, C. *Macromolecules* **1999**, *32*, 6172-6179.

(85)Grunlan, J. C.; Gerberich, W. W.; Francis, L. F. *J. Appl. Polym. Sci.* **2001**, *80*, 692-705.

(86)Lutkenhaus, J. L.; Hrabak, K. D.; McEnnis, K.; Hammond, P. T. *J. Am. Chem. Soc.* **2005**, *127*, 17228-17234.

(87)Földes, E.; Tóth, A.; Kálmán, E.; Fekete, E.; Tomasovszky-Bobák, A. *J. Appl. Polym. Sci.* **2000**, *76*, 1529-1541.

(88)Yu, J.; Zhang, L. Q.; Rogunova, M.; Summers, J.; Hiltner, A.; Baer, E. *J. Appl. Polym. Sci.* **2005**, *98*, 1799-1805.

(89)Sun, Y. P.; Fu, K.; Lin, Y.; Huang, W. *Acc. Chem. Res.* **2002**, *35*, 1096-1104.

(90)Dyke, C. A.; Tour, J. M. *J. Phys. Chem. A* **2004**, *108*, 11151-11159.

(91)Tasis, D.; Tagmatarchis, N.; Bianco, A.; Prato, M. *Chem. Rev.* **2006**, *106*, 1105-1136.

(92)Chen, J.; Hamon, M. A.; Hu, H.; Chen, Y.; Rao, A. M.; Eklund, P. C.; Haddon, R. C. *Science* **1998**, *282*, 95-98.

(93)Price, B. K.; Tour, J. M. *J. Am. Chem. Soc.* **2006**, *128*, 12899-12904.

(94)Liang, F.; Sadana, A. K.; Peera, A.; Chattopadhyay, J.; Gu, Z.; Hauge, R. H.; Billups, W. E. *Nano Lett.* **2004**, *4*, 1257-1260.

(95)Coleman, K. S.; Bailey, S. R.; Fogden, S.; Green, M. L. H. *J. Am. Chem. Soc.* **2003**, *125*, 8722-8723.

(96)Qin, S.; Qin, D.; Ford, W. T.; Resasco, D. E.; Herrera, J. E. *J. Am. Chem. Soc.* **2004**, *126*, 170-176.

(97)Qu, L.; Veca, L. M.; Lin, Y.; Kitaygorodskiy, A.; Chen, B.; McCall, A. M.; Connell, J. W.; Sun, Y. P. *Macromolecules* **2005**, *38*, 10328-10331.

(98)Bergbreiter, D. E.; Kippenberger, A. M. *Adv. Polym. Sci.* **2006**, *198*, 1-49.

(99)Kim, Y.-S.; Liao, K.-S.; Jan, C. J.; Bergbreiter, D. E.; Grunlan, J. C. *Chem. Mater.* **2006**, *18*, 2997-3004.

(100)Liu, Y.; Wu, D.-C.; Zhang, W.-D.; Jiang, X.; He, C.-B.; Chung, T. S.; Goh, S. H.; Leong, K. W. *Angew. Chem., Int. Ed.* **2005**, *44*, 4782-4785.

(101)Hirsch, A.; Li, Q.; Wudl, F. *Angew. Chem., Int. Ed. Engl.* **1991**, *30*, 1309-1310.

(102)Basiuk, E. V.; Monroy-Pelaez, M.; Puente-Lee, I.; Basiuk, V. A. *Nano Lett.* **2004**, *4*, 863-866.

(103)Gao, L.; McCarthy, T. J. *Langmuir* **2006**, *22*, 5998-6000.

(104)Hong, X.; Gao, X.; Jiang, L. *J. Am. Chem. Soc.* **2007**, *129*, 1478-1479.

(105)Li, X.-M.; Reinhoudt, D.; Crego-Calama, M. *Chem. Soc. Rev.* **2007**, *36*, 1350-1368.

(106)Takei, G.; Nonogi, M.; Hibara, A.; Kitamori, T.; Kim, H.-B. *Lab Chip* **2007**, *7*, 596-602.

(107)Wang, T.; Hu, X.; Dong, S. *Chem. Commun.* **2007**, 1849-1851.

(108)Gao, L.; McCarthy, T. J. *Langmuir* **2006**, *22*, 2966-2967.

(109)Gao, L.; McCarthy, T. J. *Langmuir* **2006**, *22*, 6234-6237.

(110)Cao, L.; Hu, H. H.; Gao, D. *Langmuir* **2007**, *23*, 4310-4314.

(111)Gao, L.; McCarthy, T. J. *Langmuir* **2007**, *23*, 3762-3765.

(112)McHale, G. *Langmuir* **2007**, *23*, 8200-8205.

(113)Barthlott, W.; Neinhuis, C. *Planta* **1997**, *202*, 1-8.

(114)Feng, L.; Li, S.; Li, Y.; Li, H.; Zhang, L.; Zhai, J.; Song, Y.; Liu, B.; Jiang, L.; Zhu, D. *Adv. Mater.* **2002**, *14*, 1857-1860.

(115)Gao, X.; Jiang, L. *Nature* **2004**, *432*, 36-36.

(116)Jin, M.; Feng, X.; Feng, L.; Sun, T.; Zhai, J.; Li, T.; Jiang, L. *Adv. Mater.* **2005**, *17*, 1977-1981.

(117)Lee, J. A.; McCarthy, T. J. *Macromolecules* **2007**, *40*, 3965-3969.

(118)Huang, L.; Lau, S. P.; Yang, H. Y.; Leong, E. S. P.; Yu, S. F.; Prawer, S. *J. Phys. Chem. B* **2005**, *109*, 7746-7748.

(119)Bravo, J.; Zhai, L.; Wu, Z.; Cohen, R. E.; Rubner, M. F. *Langmuir* **2007**, *23*, 7293-7298.

(120)Larmour, I. A.; Bell, S. E. J.; Saunders, G. C. *Angew. Chem., Int. Ed.* **2007**, *46*, 1710-1712.

(121)Jisr, R. M.; Rmaile, H. H.; Schlenoff, J. B. *Angew. Chem., Int. Ed.* **2005**, *44*, 782-785.

(122)Huang, Z.; Zhu, Y.; Zhang, J.; Yin, G. *J. Phys. Chem. C* **2007**, *111*, 6821-6825.

(123)Li, Y.; Huang, X. J.; Heo, S. H.; Li, C. C.; Choi, Y. K.; Cai, W. P.; Cho, S. O. *Langmuir* **2007**, *23*, 2169-2174.

(124)Li, Y.; Li, C.; Cho, S. O.; Duan, G.; Cai, W. *Langmuir* **2007**, *23*, 9802-9807.

(125)Zhou, F.; Huck, W. T. S. *Phys. Chem. Chem. Phys.* **2006**, *8*, 3815-3823.

(126)Kumar, A.; Srivastava, A.; Galaev, I. Y.; Mattiasson, B. *Prog. Polym. Sci.* **2007**, *32*, 1205-1237.

(127)Luzinov, I.; Minko, S.; Tsukruk, V. V. *Soft Matter* **2008**, *4*, 714-725.

(128)Wang, S.; Liu, H.; Liu, D.; Ma, X.; Fang, X.; Jiang, L. *Angew. Chem. Int. Ed.* **2007**, *46*, 3915-3917.

(129)Connal, L. A.; Li, Q.; Quinn, J. F.; Tjipto, E.; Caruso, F.; Qiao, G. G. *Macromolecules* **2008**.

(130)Fu, Q.; RamaRao, G. V.; Basame, S. B.; Keller, D. J.; Artyushkova, K.; Fulghum, J. E.; Lopez, G. P. *J. Am. Chem. Soc.* **2004**, *126*, 8904-8905.

(131)Sun, T.; Wang, G.; Feng, L.; Liu, B.; Ma, Y.; Jiang, L.; Zhu, D. *Angew. Chem. Int. Ed.* **2004**, *43*, 357-360.

(132)Ivanov, A. E.; Ekeroth, J.; Nilsson, L.; Mattiasson, B.; Bergenstahl, B.; Galaev, I. Y. *J. Colloid Interface Sci.* **2006**, *296*, 538-544.

(133)Yuan, W.; Jiang, G.; Wang, J.; Wang, G.; Song, Y.; Jiang, L. *Macromolecules* **2006**, *39*, 1300-1303.

(134)He, Q.; Kuller, A.; Grunze, M.; Li, J. *Langmuir* **2007**, *23*, 3981-3987.

(135)Song, W.; Xia, F.; Bai, Y.; Liu, F.; Sun, T.; Jiang, L. *Langmuir* **2007**, *23*, 327-331.

(136)Yusa, S. i.; Fukuda, K.; Yamamoto, T.; Iwasaki, Y.; Watanabe, A.; Akiyoshi, K.; Morishima, Y. *Langmuir* **2007**, *23*, 12842-12848.

(137)Kurkuri, M. D.; Nussio, M. R.; Deslandes, A.; Voelcker, N. H. *Langmuir* **2008,** *24***,** 4238-4244.

(138)Bergbreiter, D. E.; Ponder, B. C.; Aguilar, G.; Srinivas, B. *Chem. Mater.* **1997**, *9*, 472-477.

(139)Bostrom, M.; Williams, D. R. M.; Ninham, B. W. *Langmuir* **2002**, *18*, 8609-8615.

(140)Chen, X.; Yang, T.; Kataoka, S.; Cremer, P. S. *J. Am. Chem. Soc.* **2007**, *129*, 12272-12279.

(141)Ishida, N.; Biggs, S. *Macromolecules* **2007**, *40*, 9045-9052.

(142)Zhang, Y.; Furyk, S.; Bergbreiter, D. E.; Cremer, P. S. *J. Am. Chem. Soc.* **2005**, *127*, 14505-14510.

(143)Zhang, Y.; Cremer, P. S. *Curr. Opin. Chem. Biol.* **2006**, *10*, 658-663.

(144)Bergbreiter, D. E.; Fu, H. *J. Polym. Sci., Part A: Polym. Chem.* **2008**, *46*, 186-193.

(145)Liao, K.-S.; Wan, A.; Batteas, J. D.; Bergbreiter, D. E. *Langmuir* **2008**, *24*, 4245-4253.

(146)Nishio, Y.; Chiba, R.; Miyashita, Y.; Oshima, K.; Miyajima, T.; Kimura, N.; Suzuki, H. *Polym. J.* **2002**, *34*, 149-157.

(147)Bauduin, P.; Wattebled, L.; Touraud, D.; Kunz, W. *Z. Phys. Chem.* **2004**, *218*, 631-641.

(148)Batz, H.-G.; Franzmann, G.; Ringsdorf, H. *Angew. Chem. Int. Ed. Engl.* **1972**, *11*, 1103-1104.

(149)Furyk, S.; Zhang, Y.; Ortiz-Acosta, D.; Cremer, P. S.; Bergbreiter, D. E. *J. Polym. Sci., Part A: Polym. Chem.* **2006**, *44*, 1492-1501.

VITA

Kang-Shyang Liao graduated from National Taiwan University, Taiwan in May 2000 with a B.S. in chemistry. In August 2003, he entered Texas A&M University under the advisement of Professor David E. Bergbreiter. He received his Ph.D in August 2008 and is currently pursuing a postdoctoral position with Professor Seamus Curran at the University of Houston. He can be reached at the Department of Physics, University of Houston, 617 Science & Research Bldg. 1, Houston, TX 77204-5005.